UNIVERSITY
OF WARMIA AND MAZURY
IN OLSZTYN

FACULTY OF FOOD SCIENCES
DEPARTMENT OF DAIRY SCIENCE AND QUALITY MANAGEMENT

M.Sc. Eng. Justyna Tarapata

FRACTIONATION OF MILK COMPONENTS AND VALORIZATION OF BY-PRODUCTS OBTAINED WITH MEMBRANE FILTRATION OF DAIRY STREAMS

Doctoral dissertation written under the supervision of:
dr. hab. eng. Justyna Żulewska, prof UWM
and
prof. dr. hab. eng. Marcin Zieliński

Olsztyn 2022

UNIWERSYTET
WARMIŃSKO-MAZURSKI
W OLSZTYNIE

WYDZIAŁ NAUKI O ŻYWNOŚCI
KATEDRA MLECZARSTWA I ZARZĄDZANIA JAKOŚCIĄ

mgr inż. Justyna Tarapata

FRAKCJONOWANIE SKŁADNIKÓW MLEKA I WALORYZACJA PRODUKTÓW UBOCZNYCH OTRZYMANYCH POPRZEZ FILTRACJĘ MEMBRANOWĄ W PRODUKCJI MLECZARSKIEJ

Rozprawa doktorska wykonana pod kierunkiem:
dr. hab. inż. Justyny Żulewskiej, prof UWM
i prof. dr. hab. inż. Marcina Zielińskiego

Olsztyn 2022

Acknowledgments

I would like to express my gratitude and appreciation to my academic supervisors dr. hab. eng. Justyna Żulewska, prof. UWM and prof. dr. hab. eng. Marcin Zieliński, for providing guidance and feedback throughout this project.

I am grateful to the employees of the Department of Dairy Science and Quality Management and the Department of Environmental Engineering at the University of Warmia and Mazury in Olsztyn, in which the research was carried out. Thank you for assistance in acquiring knowledge of analytical methods and laboratory skills.

I would like to acknowledge the scholarship from the Programme Interdisciplinary Doctoral Studies in Bioeconomy (POWR.03.02.00-00-I034/16-00), which is funded by the European Social Fund.

The research was financially supported by The National Centre for Research and Development, Project No. WPC1/DairyFunInn/2019, amount of funding 1,950,000.00 PLN.

Table of Contents

Abbreviations 5

Abstract 8

Streszczenie 9

1. Introduction 10

    1.1. Recovery of serum proteins from cheese whey 11

    1.2. Fractionation of buttermilk components 14

    1.3. Fouling and membrane performance 15

    1.4. Valorization of by-products generated during membrane filtration of dairy streams 17

2. Objectives 20

3. Materials and Methods 23

4. Publications 42

5. Research results in the thematically related series of publications 44

    5.1. Fouling mechanisms that affect ceramic ultrafiltration membranes using acid whey in comparison with sweet whey 44

    5.2. Microfiltration of buttermilk: efficacy of serum protein fractionation and fouling mechanisms 46

    5.3. Identification of major foulants reducing efficiency of filtration processes 49

    5.4. The relationship between the degree of lactose recovery in UF/DF permeates and the amount of biogas obtained in anaerobic digestion 50

    5.5. The use of UF/DF permeates to produce electricity and heat from the biomethane generated in the process of anaerobic digestion: the case study considering large-scale dairy plant 53

6. Summary and conclusions 55

7. References 58

Appendices 70

Abbreviations

List of symbols

AD	Anaerobic digestion
A_m	Membrane area
AMPTS	Automatic Methane Potential Test System
AW-T	Acid whey after Tvarog production
b	Rate of growth of the resistances due to adsorption and concentration polarization
BM	Buttermilk
BOD	Biochemical oxygen demand
BSA	Bovine serum albumin
C	Protein concentration in the retentate stream
c	Rate of growth of the protein mass deposited on the membrane surface
C_0	Protein concentration in feed at steady state
CF	Concentration factor
COD	Chemical oxygen demand
C_p	Protein concentration in permeate at steady state
CWF	Clean water flux
d	Constant parameter
DF	Diafiltration
DFP	Diafiltration permeate
DFP-M	Milk diafiltration permeate
DFP-MS	Milk serum diafiltration permeate
e	Constant parameter
f	Constant parameter
F_c	Fouling coefficient
FD	Fouling degree
F_e	External foulants
F_i	Internal foulants
FWF	Fouled water flux
GP	Graded permeability

J_p	Permeate flux during MF of buttermilk
$J_{p,0}$	Permeate flux at the initial time
$J_{p,f}$	Permeate flux at the end of the test
MCC	Micellar casein concentrate
m_{dep}	Protein mass deposited on the membrane surface
$m_{dep,ss}$	Protein mass deposited on the membrane surface at steady state
MF	Microfiltration
MFGM	Milk fat globule membrane
MWCO	Molecular weight cut-off
NCN	Noncasein nitrogen
NPN	Nonprotein nitrogen
NF	Nanofiltration
OLR	Organic load rate
R	Rejection of milk components
R^2	Regression coefficient
R_{ads}	Resistance due to adsorption on membrane surface and on the pore walls
$R_{ads,ss}$	Resistance due to adsorption at the steady state
R_{cl}	Resistance due to the growth of the cake layer
$R_{cl,ss}$	Resistance due to the growth of the cake layer at the steady state
R_{cp}	Resistance due to concentration polarization
$R_{cp,ss}$	Resistance due to concentration polarization at the steady state
RIS	Resistance-in-series
R_m	Membrane resistance
RO	Reverse osmosis
SD	Standard deviation
SPC	Serum protein concentrate
SW	Sweet whey
t	Filtration time
TMP	Transmembrane pressure
TN	Total nitrogen
TS	Total solids
UF	Ultrafiltration
UFP	Ultrafiltration permeate
UFP-M	Milk ultrafiltration permeate

UFP-MS	Milk serum ultrafiltration permeate
VS	Volatile solids
WP	Whey protein
WPC	Whey protein concentrate
WPI	Whey protein isolate
α-LA	α-lactalbumin
β-LG	β-lactoglobulin

μ	Viscosity of the feed solution
α	Specific cake resistance
β	Rejection of protein at a steady state in flux

Abstract

With the growing milk production, dairy plants should take actions to decrease the generation of by-products and increase their circularity. Among main dairy streams considered as by-products the following should be noted: whey, buttermilk and ultrafiltration permeates, which are highly polluting agents when they are incorporated into the wastewater of dairy plants. They are characterized by very high biochemical oxygen demand and chemical oxygen demand. Thus, it is clear that they require an appropriate treatment and their inadequate disposal creates a major environmental issues. Furthermore, the processing in XXI century means following the zero waste principle to maximize the use of all nutrients with maximum profits and minimum costs. Such an approach is justified not only economically, but also ethically and is dedicated by the action resulting from the strategy based on sustainability.

One of the important developments in dairy technology in recent decades has been the fractionation/separation of dairy streams into their principal constituents using membrane processes. However, fouling is still a major factor limiting application of membrane filtration. It changes membrane selectivity and reduces the flux during filtration time.

The objectives of the doctoral dissertation were to assess the fractionation efficiency during ultrafiltration of whey and microfiltration of buttermilk, to indicate major foulants during filtration processes, to model the flux decline of different feed tested with a resistance-in-series model and to determine a time-based evolution of model parameters. Moreover, considering the need to increase the circularity of dairy by-products, the utilization of ultra- and diafiltration permeates in an anaerobic digestion was studied.

The conducted study revealed that the major fouling agents reducing the efficiency of whey ultrafiltration were β-lactoglobulin and α-lactalbumin adsorbed to the membrane surface and to the pore walls. The performance of microfiltration membrane was reduced by the cake layer formed by caseins. A time-based evolution of resistance-in-series model parameters was determined for the first time, when filtering dairy streams obtained at industrial scale. Another novelty introduced was a general equation that accounts for the time-based changes in the mass deposited on the membrane surface during microfiltration of buttermilk. It has also been shown that with use of microfiltration to process buttermilk, which has undergone extensive heat treatment, it is possible to fractionate α-lactalbumin. The study of anaerobic digestion of ultrafiltration and diafiltration permeates has proven that tested permeates are efficient substrates in biomethane production. Based on these results, it has been calculated that for a dairy plant using ultrafiltration and diafiltration, the utilization of permeate in the methane fermentation process can provide enough energy to meet the plant's needs.

Streszczenie

Ze względu na rosnącą produkcję mleka zakłady mleczarskie powinny podjąć działania na rzecz ograniczenia produktów ubocznych i rozwoju gospodarki o obiegu zamkniętym. Wśród głównych mleczarskich produktów ubocznych można wyróżnić: serwatkę, maślankę i permeat po ultrafiltracji, które po wprowadzeniu do ścieków zakładowych są silnie zanieczyszczającymi czynnikami. Charakteryzują się bardzo wysokim biochemicznym zapotrzebowaniem na tlen oraz chemicznym zapotrzebowaniem na tlen. W związku z tym, wymagają oczyszczania, a ich nieodpowiednie zagospodarowanie stwarza poważny problem środowiskowy. Ponadto, produkcja w XXI wieku oznacza podążanie za zasadą zero waste, polegającą na maksymalizacji wykorzystania wszystkich składników odżywczych, przy maksymalnych zyskach i minimalnych kosztach. Takie podejście jest uzasadnione nie tylko ekonomicznie, ale także etycznie i polega na działaniach wynikających ze strategii opartej na zrównoważonym rozwoju.

Jednym z ważnych osiągnięć w technologii mleczarskiej na przestrzeni ostatnich dekad było frakcjonowanie/rozdzielanie składników mleka przy wykorzystaniu procesów membranowych. Jednak, zjawisko zarastania membran jest nadal głównym czynnikiem ograniczającym filtrację membranową. Zmienia selektywność membrany i zmniejsza natężenie przepływu strumienia permeatu w czasie filtracji.

Sformułowano następujące cele rozprawy doktorskiej: ocena wydajności frakcjonowania podczas ultrafiltracji serwatki i mikrofiltracji maślanki, określenie głównych czynników odpowiedzialnych za zjawisko zarastania membran, modelowanie spadku natężenia strumienia permeatu podczas filtracji różnych produktów za pomocą modelu oporów szeregowych oraz określenie zmian parametrów modelu w czasie. Ponadto, biorąc pod uwagę potrzebę rozwoju gospodarki o obiegu zamkniętym, zbadano wykorzystanie permeatów po ultra- i diafiltracji w procesie fermentacji beztlenowej.

Przeprowadzone badania wykazały, że głównymi czynnikami odpowiedzialnymi za zjawisko zarastania membran, obniżającymi wydajność ultrafiltracji serwatki były β-laktoglobulina i α-laktoalbumina zaadsorbowane na powierzchni membrany i na ścianach porów. Wydajność membrany mikrofiltracyjnej została zmniejszona przez warstwę placka utworzoną przez kazeinę. Po raz pierwszy określono zmiany parametrów modelu oporów szeregowych w czasie filtracji strumieni mleczarskich uzyskanych w warunkach przemysłowych. Kolejną nowością jest przedstawienie ogólnego równania opisującego zmiany masy osadzonej na powierzchni membrany w czasie mikrofiltracji maślanki. Wykazano również, że poprzez mikrofiltrację maślanki, która została poddana intensywnej obróbce cieplnej, możliwe jest frakcjonowanie α-laktoalbuminy. Badania nad fermentacją beztlenową permeatów po ultrafiltracji i diafiltracji wykazały, że są one wydajnymi substratami w produkcji biometanu. W oparciu o te wyniki obliczono, że w przypadku zakładu mleczarskiego stosującego ultrafiltrację i diafiltrację, utylizacja permeatu w procesie fermentacji metanowej może dostarczyć energii, w ilości która pokryje zapotrzebowanie zakładu.

1. Introduction

From 2017 to 2021, global cow milk production increased from 512 to 544 million tons (Statista, 2021). Due to such a large throughput the dairy industry faces issues related to its carbon footprint and sustainability (Granato et al., 2022). According to the United Nations Sustainable Development Goals (SDGs), by 2030, food processors should take actions to decrease the generation of by-products and increase their circularity by developing nutritious products (United Nations, 2015).

Among main dairy streams considered as by-products generated in dairy factories there are: whey, buttermilk (BM) and ultrafiltration permeates (UFPs) (Oliveira et al., 2020). In spite of the numerous properties and benefits, dairy by-products are considered a high polluting agents due to their high biochemical oxygen demand (BOD), and chemical oxygen demand (COD) (Kaur, 2021). Thus, it is clear that they require an appropriate treatment and their inadequate disposal creates a major environmental problem when they are incorporated into the wastewater of dairy plants. Furthermore, the proper management of dairy side-streams that leads to limited waste of nutrients and contribute to the development of ingredients with high added value is of great importance (Argenta & Scheer, 2020).

In order to minimize the environmental impact, as well as increase its application in the food sector, different alternatives for the use of dairy by-products have been studied. One of the important developments in dairy technology in recent years has been the fractionation of dairy streams into their principal constituents (Oliveira et al., 2020).

In this work the fractionation of serum proteins from cheese whey and separation of BM components were described. Moreover, the state of the art considering the utilization of permeates generated during membrane filtration of dairy streams as substrates in anaerobic digestion (AD) was considered. The processing of milk and dairy streams according to zero-waste principle and sustainable development requires more holistic approach to optimal design the entire processing path of particular feed material.

1.1. Recovery of serum proteins from cheese whey

At industrial-scale, serum proteins are mainly concentrated from whey. Therefore, they are usually called whey proteins (WP). Whey is a by-product of the manufacture of cheese or casein. There may be small differences in protein composition between cheese whey and permeate (milk serum) obtained during membrane-based micellar casein concentrate (MCC) production, which may serve as another source of serum proteins. For example, whey may contain: glycomacropeptide, that is released from κ-casein during cheesemaking, but it is not found in the milk serum; residual color; rennet; lactic acid and the cellular debris from starter culture and associated enzymes.

The WP comprises ~20% of the total protein in milk (Brans et al., 2004; Chandrapala et al., 2016; Rocha-Mendoza et al., 2021). The main WP are β-lactoglobulin (β-LG) (35% to 65% of WP), and α-lactalbumin (α-LA) (12% to 25% of WP). In smaller amounts, WP consist of immunoglobulins (8%), serum albumin (5%) and lactoferrin (1%). Whey proteins are rich in branched chain amino acids, such as leucine, isoleucine, and valine (Patel, 2015). They are a valuable and rich source of essential amino acids in the human diet. In comparison with chicken egg proteins, WP have a higher biological value (Szczurek, 2008). That is why cheese whey is considered a promising raw material for various commercial applications.

Additionally, there is also a large availability of cheese whey, which makes it utilization even more attractive from economical point of view. World production of whey is about 248 million tons, of which about 80% is produced in European Union and the United States of America (USDA, 2022). Large world whey production is associated with growing cheese production. According to OECD/FAO (2017), world cheese production is forecasted to increase from 2017 to 2026 by approximately 1.4% per year. This means that in 2026 the estimated total amount of cheese produced in the world will be about 26.2 million tons, which translates into about 236 million tons of drained whey. Therefore, the search for new cost-effective ways to process whey, including the optimization of WP recovery, is a constant challenge for the dairy industry.

Whey is classified into sweet whey or acid whey based on its origin. Sweet whey is obtained during production of cheese made by enzymatic coagulation (González Siso, 1996). Acid whey is generated when acid-coagulated cheeses and Greek yogurt are produced (Rocha-Mendoza et al., 2021). The most important differences in properties between sweet and acid whey are protein content (0.8–1.0% vs 0.3–0.84%, respectively),

calcium concentration (45 mg/100 g vs 103–140 mg/100 g, respectively) and pH (6–7 vs 4.21–4.60, respectively) (Fox et al., 2000; Rocha-Mendoza et al., 2021; Smith, 2014).

Sweet whey is usually further processed to produce whey powder or demineralized whey powder, lactose, whey protein concentrate (WPC) or whey protein isolate (WPI). However, the development of economically and environmentally sustainable application for acid whey is still a hurdle for dairy industry due to its composition (Zotta et al., 2020). Processing of acid whey is significantly difficult due to its low pH (<5) and the interest in using liquid whey for food production is small (Skryplonek, 2018).

Nowadays, the most common technologies of WP separation/fractionation are membrane filtration processes. Membrane filtration technology is widely used in dairy processing to concentrate, fractionate, isolate, demineralize, defat, and purify different target macro-molecules, such as proteins, phospholipids and lactose (France et al., 2021). They can be applied for the treatment of whey without reducing the quality of obtained products. Generally, the nanofiltration (NF) and reverse osmosis (RO) processes are used for whey concentration and demineralization, but microfiltration (MF) and ultrafiltration (UF) processes are more popular and applied to fractionation of whey (Argenta & Scheer, 2020). Therefore UF will be addressed with more emphasis in the following sections.

Analysis of literature data indicates that among investigated issues related to UF of whey the following should be listed: separation and recovery of protein and sugars (Galanakis et al., 2014), the changes in flux during concentration of fermented acid whey (Konrad et al., 2012a), the influence of the molecular weight cut-off (MWCO) and membrane material on the dominating fouling mechanism (Corbatón-Báguena et al., 2018), the chemical cleaning efficiency of UF membranes fouled with whey (Aghajani et al., 2018) or the relationship between cake formation and membrane rejection of lactose, proteins and salts (Brião et al., 2017). The application of UF in whey processing was recently described in detail by Argenta and Scheer (2020).

Ultrafiltration is a very important stage in serum protein recovery. That is why the research focused on process optimization is of great importance. The common issue addressed by so-far published papers is fouling of UF membranes resulting in a reduction of membrane performance and thus the process efficiency. Several attempts were made and different parameters were tested to reduce the fouling.

Among factors influencing the fouling phenomenon there is a type of membrane material used. Usually polymer UF membranes are applied (Argenta & Scheer, 2020). However, ceramic membranes are gaining more attention (Gruskevica & Mezule, 2021). The resistance against cleaning and disinfection is better for ceramic membranes (Brans et al., 2004). According to Al-Mutwalli et al., (2020) the filtration of cheese whey using ceramic membranes (i.e. inorganic membranes) shows relatively low fouling properties.

Nevertheless, the fouling phenomenon is still present during the filtration with ceramic membranes. Doyen et al. (1996) undertaken a comparative study on whey processing with polymer (PSF/PVP), ceramic (ZrO_2) and organo-mineral (ZrO_2/PSf) membranes. The MWCO ranged from 25 to 50 kDa. Despite the fact that, the permeability of the membranes was different, the plateau fluxes were comparable. It means that the experiments were conducted in the pressure independent flux regime. Depending on the concentration factor, the fluxes between 5.6×10^{-5} and 6.8×10^{-5} m/s were reached at a cross-flow velocity of 6 m/s. Therefore, the authors (Doyen et al., 1996) concluded that the fouling is the limiting factor in WP concentration and not the permeability of the membrane.

Main fouling agents present in whey are: α-LA, bovine serum albumin (BSA) and β-LG (Barukčić et al., 2015). Additionally, increased calcium content and ionic strength may enhance the deposit layer formation due to the reduction of repulsive forces in protein-membrane and protein-protein interactions (Labbez et al., 2002; Luján-Facundo et al., 2017; Steinhauer et al., 2016). The UF of acid whey obtained after Tvarog production is especially difficult to practice due to fouling associated with precipitation of calcium phosphate, the high concentration of lactic acid, minerals and the resulting insolubility of WP (Konrad et al., 2012a).

The membrane separation processes are important techniques that make it possible to exploit and add value to whey, due to its numerous advantages, notably allowing the recovery of proteins. As a drawback, membrane fouling is still a limiting factor and it was observed in the literature review (Argenta & Scheer, 2020), that several authors are seeking to understand and minimize its effects, for instance, through the manipulation of the process variables and the use of modified membranes. Currently, one of the main challenges in the fully efficient application of ceramic membranes is the need to reduce membrane fouling.

1.2. Fractionation of buttermilk components

Buttermilk is a by-product generated during butter making process. When cream is churned, an aqueous phase (BM) and a fat phase are generated (Oliveira et al., 2020).

India was the largest producer of butter in 2021, contributing 56% of the global production. The European Union was the second largest producer, averaging 2.13 million tons of butter (USDA, 2021). Assuming that butter is produced from 40% fat cream, about 107 tons of BM are generated annually. Most of BM produced today is dried and used as an ingredient with technological and functional properties in a wide range of food products (e.g. salad dressings, chocolate, cheese, ice cream or yogurt) (Dewettinck et al., 2008; Levin et al., 2016; Svanborg et al., 2015). Typically, 1000 kg of milk will yield over 45 kg of butter and 2–3 kg of BM powder (Oliveira et al., 2020).

Natural BM contains lactose (3.5–4.9%), lactic acid (0.5%), nitrogenous compounds (2.7–3.8%), fat (0.3–1.0%) and ash (0.6–0.7%). It also consist of proteins and phospholipids derived from the milk fat globule membrane (MFGM). The ratio of casein to WP in BM is similar to that in skim milk (Corredig & Dalgleish, 1977). The properties and composition of BM were described by Sodini et al. (2006) and Vanderghem et al. (2010).

The number of scientific publications on the fractionation and functionality of BM has quadrupled over the past 20 years (Oliveira et al., 2020). To date, MF has been considered an efficient technique to fractionate BM into retentate enriched in casein and MFGM components and permeate rich in serum proteins (Morin et al., 2007; Svanborg et al., 2015). The majority of the studies on BM have been focused on the selective isolation of MFGM components due to their bioactive properties (Ali, 2019). For example, Corredig et al.(2003) used sodium citrate to disperse the casein micelles and decrease its retention upon MF process, which resulted in production of phospholipid-enriched retentate. In another study, Morin et al. (2007) produced BM with a lower casein content employing MF, using cream washed with skim milk ultrafiltrate. Washing the cream prior to churning yields BM with 74% less protein than regular BM.

Since BM's chemical composition and ratio of casein to serum proteins is similar to that of skim milk (Ali, 2019; Corredig & Dalgleish, 1977), BM could serve as an appropriate raw material for fractionation of serum proteins. Such approach to BM

management could increase the value of this by-product. Svanborg et al. (2015) discussed the similarities in physical and chemical properties between serum protein concentrates produced from BM and skimmed milk. The study revealed that protein concentrate from BM was equivalent to that from skim milk in terms of chemical composition, solubility and foaming properties. Moreover, the protein profiles were comparable, but serum protein concentrate from skim milk was characterized by higher content of casein (Svanborg et al., 2015). Despite the promising properties, the process oriented on isolation of serum proteins from BM has not been thoroughly explored yet.

It is also worth noting, that BM components are subjected to extensive heat treatment at the stage of cream pasteurization. Thermal processing of proteins may cause the denaturation of serum proteins and the formation of intermolecular disulfide bonds between β-LG and κ-casein (Harland et al., 1952; Zulewska et al., 2018). That may result in the retention of some part of β-LG in the retentate and simultaneous permeation of α-LA to permeate stream, resulting in "ordinary" fractionation of serum proteins upon MF process.

It should be emphasized that the overall efficiency of the MF processing of regular BM is limited by the amount of caseins retained by the MF membrane (Morin et al., 2006). Moreover, casein is the major protein foulant that increases the hydraulic resistance and reduces passage of serum proteins through MF membranes (Zulewska & Barbano, 2013). It indicates the necessity to conduct the research focused on understanding the fouling mechanisms of MF membranes during BM processing.

1.3. Fouling and membrane performance

Membrane fouling occurring during the filtration process may be caused by different mechanisms following each other or occurring simultaneously. Among these mechanism, there are:

- adsorption, that takes place when particles present in the solution interact with the membrane material and consequently a thin layer of particles is attracted to the membrane;
- concentration polarization, that occurs when the concentration of a specific component increases at the boundary layer close to the membrane surface due to the selective transport through the membrane;

- partial or complete pore blocking, that occurs when particles present in the solution have sizes similar to pore sizes in the membrane material;
- a cake layer formation, that is formed at the membrane surface due to the aggregation of colloids and macromolecules rejected by the membrane (Gruskevica & Mezule, 2021; Luis, 2018).

Usually, the foulants has organic, inorganic, and biological origin. However, in complex substrates, inorganic, organic, and biological fouling occurs simultaneously. Inorganic fouling occurs due to the deposition of salts and inorganic elements on the membrane surface. Whereas, organic fouling refers to the adherence of hydrophilic and hydrophobic organic substances, i.e., proteins and polysaccharides on the membrane surface. Biological fouling is connected with adsorption of microorganisms (Gruskevica & Mezule, 2021).

The main effect of fouling is a decrease in flux over filtration time. During UF of whey β-LG is considered the main protein that induces membrane fouling (Wen-qiong et al., 2019). As reported by Morin et al. (2007), the flux during the MF process of BM, is mainly controlled by the adsorption of casein to the pore walls and the formation of a cake layer. Casein accumulates at the surface of the membrane and creates a porous layer that limits permeation.

The optimum flux during membrane filtration should have acceptable degree of fouling and foulants should be easily removed from membrane surface and/or pores by a standard cleaning procedure (Damar et al., 2020). Stable and high permeate fluxes can be obtained with shear-enhanced filtration processes. In order to keep such parameters in long-term operation, critical fouling conditions (the flux at which irreversible fouling appears on a membrane surface) should be studied and an optimum flux needs to be determined (Bacchin, 2004; Luo et al., 2012) .

The first and the most important stage during the development of solutions leading to fouling reduction is to understand the fouling mechanisms. According to Tan et al. (2014) it is possible to elucidate the mechanisms of membrane fouling during filtration of skim milk by identifying and quantifying the proteins and minerals involved in the external and internal membrane fouling. The method involve an extraction of foulants from the filtration unit by subsequent rinsing stages performed with RO water and identification coupled with quantification of foulants using high performance liquid chromatography.

It is also possible to get insight into the fouling mechanism by fitting experimental results (i.e. flux measurements) to mathematical models. Due to the great influence that the decline of permeate flux has on the process productivity, the research has been focused on the prediction of the time evolution of permeate flux by means of the development of mathematical models (Bolton et al., 2006; Chen & Kim, 2006; Choi et al., 2000; Ho & Zydney, 2000; Mondal & De, 2010). Among the different models available in the literature, the resistance-in-series model (RIS) is the most often used. In recent study performed by Corbatón-Báguena et al. (2018), a RIS model was fitted to the experimental data obtained during UF of whey model solutions. The fitting was characterized by very high accuracy in terms of coefficient of determination ($R^2 > 0.95$).

It seems that the fouling occurring during membrane filtration of dairy streams is quite well explored. However, majority of previously published data considers the filtration of model solutions of single or mixed whey proteins or whey derived from reconstitution of milk or whey protein concentrates (Corbatón-Báguena et al., 2018; Konrad et al., 2012a; Luján-Facundo et al., 2017). When the preparations are used to prepare the feed solution, there is a bias related to the potential influence of previous processing on protein properties and hence their interactions with other whey components and membrane material during filtration. Therefore, the research on complex industrial streams is of great importance and requires further exploration.

1.4. Valorization of by-products generated during membrane filtration of dairy streams

Membrane separation processes applied in fractionation of components of dairy streams solve the issue related to recovery of ingredients with high added value and increase their application in the food sector. However, UF of whey or milk serum generate another stream – UFP, which require further processing. Additionally, the diafiltration (DF) process is usually applied during concentration of serum proteins to obtain higher purity of retentate (Chamberland et al., 2020; Çınar, 2022; Lee et al., 2003; Lipnizki, 2010; Tomasula & Bonnaillie, 2015), resulting in doubling the amount of permeate generated. The DF process is a variation of a UF process, in which fresh solvent (usually RO water) is added to the retentate produced during the first stage of filtration (UF) to replenish the filtered volume. As a result of DF, small molecules (i.e. salts) are washed away from the retained macromolecules.

The UF/DF permeate contains mainly water, lactose, minerals, and a small amount of nitrogen containing compounds. Most of the nitrogen present in the UF/DF permeate consists of nonprotein nitrogen compounds normally found in milk (Barbano et al., 1988). Generally, the side-streams generated during milk and whey processing are characterized by an extreme COD up to approximately 70,000 mg O_2/L (Bella & Rao, 2021). These liquids are commonly regarded as the environmental problem and are creating a great difficulty for the dairy industry in their disposal (Das et al., 2016).

Since UF/DF permeate is a waste product, it can be utilized as a cheap source of lactose. The primary raw material for lactose production is the UFP of sweet/cheese whey generated during the production of WPC and WPI. About 4.2 million tons of WP powders were produced worldwide in 2018 (Research and Markets, 2019), indicating the large amount of permeate generated. The recovery of lactose can help reducing the COD loading of UF/DF permeate and can help solving the problem of environmental pollution being caused by its disposal. However, this approach is relevant only in the case of large-scale dairy factories possessing appropriate technological equipment. The production of lactose powder requires additional investment and operation costs for equipment dedicated to the further processing of the UF/DF permeate (Durham, 2009).

Anaerobic digestion was recognized as an environmentally friendly process applied for treatment of dairy wastes (Pochwatka et al., 2020; Ratanatamskul et al., 2014). Moreover, the production of biogas through the AD allows the increase in the share of renewable sources in the national energy scheme, which is the EU's goal as set out in the renewable energy directive (RED II) (RED I, 2013). Due to the growing energy demand in European Union, it is forecasted that there will be a rapid development of biogas plants needed in the nearest future (Kozłowski et al., 2016). These plants enable the production of biogas, which is a mixture of methane (45–74%) and carbon dioxide (25–54%). It may also contain a trace amounts of other components like hydrogen sulfide, ammonia, hydrogen, nitrogen or oxygen in a concentration between 1% and 2% of the total biogas volume. The composition of produced biogas is mainly affected by the components found in the substrates used in AD (Kozłowski et al., 2016). The biochemical methane potential (BMP) test is often applied to assess the anaerobic biodegradability of a substrate, whereby the produced volume of methane generated by the substrate (in terms of VS or COD added) can be determined (Escalante et al., 2018).

The vast majority of previous research has reported BMP values for cheese whey. It ranges from 0.32 to 0.85 L CH_4/g VS (Dreschke et al., 2015; Ergüder et al., 2001; Labatut et al., 2011). Although cheese whey is characterized by high organic matter content, methane yield is limited owing to the production of volatile fatty acids (VFAs) during lactose fermentation. For this reason, acid accumulation causes the decrease in pH, lead to the growth of acetogenic bacteria, and inhibition of methanogenic activity (Yang et al., 2018). In another study by Zieliński et al. (2007), it was showed that the controlled AD allows efficient disposal of the permeate obtained after NF of acid whey. To date, little is known about BMP of UF/DF permeates containing a relatively high concentration of lactose. The assessment of the possibility of valorizing the permeates generated during UF and DF by using them in biogas production remains to be exploited.

2. Objectives

The fundamentals about fractionation of dairy by-products using membrane processes have already been established over the last 50 years. Many theories and models regarding mass transfer have been developed to represent most of the existing membrane systems. However, there still exist a big gap in the area of the industrial application of the membrane processes. More specifically, several observations cannot yet be explained regarding the fouling mechanism. In this thesis, an attempt to reduce the gap in understanding the filtration of complex raw materials such as whey and buttermilk (BM) was made. Moreover, in order to minimize the environmental impact of ultrafiltration/diafiltration permeates (UFP/DFP), side-streams generated during fractionation of milk components, their application as substrates in anaerobic digestion (AD) has been studied.

The main objectives of the study were to assess the fractionation efficiency of membrane filtration of dairy streams, to indicate major foulants during filtration processes, to relate the model parameters of a resistance-in-series (RIS) model to the different feed tested and to assess the possibility of valorizing the permeates generated during diafiltration (DF) by using them in biogas production and comparing their effects with typical ultrafiltration (UF) permeates.

The specific objectives of the doctoral dissertation (which is a collection of published and thematically related scientific publications) were:

SO1 To examine the fouling mechanisms that affect ceramic UF membranes using acid whey in comparison with sweet whey, based on physicochemical analysis of external and internal foulants as well as mathematical modelling of the flux using RIS model.

SO2 To examine the microfiltration (MF) process of BM (using ceramic graded permeability membranes) in terms of the efficacy of serum protein fractionation and fouling mechanisms that affect membrane performance by physicochemical analysis of external and internal foulants as well as fitting experimental data to the RIS model.

SO3 To identify major foulants reducing the performance of UF membrane during whey processing and MF membrane during BM processing.

SO4 To estimate the relationship between the degree of lactose recovery in UF/DF permeates and the amount of biogas obtained in AD.

SO5 To analyze the possibilities of using the waste from dairy streams processing (UFP/DFP) to produce electricity and heat from the biomethane generated in the process of AD. The biochemical methane potential test was performed and its results served as one of the input variables in the case study concerning electric power and heat production from UF/DF effluents generated by large-scale dairy factory.

The research plan is presented in the Figure 1.

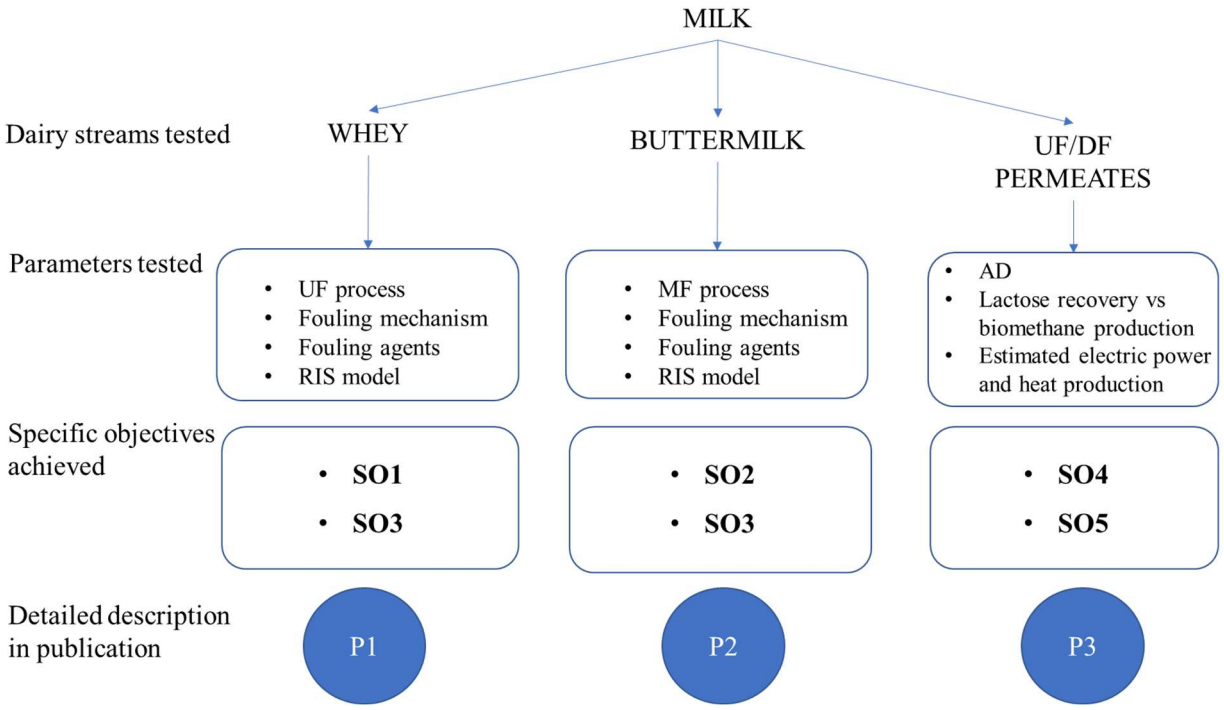


Figure 1. Schematic research plan: SO - specific objective, UF - ultrafiltration, MF- microfiltration, AD – anaerobic digestion, RIS – resistance-in-series, P1 – publication 1 (Tarapata et al., 2022a), P2 – publication 2 (Tarapata et al., 2022b), P3 – publication 3 (Tarapata et al., 2022c).

Based on the literature review **the** following **research hypothesis** were formed:

H1 RIS model accurately describes flux decline during membrane filtration of industrially obtained whey and BM.

H2 Microfiltration of thermally processed BM results in fractionation of major serum proteins under certain conditions.

H3 The concentration of lactose in UF/DF permeates affects the results of biochemical methane potential test.

H4 Ultrafiltration and diafiltration permeates are efficient substrates in biomethane production through AD.

In order to test these hypotheses, the following processes were investigated:

- UF of acid whey (generated in the dairy industry during Tvarog cheese production) and sweet whey (generated in the pilot-scale production of Gouda cheese) using ceramic (zirconia) membrane under the parameters recommended by the membrane manufacturer,
- MF of BM generated after butter making on industrial scale using graded-permeability ceramic membranes,
- biochemical methane potential test of permeates generated after UF and DF (pilot-scale) of milk and milk serum.

Detailed information on the research material, research methodology, the results and the discussion are provided in the thematically related series of scientific publications (3 research papers), which constitute a doctoral dissertation entitled "*Fractionation of milk components and valorization of by-products obtained with membrane filtration of dairy streams*".

3. Materials and Methods

3.1. Materials

The following streams were used in series of experiments carried out: sweet whey, acid whey, BM, UFPs, DFPs.

3.1.1 Whey

Sweet/cheese whey (SW) was generated during Gouda cheese production in Dairy Research and Educational Center (DREC) at University of Warmia and Mazury in Olsztyn (Poland).

Acid whey (AW-T) was supplied by the Dairy EkoŁukta Ltd. (Łukta, Poland). It was generated during Tvarog cheese (acid-coagulated cheese) production with the use of cheese milk pasteurized at 88.2 ± 2°C for 21s.

Before UF process, whey was subjected to several pre-treatment operations. Right after separation from curd grains whey was centrifuged at 45°C using LWG20 centrifuge (Spomasz, Gniezno, Poland) to remove fat and residual curd. Next, it was pasteurized at 72°C for 15s using plate heat exchanger (P20-HB; Alfa Laval, Lund, Sweden). Following the pasteurization, whey was cooled and stored (at least 24 h) at 3°C until further processing. The chemical composition and pH of tested whey types are reported in Table 1.

Table 1. The chemical composition and pH of tested whey types.

Parameter	SW	AW-T
TS [%]	$5.90^{a} \pm 0.51$	$5.53^{a} \pm 0.16$
TN [%]	$0.86^{a} \pm 0.02$	$0.50^{b} \pm 0.01$
NCN [%]	$0.82^{a} \pm 0.03$	$0.48^{b} \pm 0.02$
NPN [%]	$0.19^{a} \pm 0.02$	$0.229^{b} \pm 0.004$
Lactic acid [%]	$0.09^{b} \pm 0.01$	$0.58^{a} \pm 0.02$
Ca [mg/L]	$366^{b} \pm 49$	$1180^{a} \pm 74$
P [mg/1000g]	$363^{b} \pm 35$	$612^{a} \pm 20$
pH	$6.66^{a} \pm 0.13$	$4.66^{b} \pm 0.08$

^{a,b} - means within a row with different superscripts are different ($P < 0.05$);
TS - total solids; TN - total nitrogen; calculated as total N × 6.38; NCN - noncasein nitrogen × 6.38; NPN - nonprotein nitrogen × 6.38; Ca - calcium; P - phosphorus.
Source: Tarapata et al. (2022 **P1**).

The detailed information on raw materials subjected to UF process can be found in publication **P1** (Section 2.2, p. 2).

3.1.2. Buttermilk

Buttermilk was supplied by the Dairy Cooperative SM Mlekovita (Poland) and delivered to the DREC located at the University of Warmia and Mazury in Olsztyn. Upon arrival at the DREC, the BM was skimmed by centrifugation (LWG20 centrifuge, Spomasz) to ~0.3% fat at 45°C. Next, the BM was subjected to pasteurization using heat plate exchanger (P20-HB; Alfa Laval) at 72°C for 15s. After the pasteurization process, the BM was cooled to microfiltration temperature of 50°C and processed. The chemical composition and pH of BM are reported in Table 2.

Table 2. The chemical composition and pH of buttermilk.

Parameter	Value
TS [%]	8.61 ± 0.22
TN [%]	2.80 ± 0.10
NCN [%]	0.31 ± 0.01
NPN [%]	0.16 ± 0.02
Fat [%]	0.27 ± 0.02
Ca [mg/L]	843 ± 379
P [mg/1000g]	666 ± 47
pH	6.68 ± 0.10

TS - total solids; TN - total nitrogen; calculated as total N × 6.38; NCN - noncasein nitrogen × 6.38; NPN - nonprotein nitrogen × 6.38; Ca - calcium; P - phosphorus.
Source: Tarapata et al. (2022 **P2**).

The detailed information on raw material subjected to MF process can be found in publication **P2** (Section 2.2, p. 3).

3.1.3. Ultrafiltration/diafiltration permeates (substrates for anaerobic digestion)

The UF permeates (UFP) and diafiltration permeates (DFP) were generated during UF/DF processes curried out in DREC at University of Warmia and Mazury in Olsztyn. The UF/DF experiments were performed with a pilot-scale filtration unit (Koch Membrane Systems, Wilmington, MA, USA). The system was equipped with a spiral-wound polyethersulfone (PES) UF membrane (model 3838-HFK-131) with a molecular weight cut-off of 10 kDa and a feed spacer model N 31 mil (manufacturer's specifications). Total membrane surface area was 6.7 m^2. Two different dairy streams, namely skimmed milk and milk serum were ultra- and diafiltered according to the procedures described below.

UF/DF of milk

Raw milk was purchased from a local dairy manufacturer and skimmed at 45°C using LWG20 centrifuge (Spomasz). Then, it was pasteurized at 72°C for 15s using plate heat exchanger (P20-HB; Alfa Laval). Next, it was cooled down to 50°C and subjected to UF/DF processes in order to produce milk protein concentrate (MPC). Three 170 kg batches of skimmed milk were ultra- and diafiltered to reach a final protein content in retentate of approximately 13.5%. The UF/DF system was operated in a batch mode at 50°C, under a constant transmembrane pressure (TMP) of 4 bar. Skim milk was ultrafiltered until concentration factor (CF) of 4.6×. Once the target CF was reached, the DF (CF of 6.6×) was carried out by adding the reverse osmosis (RO) water (50°C) to UF retentate to bring the weight back to the original total weight of the starting feed. Samples of the permeate generated after UF step, and the permeate generated at the end of DF step were collected and stored at 4°C before being subjected to anaerobic digestion (AD) described in section 3.8. The physicochemical parameters of UF/DF permeates generated after milk filtration are reported in Table 3.

Table 3. The physicochemical parameters of UF/DF permeates generated after filtration of milk (M).

Parameter	Permeate	
	UFP-M	**DFP-M**
TS [%]	$5.60^{a} \pm 0.06$	$1.81^{b} \pm 0.05$
VS [%]	$5.13^{a} \pm 0.06$	$1.6^{b} \pm 0.08$
Ash [%]	$0.45^{a} \pm 0.01$	$0.15^{b} \pm 0.01$
Ca [mg/L]	$185.5^{a} \pm 9.6$	$34.8^{b} \pm 2.0$
TN [%]	$0.18^{a} \pm 0.03$	$0.06^{b} \pm 0.01$
Lactose [%]	$4.97^{a} \pm 0.02$	$1.59^{b} \pm 0.18$
pH	$6.55^{a} \pm 0.18$	$6.84^{b} \pm 0.10$
COD [mg O_2/L]	$57{,}020^{a} \pm 510$	$19{,}150^{b} \pm 1500$

[a,b] - means within a row with different superscripts are different ($P < 0.05$);
TS - total solids; VS – volatile solids; TN - total nitrogen; calculated as total N × 6.38; Ca – calcium; COD – chemical oxygen demand.
Source: Tarapata et al. (2022 **P3**).

UF/DF of milk serum

Milk serum was produced in DREC in University of Warmia and Mazury in Olsztyn. Raw milk was purchased from a local dairy manufacturer and skimmed at 45°C using LWG20 centrifuge (Spomasz). Then, it was pasteurized at 72°C for 15s using plate heat exchanger (P20-HB; Alfa Laval). Next, it was cooled down to 50°C and subjected to MF/DF processes typically applied during production of micellar casein concentrates (MCC). Three 160 kg batches of skimmed milk were micro- and diafiltered to reach a final protein content in retentate of approximately 7%. The detailed description of MF unit used was provided in section 3.2 (below). The MF/DF system was operated in batch mode at 50°C, under a constant TMP of 1.9 bar. Skim milk was microfiltered until CF of 3.0×. Once the target CF was reached, two DF stages (DF1 and DF2) were carried out using RO water (50°C) as a diafiltrant. The target CF of both DF stages was 3.0×. The permeates generated after MF and DF1 stages (milk serum) were mixed and stored at 4°C until further processing with UF/DF unit. In order to produce serum protein concentrate (SPC).

Three 170 kg batches of milk serum were ultra- and diafiltered to reach a final protein content in a retentate of approximately 2.2%. The UF-DF system was operated in a batch mode at 50°C, under a constant TMP of 4 bar. Milk serum was ultrafiltered until CF of 5.5×. Once the target CF was reached, the DF (CF of 8.5×) was carried out with RO water as diafiltrant. Samples of the permeate generated after UF step, and the permeate generated at the end of DF step were collected and stored at 4°C before being subjected to AD described in section 3.8. The physicochemical parameters of UF/DF permeates generated after milk serum filtration are reported in Table 4.

Table 4. The physicochemical parameters of UF/DF permeates generated after filtration of milk serum (MS).

Parameter	Permeate	
	UFP-M	**DFP-M**
TS [%]	$3.80^{a} \pm 0.02$	$0.86^{b} \pm 0.09$
VS [%]	$3.40^{a} \pm 0.07$	$0.79^{b} \pm 0.03$
Ash [%]	$0.332^{a} \pm 0.004$	$0.07^{b} \pm 0.01$
Ca [mg/L]	$54.4^{a} \pm 2.1$	$3.6^{b} \pm 0.1$
TN [%]	$0.097^{a} \pm 0.003$	$0.021^{b} \pm 0.002$
Lactose [%]	$3.37^{a} \pm 0.02$	$0.76^{b} \pm 0.01$
pH	$6.84^{a} \pm 0.04$	$7.03^{b} \pm 0.06$
COD [mg O_2/L]	$38{,}600^{a} \pm 780$	$7610^{b} \pm 430$

[a,b] - means within a row with different superscripts are different ($P < 0.05$);
TS - total solids; VS – volatile solids; TN - total nitrogen; calculated as total N × 6.38; Ca – calcium; COD – chemical oxygen demand.
Source: Tarapata et al. (2022 **P3**).

The detailed information on raw materials subjected to AD process can be found in publication **P3** (Section 2.1, p. 3-5).

3.1.4. The fermentative inoculum

The source of methanogenic bacteria was an anaerobic sludge, which came from a bioreactor operating under mesophilic conditions (36 ± 1°C). The reactor was installed in the Department of Environmental Engineering, University of Warmia and Mazury in Olsztyn. The parameters of the sludge are reported in Table 5.

Table 5. The parameters of fermentative inoculum used in anaerobic digestion.

Parameter	Value
TS [%]	6.8 ± 0.2
VS [% TS]	73.5 ± 0.9
Ash [% TS]	26.5 ± 0.9
C [% TS]	41.1 ± 0.8
N [% TS]	3.7 ± 0.0
C/N ratio	11.2 ± 0.2

TS – total solids; VS – volatile solids; C – carbon; N – nitrogen; C/N – carbon to nitrogen; ± standard deviation.
Source: Tarapata et al. (2022 **P3**).

The detailed information on inoculum used in AD process can be found in publication **P3** (Section 2.1, p. 5).

3.2. Filtration units and membranes

Ultrafiltration of SW and AW-T was performed using a laboratory-scale unit (Pall Membralox XLAB 5, Pall Corp, Port Washington, NY) described previously by Zulewska et al. (2018). The 3.5-L stainless steel feed tank was connected to a progressive cavity feed pump with frequency converter, powering the whole unit. Two manometers were located at each side of the membrane module to control the TMP. The unit was equipped with a temperature control system and UF monochannel ceramic membrane (model ET1-070, zirconia, Pall Corp.). The membrane was 250 mm long with channel diameter of 7 mm and pore size of 20 nm. Total membrane surface area was 0.005 m^2.

Microfiltration of BM was performed on a pilot-scale graded permeability (GP) MF system. The 60-L stainless steel feed tank was connected to a feed pump (model LKH-10-155-FSS-DIN, 3.0 kW, Alfa Laval, Kansas City, MO, USA). The system was also

equipped with a retentate recirculation pump (model LKH-10-155-FSSDIN 4.0 kW, Alfa Laval, Kansas City, MO, USA). Three ceramic MF membranes (tubes, model EP1940GL0.1mAGP1020, alumina, Pall Corp., East Hills, NY, USA) were mounted vertically in a tubular single stainless steel module. The membranes were 1.02 m long with 19 channels each and 4-mm channel diameter. Total membrane surface area was 0.72 m^2 (0.24 m^2 per membrane).

The detailed information on: UF unit can be found in publication **P1** (Sections 2.1 and 2.2, p. 2); MF unit can be found in publication **P2** (Section 2.3, p. 3).

3.3. UF of Whey and Membrane Cleaning Procedure

The main processing conditions applied during UF of whey are summarized in Table 6.

Table 6. The processing conditions applied during UF of whey.

Parameter	**Description**
Filtration unit	• laboratory-scale UF system (Pall Membralox XLAB 5, Pall Corp.)
Membrane used	• single ceramic unit (model ET1-070, zirconia, Pall Corp.), • membrane length: 250 mm, • channel diameter: 7mm, • pore size: 20 nm, • surface area: 0.005 m^2
Cleaning procedure before running experiment	• short cleaning procedure previously described by Zulewska et al. (2018)
Prerun clean water flux (CWF) measurement	• RO water flushing at 25°C until neutral pH, • the retentate outlet valve opened to obtain TMP of 1 bar, the permeate outlet valve fully opened, • calculations based on permeate weight collected in 120 s

UF process	
Feed	• 3.5 kg of AW-T (1 batch), • 3.5 kg of SW (1 batch)
Mode	• first 5 min before opening the permeate valve – total recirculation mode, • after opening the permeate valve – recirculation of retentate, permeate was collected
Temperature	• 50°C
Filtration time	• 180 min
Pump settings	• pump motor frequency of 28.3 Hz, • frequency converter adjusted to 5 on 0 to 10 scale
Crossflow velocity	• 4.1 m/s, • turbulent flow of whey through the unit (Re ~38,000)
TMP	• 3 bar (0.3 MPa)
Flux measurements	• measured every 15 min based on the weight of permeate obtained during this time
RO water flushing after UF process	• flushing with RO water (50°C), to wash out whey residue, • next, another rinsing steps were performed to collect foulants according to procedure described in section 3.6.
Fouled water flux (FWF) measurement	• determined using same settings as for prerun CWF, • performed after foulants collection
Cleaning procedure after UF	• cleaning procedure previously described by Zulewska et al. (2018)
Postrun CWF measurement	• determined under the same conditions as for prerun CWF

The detailed information on UF of whey and cleaning procedure can be found in publication **P1** (Sections 2.1- 2.3, p. 2).

3.4. MF of Buttermilk and Membrane Cleaning Procedure

The main processing conditions applied during MF of BM are summarized in Table 7.

Table 7. The processing conditions applied during MF of BM.

Parameter	**Description**
Filtration unit	• a pilot-scale GP MF system
Membrane used	• 3× ceramic tubes (model EP1940GL0.1mAGP1020, alumina, Pall Corp.), • membrane length: 1.02 m, • no. of channels: 19, • channel diameter: 4 mm, • pore size: 0.1 μm, • surface area: 0.72 m^2 (0.24 m^2 per membrane)
Cleaning procedure before running experiment	• alkaline cleaning only, • cleaning chemicals: Divos 120CL VM9 (Diversey, Fort Mill, SC, USA) water solution at concentration of 1.0-1.5% v/v, • cleaning temperature: 75°C, • time of cleaning: 30 min, • permeate flow of approximately 1000 L/h, • retentate flow of approximately 5000 L/h, • feed and recirculation pumps on
Prerun CWF measurement	• RO water flushing at 25°C until neutral pH, • the retentate pressure at the inlet (R_{pi}) 0.32 MPa, • the retentate pressure at the outlet (R_{po}) 0.20 MPa, • the permeate outlet valve fully opened, • retentate flow of approximately 7000 L/h, • permeate flow of approximately 750 L/h, • calculations based on permeate weight collected in 90 s

MF process	
Feed	• ~160 kg of BM (1 batch)
Mode	• first 5 min before opening the permeate valve – total recirculation mode, • after opening the permeate valve – feed and bleed mode until 28 kg of retentate was collected, • next, recirculation of retentate and collection of permeate
Temperature	• 50°C
Filtration time	• ~6 h
CF	• 3×
Permeate removal rate	• 16.9 L/h
R_{pi}	• 0.25 MPa
P_{po}	• 0.15 MPa
Crossflow velocity	• 6.3 m/s,
TMP	• 2 bar (0.2 MPa)
Flux measurements	• measured every 30 min based on the weight of permeate obtained during this time
RO water flushing after MF process	• flushing with RO water (25°C), to wash out BM residue, • next, another rinsing steps were performed to collect foulants according to procedure described in section 3.6.
FWF measurement	• determined using same settings as for prerun CWF, • performed after foulants collection
Cleaning procedure after MF	Alkaline cleaning: • cleaning chemicals: Divos 120CL VM9 (Diversey) water solution at concentration of 1.0-1.5% v/v, • cleaning temperature: 70°C, • time of cleaning: 30 min, • permeate flow of approximately 1000 L/h, • retentate flow of approximately 5000 L/h, • both pumps on

	Acidic cleaning: • cleaning chemicals: Pascal VA5, conc. 1.0%, v/v, (Diversey, Fort Mill, SC, USA), • cleaning temperature: 65°C, • time of cleaning: 30 min, • permeate flow of approximately 1000 L/h, • retentate flow of approximately 5000 L/h, • both pumps on
Postrun CWF measurement	• determined under the same conditions as for prerun CWF, after alkaline cleaning

The detailed information on MF of BM and cleaning procedure can be found in publication **P2** (Section 2.3, p. 3-4).

3.5. Membrane performance

The membrane performance was characterized by calculating permeate flux, fouling coefficient, fouling degree, limiting flux and critical flux.

Permeate flow rate values were measured throughout the experiment in time intervals specified in sections 3.3 and 3.4, by weighing the permeate collected in that time intervals. Permeate flux (J_p, m^3/m^2h) values were calculated using Eq. 1:

$$J_p = \frac{M}{A_m \times t \times \rho} \quad (1)$$

where M is the permeate weight (kg), A_m is the membrane area (m^2), t is time (s), and ρ is the permeate density at the operating temperature (kg/m^3).

The fouling coefficient (*Fc*) was calculated according to Rao (2002) with Eq. (2):

$$Fc = 1 - (FWF / prerun\ CWF) \quad (2)$$

where *FWF* is fouled water flux, and *prerun CWF* is the flux of pure water measured before filtration process. The *Fc* varies between 0 (not fouled membrane) and 1 (completely fouled membrane).

The fouling degree (*FD*) was calculated by comparing the permeate flux at the start of filtration process ($J_{p,0}$) and at the end of a run ($J_{p,f}$) according to Eq. 3:

$$FD\ (\%) = [(J_{p,0} - J_{p,f})/J_{p,0}] \times 100\% \quad (3)$$

Limiting and critical flux were calculated according to Samuelsson et al. (1997) and Bacchin (2004), respectively.

3.6. Characterization of membrane fouling

The external (F_e) and internal (F_i) foulants located on the membrane surface and inside the pores, respectively were collected according to the modified method described by Tan et al. (2014). The modifications were adjusted depending on filtration unit used. The parameters of foulants collection procedure are summarized in Table 8.

Table 8. The main conditions applied during foulants collection.

Foulants	**UF of whey**	**MF of BM**
External foulants – F_e		
	• 1st flushing: 2 L of RO water at 50°C circulating in the system for 1 min to wash out whey residues (drained), • 2nd flushing: 2 L of RO water circulating in the system for 5 min to collect F_e: - the permeate valve closed, - the retentate valve opened, - pump motor frequency: 12.9 Hz	• 1st- 4th flushing: 4 × 60 L of RO water at 25°C circulating in the system for 3 min to wash out BM residues (drained), • 5th flushing: 60 L of RO water circulating in the system for 5 min to collect F_e: - the permeate valve closed, - the retentate valve opened, - crossflow velocity of 10.3 m/s

Internal foulants – F_i		
	• 3rd flushing: 2 L of RO water circulating in the system for 5 min to collect F_i: - the permeate valve opened, - the retentate valve closed, - pump motor frequency: 12.9 Hz	• 6th flushing: 60 L of RO water circulating in the system for 5 min to collect Fi: - the permeate valve opened, - the retentate valve closed, - crossflow velocity of 10.3 m/s

The detailed information on foulants collection after UF of whey can be found in **P1** (Section 2.4, p. 2-3), after MF of BM in publication **P2** (Section 2.4, p. 4).

3.7. Modelling of permeate flux with resistance-in-series model

The resistance in series model (RIS) applied in described studies considers four following filtration resistances: resistance of membrane material, resistance due to adsorption, resistance due to concentration polarization and resistance due to cake layer formation. In this regard, the permeate flux of the cross-flow filtration process (J_p) is described by Eq. (4) (Juang et al., 2008a):

$$J_p = \frac{TMP}{\mu \times \left(R_{\mathrm{m}} + R_{\mathrm{ads}} + R_{\mathrm{cp}} + R_{\mathrm{cl}}\right)} \tag{4}$$

where TMP is the transmembrane pressure, μ is the viscosity of the feed, R_{m} is the hydraulic resistance of the membrane material, R_{ads} is the resistance due to the adsorption of solute on the membrane surface, and also on the pore walls, R_{cp} is the resistance due to concentration polarization, and R_{cl} is the resistance of the cake layer.

The R_{m} is determined based on CWF measurements. According to Eq. (4), when the clean water is used as feed, the values of R_{ads}, R_{cp} and R_{cl} are negligible. Then, the formula describing R_m is given in Eq. 5:

$$R_{\mathrm{m}} = \frac{TMP}{\mu \times CWF} \tag{5}$$

According to Carrere et al. (2001) and Juang et al. (2008b), the experimental variations of R_{ads} and R_{cp} follow an exponential trend. These resistances grow at a rate constant b up to a steady-state (ss) values of $R_{ads,ss}$ and $R_{cp,ss}$. Moreover, both resistances are determined simultaneously during crossflow filtration experiments and are expressed as a one fixed value of $R_{ads,ss} + R_{cp,ss}$ (Eq. 6):

$$R_{\text{ads}} + R_{\text{cp}} = \left(R_{\text{ads,ss}} + R_{\text{cp,ss}}\right) \times [1 - \exp(-b \times t)] \tag{6}$$

where $R_{ads,ss}$ is the resistance due to solute adsorption at the steady-state and $R_{cp,ss}$ is the resistance due to concentration polarization at the steady-state, t is the filtration time. The sum of $R_{ads,ss}$+$R_{cp,ss}$ and the value of b are determined by fitting experimental data to the model equations (Corbatón-Báguena et al., 2018; Juang et al., 2008a).

The resistance due to formation of the cake layer (R_{cl}) is explained by Eq. (7):

$$R_{cl} = \left(\frac{m_{dep}}{A_m}\right) \times \alpha \tag{7}$$

where A_m is the membrane area, m_{dep} is the protein mass deposited on the membrane surface, and α is the specific cake resistance. The value of α is determined by fitting experimental data to the model equation (Corbatón-Báguena et al., 2018).

Once the J_p and rejection of protein are known, the changes in protein concentration in the retentate at each time interval can be calculated from Eq. (8) (Juang et al., 2008b):

$$C = \frac{C_0\left[V_0 - (1-\beta)A_m \int_0^t J_p dt\right]}{V_0 \; - \; A_m \int_0^t J_p dt} \tag{8}$$

where C is the protein concentration in the retentate stream, V_0 is the initial volume of the feed, and β is the rejection of protein calculated at a steady-state in flux (the last measured flux value) according to Eq. (9):

$$\beta = 1 - \left(\frac{C_p}{C_0}\right) \tag{9}$$

where C_p and C_0 are the concentration of protein in permeate at the steady-state and in the feed, respectively.

Under certain assumptions, the mass of protein deposited on the membrane surface (m_{dep}) can be estimated by means of mass equation balance (Eq. 10) (Juang et al., 2008b):

$$\frac{dm_{dep}}{dt} = A_m \times C \times \left(J_p - J_{p,f}\right) \tag{10}$$

where $J_{p,f}$ is the average permeate flux at the end of the test.

According to Carbonell-Alcaina et al. (2016), who successfully expressed R_{cl} as an exponential function of time and considering the fact that R_{cl} depends on protein mass deposited on the membrane surface, a new general equation that accounts for the protein mass deposition on the membrane surface as a function of time during MF of BM was proposed in this work and was presented as Eq. (11):

$$m_{dep} = m_{dep,ss}[1 - exp(-c \times t)] \tag{11}$$

where $m_{dep,ss}$ is the mass deposited on the membrane surface in the steady-state and c is the rate of protein mass deposit development. The $m_{dep,ss}$ and c can be determined by fitting the m_{dep} values calculated based on Eq. (10) and experimental data to the proposed model.

Substituting Eq. (6), Eq. (7) and Eq. (11) in Eq. (4), the general formula for the RIS model can be obtained (Eq. 12):

$$J_p = \frac{TMP}{\mu \times \left[R_m + \left(R_{ads,ss} + R_{cp,ss}\right) \times [1 - \exp(-b \times t)] + \left(\frac{m_{dep,ss}[1 - \exp(-c \times t)]}{A_m}\right) \times \alpha\right]} \tag{12}$$

3.8. Anaerobic digestion of UF/DF permeates

The parameters applied during AD of dairy wastes (UFPs and DFPs) are presented in the Figure 2.

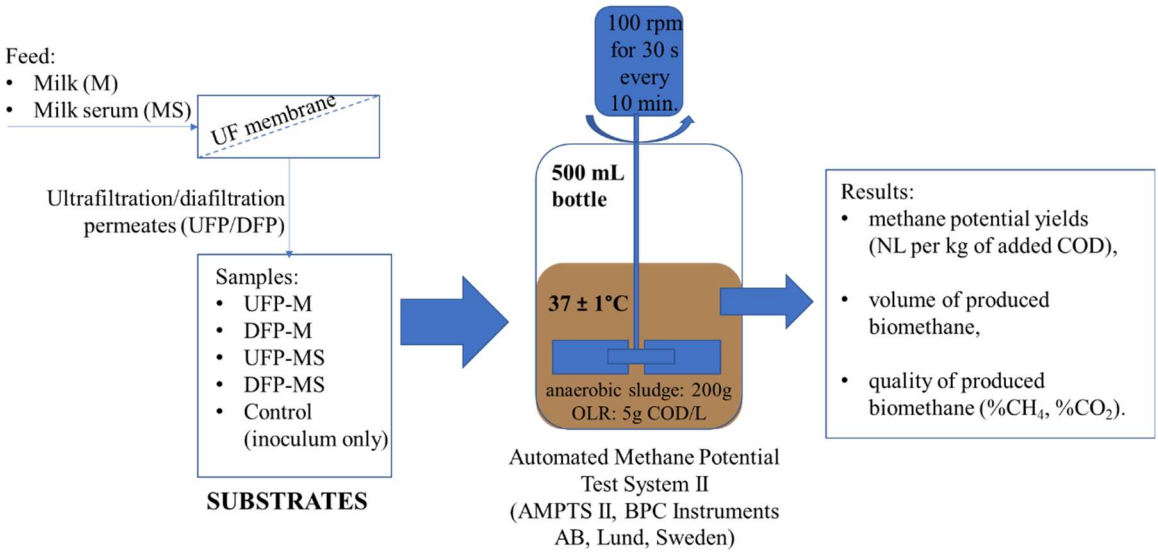


Figure 2. Parameters of anaerobic digestion of UF/DF permeates: OLR – organic load rate, COD – chemical oxygen demand.

The detailed information on AD can be found in publication **P3** (Section 2.3, p. 5-6).

3.9. Analytical methods

The feed materials, retentates, permeates and substrates used in AD were subjected to physicochemical analyses (Table 9).

Table 9. Summary of physicochemical analyses of the feed materials, retentates, permeates and substrates used in AD.

Parameter	Method/equipment	References
pH	pH meter (CP-401, Elmetron, Zabrze, Poland) equipped with an electrode IJ-44C IONODE (Elmetron)	n/a
TS	AOAC International method 990.20; 33.2.4	(AOAC, 2007)
TN	Kjeldahl method (AOAC International method 991.20; 33.2.11)	(AOAC, 2007)
Noncasein nitrogen (NCN)	Kjeldahl method (AOAC International method 998.05; 33.2.64) with modifications according to Wojciechowski and Barbano (2015)	(AOAC, 2007) (Wojciechowski and Barbano, 2015)
Nonprotein nitrogen (NPN)	Kjeldahl method (AOAC International method 991.21; 33.2.12)	(AOAC, 2007)
Fat content	Rose-Gottlieb method	(IDF, 1987a)
Lactic acid content	Calculated based on titratable acidity measurements (1◦SH = 0.0225 lactic acid %)	n/a
Lactose content	Milko-Scan™ FT2 (Foss, Hillerød, Denmark)	n/a
Ash content	The muffle furnace technique at 530°C	(PN-A-86364:1996)

Total calcium content	Atomic absorption spectrometry according to ISO 8070-2007 IDF 119:2007(E) using Thermo Scientific iCE 3000 Series AA Spectrometer (Thermo Fisher Scientific, Franklin, MA, USA) and at the wavelength of 422.7 nm	(ISO/IDF, 2007)
Total phosphorus content	A colorimetric analysis and the absorbance measured using a Carry 60 UV-Vis (Agilent) spectrophotometer at the wavelength of 610 nm	(Żegarska, 2000)
Viscosity	A rotational rheometer (RheolabQC, Anton Paar, Graz, Austria) at a shear rate of 100 s^{-1} and a temperature of 50°C	n/a
Density	An automatic handheld density meter (Densito, Mettler Toledo, Greifensee, Switzerland) with an accuracy of ± 0.001 g/cm^3	n/a
Conductivity	Conductivity benchtop meter (model InoLab Cond Level 1, WTW, Weilheim, Germany) equipped with conductivity cell TetraCon 325 (WTW)	n/a
Particle-size distribution	Dynamic light scattering, using Zetasizer NanoS (model ZEN1600, Malvern Instrument Ltd., UK)	Dybowska (2011)
VS	A gravimetric method	EPA-821-R-01-015
COD	The aid of cuvette test LCK 914 (HACH LANGE GmbH, Berlin, Germany)	n/a
The composition and percentage of individual components of the biogas outflow (CH_4, CO_2)	A gas chromatograph (GC, 7890A Agilent, Santa Clara, CA, USA) equipped with a thermoconductometric detector (TCD)	Rokicka et al. (2021)

n/a – not applicable

3.10. SDS-PAGE electrophoresis

To identify proteins present in filtration streams and proteins attached to the membrane surface and pore walls contributing to external and internal fouling, respectively, an SDS-PAGE electrophoresis on 12% polyacrylamide gel (Biorad Laboratories, Warsaw, Poland) was used. The fresh samples of BM, MF retentate, MF permeate, SW, AW-T and permeates obtained after UF of whey were diluted with a sample buffer (pH 6.8, 10 mM TrisHCl, 1.0% SDS, 20% glycerol, 0.02% bromophenol blue tracking dye, and 50 mM dithiothreitol), then immersed in boiling water for 3 min and kept frozen (-26 °C) in plastic vials (Eppendorf microtubes, 3810X; Merc, Darmstadt, Germany) until analysis. Due to the small TS content (data not shown), samples of Fe and Fi (20 g each) were first frozen at -26°C, lyophilized for 72 h at 0.18 bar (Freeze dryer Alpha 1e2 LD, Christ, Germany), then diluted with 100 µL of sample buffer, immersed in boiling water for 3 min and kept frozen (-26°C). Before the analysis, all samples were thawed at room temperature, and the wells were then loaded with 22.4 µg protein per loading for BM, MF retentate and MF permeate, 13.6 µg protein per loading in case of whey and permeates obtained after UF of whey, and with 10 µL of F_e and F_i sample per loading. In addition, 4 µL of an SDS-PAGE molecular mass standard (Dual Xtra Standard, Bio-Rad) was applied to one well. Running, staining and destaining procedures were performed according to Verdi, Barbano, Dellavalle, and Senyk (1987). The destained gels were scanned using a Lumi Bis Bioimaging Systems DNR scanner (Jerusalem, Israel) and analysed using TotalLab 1D v 11.3 (Newcastle, UK).

3.11. Kinetic analysis of methane production

According to the approach reported by Llabres-Luengo and Mata-Alvarez (1987), a nonlinear regression was used to obtain the rate constants of methane production from plots of volume of methane per mass of COD_{added} versus time.

3.12. Energetic calculation

The calculations of the energy potential of substrates (UFP-M, DFP-M, UFP-MS, and DFP-MS) were based on the conducted fermentation tests and methodology described by Cieślik et al. (2016) and Kozłowski et al. (2019). The amount of electricity and heat produced from combined heat and power (CHP) unit were estimated for the unit offered by PAKTOMA (Łódź, Poland), a Polish manufacturer of modern co-generation units for biogas plants. For the purpose of the calculation of the amount of produced electric energy, the efficiency of 43% was assumed for the unit offered by PAKTOMA. In the case of the calculation of the amount of produced heat, the efficiency of 45% was assumed for the unit offered by the same company.

The detailed information on energetic calculations can be found in publication **P3** (Section 2.5, p. 6).

3.13. Statistical analysis

The statistical analysis was performed using the Statistica software (version 13.1, 1984-2016, StatSoft, Inc., Tulsa, K, USA). The one way ANOVA ($P < 0.05$) followed by Tukey's post hoc test was performed. The Person's correlation coefficient was determined at $P < 0.05$. The RIS model was fitted to the experimental data using Microsoft Excel's add-in Solver and LabPlot software (LabPlot Team, 2022). The non-linear least-squares minimization was performed to minimize the difference between the experimental and predicted data. The fitting accuracy was evaluated using the regression coefficient (R^2) and the standard deviation (SD).

4. Publications

This thesis is a collection of three scientific publications published in international peer-reviewed journals:

P1. Tarapata, J., Dybowska, B.E., Zulewska, J. 2022. Evaluation of fouling during ultrafiltration process of acid and sweet whey. *Journal of Food Engineering,* 328, 111059. https://doi.org/10.1016/j.jfoodeng.2022.111059.
IF = 6.203; MEiN 2021 = 140 points

Author contributions
Justyna Tarapata: Conceptualization, Methodology, Investigation, Visualization, , Data curation, Resources, Writing – original draft. Estimated percentage contribution: 70%.
Brygida E. Dybowska: Methodology, Investigation. Estimated percentage contribution: 10%.
Justyna Żulewska: Conceptualization, Methodology, Funding acquisition, Project administration, Writing – review & editing, Supervision. Estimated percentage contribution: 20%.

P2. Tarapata, J., Maciejczyk, M., Zulewska, J. 2022. Microfiltration of buttermilk: Partitioning of proteins and modelling using a resistance-in-series model. *International Dairy Journal,* 134, 105445. https://doi.org/10.1016/j.idairyj.2022.105445.
IF = 3.572; MEiN 2021 = 100 points

Author contributions
Justyna Tarapata: Conceptualization, Methodology, Investigation, Modelling of fouling, Visualization, Resources, Data curation, Writing - original draft. Estimated percentage contribution: 75%.
Maciej Maciejczyk: Modelling of cake layer formation. Estimated percentage contribution: 5%.
Justyna Żulewska: Conceptualization, Methodology, Funding acquisition, Project administration, Writing - review & editing, Supervision. Estimated percentage contribution: 20%.

P3. Tarapata, J., Zieliński, M., Zulewska, J. 2022. Valorization of Dairy By-Products: Efficiency of Energy Production from Biogas Obtained in Anaerobic Digestion of Ultrafiltration Permeates. *Energies*, 15, 6829. https://doi.org/10.3390/en15186829.
IF = 3.252; MEiN 2021 = 140 points

Author contributions

Justyna Tarapata: Conceptualization, Methodology, Formal Analysis, Investigation, Writing – review & editing, Data curation, Writing – original draft, Visualization. Estimated percentage contribution: 70 %.

Marcin Zieliński: Conceptualization, Methodology, Writing – review & editing, Validation, Data curation, Supervision, Resources, Funding acquisition. Estimated percentage contribution: 20 %.

Justyna Żulewska: Conceptualization, Methodology, Writing—review & editing, Validation, Data curation, Supervision, Resources, Funding acquisition. Estimated percentage contribution: 10 %.

THE SUM OF MEiN 2021 POINTS: 380

TOTAL IF: 13.027

5. Research results in the thematically related series of publications

5.1. Fouling mechanisms that affect ceramic ultrafiltration membranes using acid whey in comparison with sweet whey

The fouling mechanisms that affect ceramic UF membranes using AW-T in comparison with SW was studied and the results are presented in the publication **P1**. In contrast to previously conducted research (Corbatón-Báguena et al., 2018; Konrad et al., 2012b; Luján-Facundo et al., 2017), the whey subjected to UF in this study was obtained from cheesemaking process instead of using model solutions, thus omitting the potential influence of processing on protein properties and hence protein-protein, protein-membrane interactions. Based on the physicochemical analysis of external and internal foulant streams as well as a mathematical modelling of the process using RIS model, a thorough investigation of the flux decline was carried out.

There were some similarities observed in the flux vs time curve plotted for AW-T and SW at the very beginning of the processing (Fig. 1, **P1**, p. 4). The flux rates for each feed material declined sharply after starting the UF. This phenomenon is related to the membrane fouling and suggests that the maximum fouling occurred once the membrane was exposed to whey flow at the start of the process. Similar results concerning milk filtration have been reported previously (Zulewska et al., 2018; Zulewska & Barbano, 2013). In the current study, after rapid decrease in flux at the start of UF, further substantial decline was observed in the case of AW-T. Whereas, in the case of SW, the plateau value of flux was reached after that rapid decline.

The average (n=3) measured flux was 2.51×10^{-5} m^3/m^2s and 1.60×10^{-5} m^3/m^2s for AW-T and SW, respectively (Table 1, **P1**, p. 4). While comparing observed permeate flux values with calculated limiting (2.62×10^{-5} m^3/m^2s) and critical flux (1.75×10^{-5} m^3/m^2s) values, it can be stated that all UF processes were conducted under limiting flux conditions, thus formation of highly irreversible fouling was prevented. Flux for AW-T was higher than the critical value indicating continuous formation of the fouling layer causing subsequent increase in the hydraulic resistance, which was in agreement with the course of the curve plotted for the total resistance vs time. According to Diagne et al. (2013), the critical flux is the flux below which the fouling is fully reversible, whereas above the critical value irreversible fouling starts to occur. It proves that during UF

of AW-T conducted in this experiment the irreversible deposition of material occurred. The permeation during UF of SW was lower than the critical flux suggesting that fouling was fully reversible. However, it is worth noting, that the critical flux value was compared with an average value of flux observed throughout the processing time. The initial flux for SW was much higher than the critical value (2.09×10^{-5} m^3/m^2s vs 1.75×10^{-5} m^3/m^2s), causing irreversible fouling layer formation. This layer had formed after 30 min of UF resulting in increase in total resistance leading to plateau value of flux of approx. 1.57×10^{-5} m^3/m^2s (close to the average value of 1.60×10^{-5} m^3/m^2s) that remained constant till the end of processing, confirming reversible fouling (i.e. concentration polarization with adsorption fouling) occurring after formation of irreversible layer.

To get better insight into the type of fouling dominating during UF of whey, the time profile of the hydraulic resistances included in RIS model was developed (Fig. 8, **P1**, p. 9). It has been revealed that, the fouling related to the adsorption of particles on the membrane surface and inside the pores as well as concentration polarization (R_{ads}+R_{cp}) occurred at the very beginning of processing and therefore these are main mechanisms responsible for the sharp decrease in permeate flux at the start of UF process. Similar observations were previously reported by Juang et al. (2010) and Villeneuve et al. (2021). Moreover, resistances R_{ads}+ R_{cp} were predominant over the entire processing time regardless the whey type tested. The total hydraulic resistance during UF of SW and AW-T increased in time because of gradual accumulation of the cake layer. There was an initial period of rapid protein adsorption on the membrane surface followed by a gradual growth of resistance until constant value of R_{cl} was reached. The obtained time profile of cake layer formation for AW-T indicated that cake layer was formed slower than in case of SW, which was reflected in the profile of flux vs time curve. At the end of AW-T ultrafiltration, resistance reflecting cake formation (R_{cl}) was almost equal to that caused by adsorption and concentration polarization (R_{ads}+R_{cp}).

The $R_{ads,ss}$+$R_{cp,ss}$ value noted for AW-T (10.053×10^{12} m^{-1}; 0.27% true protein in feed and 0.42% in retentate) was smaller than for SW (17.445×10^{12} m^{-1}; 0.67% true protein in feed and 0.92% in retentate) (Table 2, **P1**, p. 4; Table 4, **P1**, p. 5; Table 5, **P1**, p. 8). These data are in agreement with literature data (Carić et al., 2000), stating that fouling resistance caused by protein adsorption increases as protein concentration increases. According to Cheryan (1986) and Baldasso et al. (2011) the more concentrated the solution of protein the lower the permeate fluxes. It results from the higher osmotic

pressure and the greater accumulation of solute molecules in the polarized layer increasing its thickness and thus its resistance to filtration. The $R_{cl,ss}$ and the determined specific cake resistance coefficient α were higher during SW processing (7.132×10^{12} m^{-1} and 12.859×10^{13} m/kg, respectively) than during AW-T processing (7.033×10^{12} m^{-1} and 8.852×10^{13} m/kg, respectively) (Table 5, **P1**, p. 8). It can be observed that the values of parameter α increased as the size of the molecules in the feed decreased (approx. 245 nm for AW-T and 208 nm for SW). Similar relation was reported previously by Salinas-Rodriguez et al. (2015) and Corbatón-Báguena (2018). The RIS model fitted the experimental data with high accuracy in terms of R^2 (0.979 and 0.994 for AW-T and SW, respectively) and SD (0.003 and 0.007 for AW-T and SW, respectively) (Table 5, **P1**, p. 8).

In summary, the knowledge generated in this study advances the understanding of fouling in UF of polydisperse systems like Tvarog acid whey in which diffusive transport is complex and not yet fully understood. The RIS model, tested in this work, based on cake formation, concentration polarization and adsorption mechanisms, fitted the experimental data with high accuracy in terms of the regression coefficient and standard deviation. Thus, it can be concluded that this model is appropriate to describe the evolution of permeate flux during UF (with 20 nm ceramic membranes, at TMP of 3 bar, crossflow velocity of 4.1 m/s) of acid and sweet whey obtained after cheese manufacture.

5.2. Microfiltration of buttermilk: efficacy of serum protein fractionation and fouling mechanisms

The MF process of BM (using ceramic GP membranes) was examined in terms of the efficacy of serum proteins fractionation and fouling mechanisms that affect membrane performance and the results are presented in the publication **P2**. The RIS model was fitted to experimental data. An evolution of model parameters in filtration time was determined, and the predominance of each fouling resistance as a function of time was investigated. Moreover, exponential time dependence was proposed to describe changes in protein mass deposited on the membrane surface during MF.

The efficiency of serum protein fractionation in MF of BM was assessed by the evaluation of protein profile with SDS-PAGE electrophoresis. Caseins and MFGM proteins were main components retained by the membrane in the retentate stream

(Fig. 7, **P2**, p. 8). The relative ratio of β-LG to α-LA assessed with densitometry analysis was 71:29 in feed, 81:19 in retentate and 40:60 in permeate. Based on this results, it was stated that the selective transmission of α-LA to permeate stream occurred. This phenomenon can be explained with the observations described in previous research. According to Harland, Coulter, & Jenness (1952) and Zulewska et al. (2018), thermal processing of milk proteins may cause the denaturation of serum proteins and the formation of intermolecular disulfide bonds between β-LG and κ-casein. Since, cream used in this study was subjected to high heat treatment before butter making process, some part of β-LG could remain in the retentate stream due to the interactions described above. However, the yield of serum proteins in the permeate stream, only 27% of SP in the feed actually partitioned to the permeate, was low. It indicated the low feasibility of fractionation process. Densitometry analysis of the gels also revealed almost unchanged ratio of MFGM proteins to caseins when comparing BM with obtained retentate (13:87 vs 15:85). The presence of skim milk solids in BM, especially casein micelles, restricts the concentration of MFGM, as the MFGM particles and casein micelles are comparable in size (Oliveira et al., 2020). The study by Morin et al. (2004) showed that MF alone cannot achieve optimal separation of lipids and proteins for the production of novel ingredients from BM.

The calculated fouling coefficient (*Fc*) was 0.88 ± 0.01, indicating severe fouling of the ceramic membrane used. The RIS model was fitted to the experimental data to get some insight into the fouling mechanism governing MF of BM. As the R_{cl} can be expressed as an exponential function of time (Carbonell-Alcaina et al., 2016) and depends on protein mass deposited on the membrane surface, a new general equation that accounts for the protein mass deposition on the membrane surface as a function of time was proposed in this work (Eq. 11 explained in detail in Section 3.7):

$$m_{dep} = m_{dep,ss}[1 - exp(-c \times t)] \quad (11)$$

After fitting Eq.11 to experimental data, the noticeable disturbance of exponential growth of the deposited mass in the approximate time interval 1 - 4 h during MF of BM was observed (Fig. 4, **P2**, p.6). It should be noted that the investigated process was affected by the change of processing conditions from feed and bleed mode to recirculation mode, which generated that deviation. Therefore, an analytical polynomial correction

of the fitted function which models this effect was proposed and fitted to the experimental data (Eq. 13):

$$m_{dep}(t) = m_{dep,ss}[1 - g(t) \times exp(-c \times t)] \quad (13)$$

where $g(t) = d \times t^2 + e \times t + f$ is the polynomial correction of the exponential growth. The corrected equation (Eq. 13) more accurately fitted the experimental data in terms of $R^2 = 0.99$ compared to 0.93 obtained for Eq. 11.

It should be noted that the time-dependence of this process does not depend only on parameter c (a time constant which describes the speed of the cake formation) in the corrected model but also on d, e and f parameters. Therefore, further research is needed to gain insight into the definition and interpretation of additional parameters.

Since the $R_{cl,ss}$ obtained in this study was greater than $R_{ads,ss} + R_{cp,ss}$ (3×10^{13} versus 8×10^{12} m^{-1}) (Table 4, **P2**, p.7), the cake formation mechanism dominated at the steady-state for the operating parameters applied. It can be observed that at the beginning of the MF process, the dominant resistance was due to adsorption (either on the surface or on the pore walls of the membrane) and concentration polarization (Fig. 5, **P2**, p. 7). The change in the dominant fouling mechanism from adsorption and concentration polarization to the cake layer formation was noted in this experiment after less than 1 h of the MF process.

To the best of the author's knowledge, there is limited number of studies considering the RIS model that accounts for the time evolution of the fouling resistances during membrane filtration of liquid dairy products. Recently, Corbatón-Báguena (2018) reported on the fitting accuracy of the RIS model to the permeation resistance noted during UF of whey model solutions. Based on that research, some similarities between the UF of whey model solutions performed with 15 kDa ceramic membrane and the MF process performed in the current study can be identified. During the UF of WPC solution (44.4 g/L), the resistance due to cake formation increased over the entire UF time, being predominant at the end of the filtration process (Corbatón-Báguena, 2018). Moreover, the parameter $R_{cl,ss}$ (characterizing the resistance due to the cake layer at the steady-state in the UF process of WPC solutions) was similar to that obtained during the filtration of BM in the current study (~3×10^{13} m^{-1}). However, the structure of this layer would differ significantly due to the different protein compositions of tested feeds.

In summary, this study demonstrates that the RIS model accounting for the time evolution of the fouling resistances during MF of BM accurately fit the experimental data in terms of high R^2 and low SD. The resistance due to adsorption and concentration polarization was predominant during the first minutes of operation as it sharply increased with time. However, the resistance due to the cake formation increased over the entire microfiltration time, being predominant at the latter stages of the filtration process. It was observed that the cake layer was mainly composed of casein and high molecular weight serum proteins. Apart from cake layer formation, casein was also involved in the pore-blocking mechanism. The results showed that applied processing parameters (GP ceramic membranes, pore size of 0.1μm, TMP of 2 bar, crossflow velocity of 6.3 m/s) enabled selective partitioning of α-LA, resulting in transmission of this protein to the permeate stream. Nevertheless, further studies on optimized MF conditions enhancing the efficiency of the fractionation process should be performed.

5.3. Identification of major foulants reducing efficiency of filtration processes

The identification of major foulants reducing the membrane performance during UF of whey and MF of BM was performed and the results are presented in the publications **P1** and **P2**.

In the case of whey UF (**P1**), external foulants consisted of all major WPs as showed by the results of SDS-PAGE electrophoresis (Fig. 3, **P1**, p. 6). β-LG and α-LA did appear to be the major cause of pore blocking. Dynamic light scattering analysis of particle-size distribution showed multimodal size distribution in permeate streams shifted towards smaller particle sizes in contrast to unimodal (SW) and bimodal (AW-T) particle size distribution in feed (Fig. 5, **P1**, p. 7). It suggests that the shear stress during processing caused breakdown of aggregates, enhancing transmission of smaller particles (α-LA and β-LG) to the permeate stream and thus its adsorption inside the pores. Higher Ca content in AW-T in comparison with SW (1180 mg/L vs 366 mg/L, respectively) contributed to significantly higher Ca content in stream containing internal foulants (3.7 mg/L vs 2.2 mg/L) (Fig. 6, **P1**, p. 8). According to Steinhauer et al. (2016) the presence of salt ions has a major impact on protein interaction forces and at higher ion concentrations the deposition probability is higher because of reduced particle repulsions. This may explain why flux decline noted during UF of SW (26%) was significantly lower ($P < 0.05$) than for AW-T (37%) (Table1, **P1**, p. 4). In addition,

the postrun CWF measured in this experiment after cleaning the fouled membrane was close to prerun CWF, so the fouling layer was chemically removed which means it was reversible fouling.

Concerning MF of BM (**P2**), casein was the major protein responsible for both pore blocking and cake layer formation as revealed by the results of SDS-PAGE electrophoresis of the foulants (Fig. 3, **P2**, p. 6). However, apart from casein, the cake layer was also composed of high molecular mass serum proteins (i.e., lactoferrin). According to Morin et al. (2007), casein accumulates at the surface of the membrane, creating a porous layer that limits permeation. Therefore, it can be stated that during the MF process of BM, the flux is mainly controlled by the adsorption of casein to the pore walls and the formation of a cake layer composed of casein and high molecular mass WPs. Additionally, based on similar prerun and postrun CWF values, it can be stated that water flux was restored after the cleaning procedure, indicating a reversible form of fouling occurred in this experiment.

The phenomenon of fouling occurring during the filtration of various raw materials (containing only WPs (whey) or a mixture of WPs and casein (BM)) was compared based on the results described in publications **P1** and **P2**. In general, the mechanism of cake layer formation dominated during MF of BM in contrast to UF of whey, when the decrease in membrane performance was caused mainly by adsorption and concentration polarization (Fig. 8, **P1**, p. 9 & Fig. 5, **P2**, p. 7). It can be stated that the casein content determines the type of fouling mechanism occurring during membrane filtration. Its presence induces formation of cake layer.

5.4. The relationship between the degree of lactose recovery in UF/DF permeates and the amount of biogas obtained in anaerobic digestion

The possibility of valorization of permeates generated during DF processes by using them in biogas production and comparing their effects with typical UF permeates was assessed in publication **P3**. The raw material subjected to UF/DF processes were milk and milk serum (permeate obtained after the MF of milk during concentration of casein micelles) (Fig.2, **P3**, p. 4). Attempts were made to estimate the relationship between the degree of lactose recovery and the amount of biogas obtained.

The permeates obtained in the UF and DF stages, during either the milk or milk serum filtration, contained mostly water and a very low amount of solids (5.6% TS in UFP-M,

1.81% TS in DFP-M, 3.8% TS in UFP-MS and 0.86% TS in DFP-M) (Table 2, **P3**, p. 7). The respective streams obtained either during UF (UFP-M vs. UFP-MS) or DF (DFP-M vs. DFP-MS) were characterized by higher TS content when milk was subjected to filtration in comparison with milk serum.

The waste load equivalents of TS constituents are: 1 kg of fat, which contributes to 3 kg of COD; 1 kg of protein, which contributes to 1.36 kg of COD; and 1 kg of lactose, which contributes to 1.13 kg of COD (Ahmad et al., 2019; Bella & Rao, 2021). According to Barbano et al. (1988), the permeates generated after the UF/DF process in the dairy industry contribute to a high COD as they are rich in lactose. Lactose contributes around 90% of the COD (Bella & Rao, 2021). The lactose content measured in substrates tested in the current work was as follows: 4.97% in UFP-M, 1.59% in DFP-M, 3.37% in UFP-MS and 0.76% in DFP-MS (Table 2, **P3**, p. 7). As confirmed by the Pearson's correlation coefficient (r = 1), the lactose content determined the COD of tested wastes (Table 3, **P3**, p. 8).

High COD values indicate that the dairy wastes produced are strong and fluctuating types (Bella & Rao, 2021). The COD of the permeates, coming from UF process conducted in this study, were 38,600 and 57,020 mg O_2/L for UFP-MS and UFP-M, respectively (Table 2, **P3**, p. 7). Whereas the COD values of the permeates obtained during the DF stage were equal to 7610 and 19,150 mg O_2/L for DFP-MS and DFP-M, respectively.

The methane potential of the UF/DF permeates ranged from 149 to 181 NL CH_4 per kg of added COD (Table 4, **P3**, p. 8). When the volume of the substrate characterized by higher COD value was analyzed, higher biogas volume was observed. However, there were no significant ($P > 0.05$) differences detected between the methane yields noted at the end of the experiment calculated as NL per kg of added COD for four tested waste samples. The experimental methane yield was fitted to the first order regression with high accuracy ($R^2 > 0.87$). The reaction rates were similar for four substrates tested as there were no significant differences noted between calculated kinetic constant k. It ranged from 0.29/day for DFP-MS to 0.37/day for UFP-M and DFP-M (Table 4, **P3**, p.8). The results of kinetic analysis were in agreement with the results of methane yield. As coefficients of methane production expressed in NL per kg of added COD were similar for all tested samples, the kinetic of methane production was also comparable. The methane content in the biogas did not differ significantly ($P > 0.05$) among the four tested samples and reached about 69%. The amount of CO_2 reached 31% (Table 5, **P3**, p. 9).

The quality of obtained biogas indicated that all samples subjected to AD were equally good substrates for biomethane production.

The efficiency of biomethane production from dairy waste varies across literature data and depends on the applied parameters and substrates. For example, Fernández et al. (2015), reported a yield of 314 L CH_4/kg COD_{added} during single stage AD of whey under thermophilic conditions, with an OLR up to 1.5 kg O_2/m^3day. In another study by Kisielewska et al.(2014), the digestion of a solution of dried ultrafiltrated whey permeate in a mesophilic system (UASB methanogenic reactor; 35 °C) at OLR rates from 4.6 to 6.9 kg COD/m^3 was tested. The obtained methane yield reached about 120 L CH_4/kg COD_{added}.

The kinetic constant obtained in this experiment was comparable with the kinetic constants reported in the literature for dairy liquid wastes such as cheese whey (with a hydrolysis constant k between 0.36–0.55/day; a COD of substrates between 50,000–78,000 mg/L; an inoculum/substrate ratio of 6; and a temp. of 35°C) (Mainardis et al., 2019). The results obtained in this experiment indicated that majority of components present in tested permeates were easily biodegradable by the biomass used.

In summary, lactose content was highly correlated with the COD value of tested substrates. Analyzed biochemical methane potential for DFPs and UFPs showed similar values of methane production yield. Calculation per kg of COD added indicates a lack of significant differences. Anaerobic co-digestion can overcome most of the limitations of anaerobic mono-digestion by producing more CH_4 due to the synergy of the substrates and the supplementation of the missing nutrients by the co-substrates (Bolen et al., 2022; Mata-Alvarez et al., 2014). Comino et al. (2012) indicated that the co-digestion of a high volume of whey (up to 65% in volume) and cattle slurry is possible without the use of chemicals for pH correction, and additionally this kind of mix has a similar energetic potential for an AD as energy crops such as maize.

5.5. The use of UF/DF permeates to produce electricity and heat from the biomethane generated in the process of anaerobic digestion: the case study considering large-scale dairy plant

The potential heat and electric energy production from biogas obtained in AD of UF/DF permeates acquired in the amounts comparable with that generated during protein concentration in a large-scale dairy plant was described in publication **P3**. Permeates yield were estimated based on the raw milk and whey throughput and processing using membrane technology. The assumption was that the dairy plant process daily about 1200 t of raw milk, which is solely dedicated for the production of milk concentrates and 800 t of whey. Considering the amount of raw material processed in the analyzed dairy plant, the membrane filtration processes applied in valorization of milk and whey would generate about 864 t of permeate per stage of filtration in the case of milk and 706 t of permeate per stage of filtration in the case of whey. Additionally, the daily large-scale dairy plant demand for electric power was estimated at 11 MWh/day.

The maximum generated electric power was estimated at 10,632 MWh/a for UFP-M and a minimum of 1374 MWh/a for DFP-MS (Table 6, **P3**, p. 11). In general, the higher the COD of the substrates, the higher the electric power produced and thus the higher profitability of the biogas plant. In the work by Kozłowski et al. (2019), the energy data from a dairy factory, producing 400 t of whey per day (two times lower than in the case of the dairy plant considered in this case study), were reported: they claimed a biomethane yield of 3,508,487 m^3 per annum, which is a significantly greater amount than the summarized methane yield (2,167,430 m^3/a) noted for UF/DF permeates (UFP-MS and DFP-MS) generated after milk serum filtration conducted in this study. It is also important to highlight that in the research conducted by Kozłowski et al. (2019), whey was used as a fermentation substrate, and its amount was almost half of that of UFP-MS. Whey contains more COD than UF/DF permeate, which is why the amount of biogas generated is expected to be higher than that from milk serum permeates. Therefore, in the future research, the co-digestion of UF/DF permeates in combination with other wastes should also be considered.

As calculated, the dairy plant can generate approximately 23,000 MWh/a of electricity and about 85,500 GJ of heat on an annual basis while using all the generated permeates considered in this study (Table 6, **P3**, p. 11). The total electric energy output

value corresponds to approximately 2.8 MW of the gross nominal capacity, which not only covers the annual demand of the whole factory (0.5 MW, calculated based on the daily demand of 11 MWh/d) but also enables the sale of remaining energy. It is assumed that a 3 MW biogas plant is capable of generating 24,000 MWh per year of electric power (Kozłowski et al., 2019), which means that in the analyzed case there is still an approx. 4% power reserve for a potential increase in waste processing.

Additionally, apart from serving as potential substrates for AD, the analyzed UF/DF permeates may also be considered a profitable source material for lactose production. In purely financial terms, food-grade lactose production exceeds the profitability of biogas production in the on-site biogas plant (19.7 mln EUR/a vs 2.9 mln EUR/a) (Table 6, **P3**, p. 12). However, other aspects such as the renewable energy demand and the geopolitical situation should also be considered by the plant owners. It is worth noting that one of the current objectives of the Bioeconomy Strategy for the EU is a reduction in energy dependence on non-renewable and unsustainable sources (European Commission, 2018).

In summary, the UF/DF permeates are efficient substrates in biomethane production through the AD. The amount of biomethane generated is enough to cover the total heat and electric power requirements of a large-scale dairy factory that reuses its own effluents.

6. Summary and conclusions

In summary, the results presented in the thematically related series of published papers, constituting a doctoral dissertation entitled "***Fractionation of milk components and valorization of by-products obtained with membrane filtration of dairy streams***", are of a cognitive nature. They provide new information in the subject of fouling mechanism occurring during membrane filtration and in the field of environmental science focused on disposal of dairy wastes. The causes of flux decline during UF and MF of dairy by-products i.e., whey and BM were discussed. The explanation of fouling mechanism was provided by fitting the experimental data to the RIS model. Additionally, considering the need to increase the circularity of dairy by-products, the utilization of UF/DF permeates in AD was studied.

Novelty of the study:

1. A time-based evolution of RIS model parameters was determined for the first time, when filtering dairy streams obtained at industrial scale.
2. A general equation that accounts for the time-based changes in the mass deposited on the membrane surface during MF of BM (an exponential function and its polynomial correction) was newly proposed.
3. It has been shown that it is possible to fractionate α-LA when the process of MF is applied to BM, which has undergone extensive heat treatment.
4. The assessment of the possibility of valorizing the permeates generated during DF by using them in biogas production and comparing their effects with typical UF was a new approach in studies on AD.
5. This research has shown that the amount of permeate generated by large-scale dairy factory can be enough to meet its demand for electric power and heat.

Taking into account recent achievements, it should be emphasized that besides previously mentioned further exploration of buttermilk microfiltration as an efficient way in fractionation of serum proteins, further research is also required in the field of AD of UF/DF permeates. Anaerobic co-digestion seems to be another stage of optimization of biomethane production from this kind of dairy effluents. It should be of a great importance since the availability of permeate is very high due to growing production in the dairy sector.

The research carried out allowed to verify research hypotheses:

1. Resistance-in series model is an accurate model to describe flux decline during UF of whey and MF of BM generated in industrial or pilot scale.
2. Microfiltration (GP ceramic membranes, pore size of 0.1μm, TMP of 2 bar, crossflow velocity of 6.3 m/s) of thermally processed BM results in enhanced transmission of α-LA to permeate stream in comparison with enhanced retention of β-LG in retentate stream.
3. The higher the lactose content in permeate the more efficient CH_4 production can be achieved per volume unit. Unit coefficients of methane production calculated as volume of methane per kg of COD added were similar in all tested types of permeates indicating that DFPs can be equally good substrates in AD as UFPs.
4. Ultrafiltration/diafiltration permeates can be efficient substrates in biomethane production through AD.

Based on the research carried out the following conclusions were drawn:

1. The RIS model allows to describe the evolution of permeate flux during UF of acid and sweet whey obtained after cheesemaking when the process is carried out with 20 nm ceramic membranes, at TMP of 3 bar, and crossflow velocity of 4.1 m/s.
2. The RIS model accurately describes the evolution of permeate flux during MF of BM when the process is carried out with 0.1 μm ceramic membranes, at TMP of 2 bar, and crossflow velocity of 6.3 m/s.
3. Polynomial correction of function describing mass deposited on the membrane surface during MF of BM enables accurate (R^2 = 0.99) prediction of cake layer formation.
4. The adsorption and concentration polarization were predominant fouling mechanisms during UF of acid and sweet whey.
5. The major WPs (β-LG and α-LA) are adsorbed on the membrane surface and/or the pore walls during UF of whey.
6. The adsorption and concentration polarization cause sudden permeate flux decline at the early stages of MF of BM and cake layer formation dominates at the latter stages of processing.

7. Microfiltration of BM is mainly restricted by cake layer composed of casein and high molecular weight serum proteins.
8. The mechanism of fouling is determined by the composition of feed. When whey proteins are main components of dairy streams the adsorption and concentration polarization resistance dominates during membrane filtration. When casein is main protein fraction the membrane performance is mainly restricted by cake layer formation.
9. Lactose content is highly correlated with the COD value of UF/DF permeates.
10. Unit coefficients of methane production, which correspond to kg od added COD, were similar in all tested types of permeates, however, higher amounts of DFPs (characterized by lower COD values than UFPs) in comparison to UFPs are required to obtain the same methane volume during AD.
11. The amount of UF/DF permeate generated by large-scale dairy factory may enable the production of biomethane that can serve as a source for heat and electric power generation covering the factory demand for energy.

7. References

1. Aghajani, M., Rahimpour, A., Amani, H., & Taherzadeh, M. J. (2018). Rhamnolipid as new bio-agent for cleaning of ultrafiltration membrane fouled by whey. *Engineering in Life Sciences*, *18*(5), 272–280. https://doi.org/10.1002/elsc.201700070.
2. Ahmad, T., Aadil, R. M., Ahmed, H., Rahman, U. ur, Soares, B. C. V., Souza, S. L. Q., Pimentel, T. C., Scudino, H., Guimarães, J. T., Esmerino, E. A., Freitas, M. Q., Almada, R. B., Vendramel, S. M. R., Silva, M. C., & Cruz, A. G. (2019). Treatment and utilization of dairy industrial waste: A review. *Trends in Food Science & Technology*, *88*, 361–372. https://doi.org/10.1016/J.TIFS.2019.04.003.
3. Ali, A. H. (2019). Current knowledge of buttermilk: Composition, applications in the food industry, nutritional and beneficial health characteristics. *International Journal of Dairy Technology*, *72*(2), 169–182. https://doi.org/10.1111/1471-0307.12572.
4. Al-Mutwalli, S. A., Dilaver, M., & Koseoglu-Imer, D. Y. (2020). Performance evaluation of ceramic membrane on ultrafiltration and diafiltration modes for efficient recovery of whey protein. *Journal of Membrane Science and Research*, *6*(2), 138–146. https://doi.org/10.22079/JMSR.2019.115152.1295.
5. Argenta, A. B., & Scheer, A. D. P. (2020). Membrane Separation Processes Applied to Whey: A Review. *Food Reviews International, 36*(5), pp. 499–528. https://doi.org/10.1080/87559129.2019.1649694.
6. Bacchin, P. (2004). A possible link between critical and limiting flux for colloidal systems: consideration of critical deposit formation along a membrane. *Journal of Membrane Science*, *228*(2), 237–241. https://doi.org/10.1016/J.MEMSCI.2003.10.012.
7. Baldasso, C., Barros, T. C., & Tessaro, I. C. (2011). Concentration and purification of whey proteins by ultrafiltration. *Desalination*, *278*(1–3), 381–386. https://doi.org/10.1016/J.DESAL.2011.05.055.
8. Barbano, D. M., Sciancalepore, V., & Rudan, M. A. (1988). Characterization of Milk Proteins in Ultrafiltration Permeate. *Journal of Dairy Science*, *71*(10), 2655–2657. https://doi.org/10.3168/JDS.S0022-0302(88)79858-6.
9. Barukčić, I., Božanić, R., & Kulozik, U. (2015). Influence of process temperature and microfiltration pre-treatment on flux and fouling intensity during cross-flow

ultrafiltration of sweet whey using ceramic membranes. *International Dairy Journal*, *51*, 1–7. https://doi.org/10.1016/j.idairyj.2015.07.002.

10. Bella, K., & Rao, P. V. (2021). Anaerobic digestion of dairy wastewater: effect of different parameters and co-digestion options—a review. *Biomass Conversion and Biorefinery*, ://doi.org/10.1007/s13399-020-01247-2.
11. Bolen, T. J., Hasan, M., Conway, T., Stéphane Yaméogo, D. D., Sanchez, P., Rahman, A., & Azam, H. (2022). Feasibility assessment of biogas production from the anaerobic co-digestion of cheese whey, grease interceptor waste and pulped food waste for WRRF. *Energy*, *254*, 124144. https://doi.org/10.1016/J.ENERGY.2022.124144.
12. Bolton, G., LaCasse, D., & Kuriyel, R. (2006). Combined models of membrane fouling: Development and application to microfiltration and ultrafiltration of biological fluids. *Journal of Membrane Science*, *277*(1–2), 75–84. https://doi.org/10.1016/J.MEMSCI.2004.12.053.
13. Brans, G., Schroën, C. G. P. H., van der Sman, R. G. M., & Boom, R. M. (2004). Membrane fractionation of milk: State of the art and challenges. *Journal of Membrane Science*, *243*(1–2), 263–272. https://doi.org/10.1016/j.memsci.2004.06.029.
14. Brião, V. B., Seguenka, B., Zanon, C. D., & Milani, A. (2017). Cake formation and the decreased performance of whey ultrafiltration. *Acta Scientiarum. Technology*, *39*(5), 517. https://doi.org/10.4025/actascitechnol.v39i5.27585.
15. Carbonell-Alcaina, C., Corbatón-Báguena, M. J., Álvarez-Blanco, S., Bes-Piá, M. A., Mendoza-Roca, J. A., & Pastor-Alcañiz, L. (2016). Determination of fouling mechanisms in polymeric ultrafiltration membranes using residual brines from table olive storage wastewaters as feed. *Journal of Food Engineering*, *187*, 14–23. https://doi.org/10.1016/j.jfoodeng.2016.04.016.
16. Carić, M. D. X., Milanović, S. D., Krstić, D. M., & Tekić, M. N. (2000). Fouling of inorganic membranes by adsorption of whey proteins. *Journal of Membrane Science*, *165*(1), 83–88. https://doi.org/10.1016/S0376-7388(99)00221-5.
17. Carrere, H., Blaszkow, F., & de Balmann, H. R. (2001). Modelling the clarification of lactic acid fermentation broths by cross-flow microfiltration. *Journal of Membrane Science*, *186*(2), 219–230. https://doi.org/10.1016/S0376-7388(00)00677-3.
18. Chamberland, J., Bouyer, A., Benoit, S., Provault, C., Bérubé, A., Doyen, A., & Pouliot, Y. (2020). Efficiency assessment of water reclamation processes in milk protein concentrate manufacturing plants: A predictive analysis. *Journal of Food Engineering*, *272*, 109811. https://doi.org/10.1016/J.JFOODENG.2019.109811.

19. Chandrapala, J., Gray, S. R., Duke, M. C., Palmer, M., Vasiljevic, T., & Weeks, M. (2016). Strategies for maximizing removal of lactic acid from acid whey – Addressing the un-processability issue. *Separation and Purification Technology*, *172*, 489–497. https://doi.org/10.1016/j.seppur.2016.09.004.
20. Chen, H., & Kim, A. S. (2006). Prediction of permeate flux decline in crossflow membrane filtration of colloidal suspension: a radial basis function neural network approach. *Desalination*, *192*(1–3), 415–428. https://doi.org/10.1016/J.DESAL.2005.07.045.
21. Cheryan, M. (1986). *Ultrafiltration handbook. Technomic Publishing Co. Inc., Lancaster, PA, USA.*
22. Choi, S. W., Yoon, J. Y., Haam, S., Jung, J. K., Kim, J. H., & Kim, W. S. (2000). Modeling of the Permeate Flux during Microfiltration of BSA-Adsorbed Microspheres in a Stirred Cell. *Journal of Colloid and Interface Science*, *228*(2), 270–278. https://doi.org/10.1006/JCIS.2000.6940.
23. Cieślik, M., Dach, J., Lewicki, A., Smurzyńska, A., Janczak, D., Pawlicka-Kaczorowska, J., Boniecki, P., Cyplik, P., Czekała, W., & Jóźwiakowski, K. (2016). Methane fermentation of the maize straw silage under meso- and thermophilic conditions. *Energy*, *115*(Part 2), 1495–1502. https://doi.org/10.1016/J.ENERGY.2016.06.070.
24. Çınar, K. (2022). Membrane Filtration of Milk: Separation and Fractionation of Milk Proteins. *Journal of Innovative Science and Engineering, 6*(1), 61–75. https://doi.org/10.38088/jise.951179.
25. Comino, E., Riggio, V. A., & Rosso, M. (2012). Biogas production by anaerobic co-digestion of cattle slurry and cheese whey. *Bioresource Technology*, *114*, 46–53. https://doi.org/10.1016/J.BIORTECH.2012.02.090.
26. Corbatón-Báguena, M. J., Álvarez-Blanco, S., & Vincent-Vela, M. C. (2018). Evaluation of fouling resistances during the ultrafiltration of whey model solutions. *Journal of Cleaner Production*, *172*, 358–367. https://doi.org/10.1016/j.jclepro.2017.10.149.
27. Corredig, M., & Dalgleish, D. G. (1977). Isolates from Industrial Buttermilk: Emulsifying Properties of Materials Derived from the Milk Fat Globule Membrane. *J. Agric. Food Chem.*, *45*(12), 4595–4600.

28. Corredig, M., Roesch, R. R., & Dalgleish, D. G. (2003). Production of a Novel Ingredient from Buttermilk. *Journal of Dairy Science*, *86*(9), 2744–2750. https://doi.org/10.3168/JDS.S0022-0302(03)73870-3.
29. Damar, I., Cinar, K., & Gulec, H. A. (2020). Concentration of whey proteins by ultrafiltration: Comparative evaluation of process effectiveness based on physicochemical properties of membranes. *International Dairy Journal*, *111,* 104823. https://doi.org/10.1016/j.idairyj.2020.104823.
30. Das, B., Sarkar, S., Sarkar, A., Bhattacharjee, S., & Bhattacharjee, C. (2016). Recovery of whey proteins and lactose from dairy waste: A step towards green waste management. *Process Safety and Environmental Protection*, *101*, 27–33. https://doi.org/10.1016/J.PSEP.2015.05.006.
31. Dewettinck, K., Rombaut, R., Thienpont, N., Le, T. T., Messens, K., & van Camp, J. (2008). Nutritional and technological aspects of milk fat globule membrane material. *International Dairy Journal*, *18*(5), 436–457. https://doi.org/10.1016/J.IDAIRYJ.2007.10.014.
32. Doyen, W., Adriansens, W., Molenberghs, B., & Leysen, R. (1996). A comparison between polysulfone, zirconia and organo-mineral membranes for use in ultrafiltration. *Journal of Membrane Science*, *113*(2), 247–258. https://doi.org/10.1016/0376-7388(95)00124-7.
33. Dreschke, G., Probst, M., Walter, A., Pümpel, T., Walde, J., & Insam, H. (2015). Lactic acid and methane: Improved exploitation of biowaste potential. *Bioresource Technology*, *176*, 47–55. https://doi.org/10.1016/J.BIORTECH.2014.10.136.
34. Durham, R. J. (2009). Modern approaches to lactose production. In M. Corredig (Ed.), *Dairy-Derived Ingredients: Food and Nutraceutical Uses* (pp. 103–144). Woodhead Publishing, Cambridge, UK. https://doi.org/10.1533/9781845697198.1.103.
35. Dybowska, B. E. (2011). Whey protein-stabilized emulsion properties in relation to thermal modification of the continuous phase. *Journal of Food Engineering*, *104*(1), 81–88. https://doi.org/10.1016/j.jfoodeng.2010.11.030.
36. Ergüder, T. H., Tezel, U., Güven, E., & Demirer, G. N. (2001). Anaerobic biotransformation and methane generation potential of cheese whey in batch and UASB reactors. *Waste Management*, *21*(7), 643–650. https://doi.org/10.1016/S0956-053X(00)00114-8.
37. Escalante, H., Castro, L., Amaya, M. P., Jaimes, L., & Jaimes-Estévez, J. (2018). Anaerobic digestion of cheese whey: Energetic and nutritional potential for the dairy

sector in developing countries. *Waste Management*, *71*, 711–718. https://doi.org/10.1016/J.WASMAN.2017.09.026.

38. European Commission. (2018). European Commission Bioeconomy Strategy. A Sustainable Bioeconomy for Europe: Strengthening the Connection between Economy, Society and the Environment; European Commission: Brussels, Belgium, 2018. Available online: https://ec.europa.eu/research/bioeconomy/pdf/ec_bioeconomy_strategy_2018.pdf (accessed on 25th February 2020).
39. FAO. (2017). *OECD-FAO Agricultural Outlook 2017-2026*.
40. Fernández, C., Cuetos, M. J., Martínez, E. J., & Gómez, X. (2015). Thermophilic anaerobic digestion of cheese whey: Coupling H2 and CH4 production. *Biomass and Bioenergy*, *81*, 55–62. https://doi.org/10.1016/J.BIOMBIOE.2015.05.024.
41. Fox, P. F., Guinee, T. P., Cogan, T. M., & McSweeney, P. L. H. (2000). *Fundamentals of Cheese Science. Aspen Publishers Inc., Gaithersburg, USA. https://link.springer.com/content/pdf/10.1007/978-1-4899-7681-9.pdf* (accessed on 20th September 2022).
42. France, T.C., Kelly, A.L., Crowley, S.V., O'Mahony, J.A. 2021. Cold Microfiltration as an Enabler of Sustainable Dairy Protein Ingredient Innovation. *Foods, 10*(9), 2091. https://doi.org/10.3390/foods10092091.
43. Galanakis, C. M., Chasiotis, S., Botsaris, G., & Gekas, V. (2014). Separation and recovery of proteins and sugars from Halloumi cheese whey. *Food Research International*, *65*(Part C), 477–483. https://doi.org/10.1016/J.FOODRES.2014.03.060.
44. González Siso, M. I. (1996). The biotechnological utilization of cheese whey: A review. *Bioresource Technology*, *57*(1), 1–11. https://doi.org/10.1016/0960-8524(96)00036-3.
45. Granato, D., Carocho, M., Barros, L., Zabetakis, I., Mocan, A., Tsoupras, A., Cruz, A. G., & Pimentel, T. C. (2022). Implementation of Sustainable Development Goals in the dairy sector: Perspectives on the use of agro-industrial side-streams to design functional foods. *Trends in Food Science & Technology*, *124*, 128–139. https://doi.org/10.1016/J.TIFS.2022.04.009.
46. Gruskevica, K., & Mezule, L. (2021). Cleaning methods for ceramic ultrafiltration membranes affected by organic fouling. *Membranes*, *11*(2), 131. https://doi.org/10.3390/membranes11020131.
47. Harland, H. A., Coulter, S. T., & Jenness, R. (1952). The Effect of the Various Steps in the Manufacture on the Extent of Serum Protein Denaturation in Nonfat Dry Milk

Solids. *Journal of Dairy Science*, *35*(4), 363–368. https://doi.org/10.3168/JDS.S0022-0302(52)93715-6.

48. Ho, C. C., & Zydney, A. L. (2000). A Combined Pore Blockage and Cake Filtration Model for Protein Fouling during Microfiltration. *Journal of Colloid and Interface Science*, *232*(2), 389–399. https://doi.org/10.1006/JCIS.2000.7231.
49. Juang, R. S., Chen, H. L., & Chen, Y. S. (2008a). Resistance-in-series analysis in cross-flow ultrafiltration of fermentation broths of Bacillus subtilis culture. *Journal of Membrane Science*, *323*(1), 193–200. https://doi.org/10.1016/j.memsci.2008.06.032.
50. Juang, R. S., Chen, H. L., & Chen, Y. S. (2008b). Membrane fouling and resistance analysis in dead-end ultrafiltration of Bacillus subtilis fermentation broths. *Separation and Purification Technology*, *63*(3), 531–538. https://doi.org/10.1016/j.seppur.2008.06.011.
51. Juang, R. S., Lin, S. H., & Peng, L. C. (2010). Flux decline analysis in micellar-enhanced ultrafiltration of synthetic waste solutions for metal removal. *Chemical Engineering Journal*, *161*(1–2), 19–26. https://doi.org/10.1016/J.CEJ.2010.04.007.
52. Kaur, N. (2021). Different treatment techniques of dairy wastewater. *Groundwater for Sustainable Development*, *14*, 100640. https://doi.org/10.1016/J.GSD.2021.100640.
53. Kisielewska, M., Wysocka, I., & Rynkiewicz, M. R. (2014). Continuous biohydrogen and biomethane production from whey permeate in a two-stage fermentation process. *Environmental Progress and Sustainable Energy*, *33*(4), 1411–1418. https://doi.org/10.1002/ep.11890.
54. Konrad, G., Kleinschmidt, T., & Faber, W. (2012a). Ultrafiltration flux of acid whey obtained by lactic acid fermentation. *International Dairy Journal*, *22*(1), 73–77. https://doi.org/10.1016/j.idairyj.2011.08.005.
55. Konrad, G., Kleinschmidt, T., & Faber, W. (2012b). Ultrafiltration flux of acid whey obtained by lactic acid fermentation. *International Dairy Journal*, *22*(1), 73–77. https://doi.org/10.1016/J.IDAIRYJ.2011.08.005.
56. Kozłowski, K., Dach, J., Lewicki, A., Cieślik, M., Czekała, W., & Janczak, D. (2016). ENVIRONMENTAL AND PROCESS PARAMETERS OF METHANE FERMENTATION IN CONTINUOSLY STIRRED TANK REACTOR (CSTR). *Inżynieria Ekologiczna*, *50*, 153–160. https://doi.org/10.12912/23920629/65490.
57. Kozłowski, K., Pietrzykowski, M., Czekała, W., Dach, J., Kowalczyk-Juśko, A., Jóźwiakowski, K., & Brzoski, M. (2019). Energetic and economic analysis of biogas

plant with using the dairy industry waste. *Energy*, *183*, 1023–1031. https://doi.org/10.1016/j.energy.2019.06.179.

58. Labatut, R. A., Angenent, L. T., & Scott, N. R. (2011). Biochemical methane potential and biodegradability of complex organic substrates. *Bioresource Technology*, *102*(3), 2255–2264. https://doi.org/10.1016/J.BIORTECH.2010.10.035.
59. Labbez, C., Fievet, P., Szymczyk, A., Vidonne, A., Foissy, A., & Pagetti, J. (2002). Analysis of the salt retention of a titania membrane using the "DSPM" model: effect of pH, salt concentration and nature. *Journal of Membrane Science*, *208*(1–2), 315–329. https://doi.org/10.1016/S0376-7388(02)00310-1.
60. Lee, Y., Koros, W.J. (2003). Membranes, Synthetic, Applications. In: R.A. Meyers (Ed.), Encyclopedia of Physical Science and Technology (Third Edition) (pp. 279-344). Academic Press, Cambridge, Mass., USA. https://doi.org/10.1016/B0-12-227410-5/00419-1.
61. Levin, M. A., Burrington, K. J., & Hartel, R. W. (2016). Whey protein phospholipid concentrate and delactosed permeate: Applications in caramel, ice cream, and cake. *Journal of Dairy Science*, *99*(9), 6948–6960. https://doi.org/10.3168/JDS.2016-10975.
62. Lipnizki, F. (2010). Membrane Processes for the Production of Bulk Fermentation Products. In: Z.F. Cui & H.S. Muralidhara (Eds.) *Membrane Technology (pp. 121-153)*. Butterworth-Heinemann, Oxford, UK. https://doi.org/10.1016/B978-1-85617-632-3.00007-0.
63. Llabrés-Luengo, P., & Mata-Alvarez, J. (1987). Kinetic study of the anaerobic digestion of straw-pig manure mixtures. *Biomass*, *14*(2), 129–142. https://doi.org/10.1016/0144-4565(87)90015-1.
64. Luis, P. (2018). Introduction. In: P. Luis (Ed.) *Fundamental Modeling of Membrane Systems: Membrane and Process Performance* (pp. 1–23). Elsevier, Amsterdam, Netherlands. https://doi.org/10.1016/B978-0-12-813483-2.00001-0.
65. Luján-Facundo, M. J., Mendoza-Roca, J. A., Cuartas-Uribe, B., & Álvarez-Blanco, S. (2017). Membrane fouling in whey processing and subsequent cleaning with ultrasounds for a more sustainable process. *Journal of Cleaner Production*, *143*, 804–813. https://doi.org/10.1016/j.jclepro.2016.12.043.
66. Luo, J., Ding, L., Wan, Y., & Jaffrin, M. Y. (2012). Threshold flux for shear-enhanced nanofiltration: Experimental observation in dairy wastewater treatment. *Journal of Membrane Science*, *409–410*, 276–284. https://doi.org/10.1016/J.MEMSCI.2012.03.065.

67. Mainardis, M.; Flaibani, S.; Trigatti, M.; Goi, D. (2019). Techno-Economic Feasibility of Anaerobic Digestion of Cheese Whey in Small Italian Dairies and Effect of Ultrasound Pre-Treatment on Methane Yield. *J. Environ. Manag.* 246, 557–563. https://doi.org/10.1016/j.jenvman.2019.06.014.
68. Mata-Alvarez, J., Dosta, J., Romero-Güiza, M. S., Fonoll, X., Peces, M., & Astals, S. (2014). A critical review on anaerobic co-digestion achievements between 2010 and 2013. *Renewable and Sustainable Energy Reviews*, *36*, 412–427. https://doi.org/10.1016/J.RSER.2014.04.039.
69. Mondal, S., & De, S. (2010). A fouling model for steady state crossflow membrane filtration considering sequential intermediate pore blocking and cake formation. *Separation and Purification Technology*, *75*(2), 222–228. https://doi.org/10.1016/J.SEPPUR.2010.07.016.
70. Morin, P., Britten, M., Jiménez-Flores, R., & Pouliot, Y. (2007). Microfiltration of buttermilk and washed cream buttermilk for concentration of milk fat globule membrane components. *Journal of Dairy Science*, *90*(5), 2132–2140. https://doi.org/10.3168/jds.2006-832.
71. Morin, P., Jiménez-Flores, R., & Pouliot, Y. (2004). Effect of temperature and pore size on the fractionation of fresh and reconstituted buttermilk by microfiltration. *Journal of Dairy Science*, *87*(2), 267–273. https://doi.org/10.3168/jds.S0022-0302(04)73165-3.
72. Morin, P., Pouliot, Y., & Jiménez-Flores, R. (2006). A comparative study of the fractionation of regular buttermilk and whey buttermilk by microfiltration. *Journal of Food Engineering*, *77*(3), 521–528. https://doi.org/10.1016/j.jfoodeng.2005.06.065.
73. Oliveira, D., Fox, P., & O'Mahony, J. A. (2020). Byproducts from Dairy Processing. In: B.K. Simpson, A.N. Aryee, F. Toldra (Eds.) Byproducts from Agriculture and Fisheries: Adding Value for Food, Feed, Pharma, and Fuels (pp. 57-106). Wiley, Hoboken, USA.
74. Patel, S. (2015). Functional food relevance of whey protein: A review of recent findings and scopes ahead. *Journal of Functional Foods*, *19 (Part A)*, 308–319. https://doi.org/10.1016/j.jff.2015.09.040.
75. Pochwatka, P., Kowalczyk-Juśko, A., Sołowiej, P., Wawrzyniak, A., & Dach, J. (2020). Biogas plant exploitation in a middle-sized dairy farm in Poland: Energetic and economic aspects. *Energies*, *13*(22), 6058. https://doi.org/10.3390/en13226058.

76. Rao, H. G. R. (2002). Mechanisms of flux decline during ultrafiltration of dairy products and influence of pH on flux rates of whey and buttermilk. *Desalination*, *144* (1-3), 319–324. https://doi.org/10.1016/S0011-9164(02)00336-3.
77. Ratanatamskul, C., Onnum, G., & Yamamoto, K. (2014). A prototype single-stage anaerobic digester for co-digestion of food waste and sewage sludge from high-rise building for on-site biogas production. *International Biodeterioration & Biodegradation*, *95*(Part A), 176–180. https://doi.org/10.1016/J.IBIOD.2014.06.010.
78. RED I. (2013). *RED I. Renewable Energy—Recast to 2030 (RED II) EU Science Hub. 2013. Available online: https: //ec.europa.eu/jrc/en/jec/renewable-energy-recast-2030-red*-ii (accessed on 10th October 2020*).*
79. Research and Markets. (2019). *Global Whey Protein (Powder & Concentrate) Market Study 2019-2024 - ResearchAndMarkets.com; https://www.businesswire.com/news/home/20190417005321/en/Global-Whey-Protein-Powder-Concentrate-Market-Study-2019-2024---ResearchAndMarkets.com* (accessed on 16th September 2020).
80. Rocha-Mendoza, D., Kosmerl, E., Krentz, A., Zhang, L., Badiger, S., Miyagusuku-Cruzado, G., Mayta-Apaza, A., Giusti, M., Jiménez-Flores, R., & García-Cano, I. (2021). Invited review: Acid whey trends and health benefits. *Journal of Dairy Science*, 104(2), 1262–1275. https://doi.org/10.3168/jds.2020-19038.
81. Rokicka, M., Zieliński, M., Dudek, M., Dębowki, M. (2021). Effects of Ultrasonic and Microwave Pretreatment on Lipid Extraction of Microalgae and Methane Production from the Residual Extracted Biomass. *BioEnergy Research, 14, 752-760.* https://doi.org/10.1007/s12155-020-10202-y.
82. Salinas-Rodriguez, S. G., Amy, G. L., Schippers, J. C., & Kennedy, M. D. (2015). The Modified Fouling Index Ultrafiltration constant flux for assessing particulate/colloidal fouling of RO systems. *Desalination*, *365*, 79–91. https://doi.org/10.1016/j.desal.2015.02.018.
83. Samuelsson, G., Huisman, I. H., Trägårdh, G., & Paulsson, M. (1997). Predicting limiting flux of skim milk in crossflow microfiltration. *Journal of Membrane Science*, *129*(2), 277–281. https://doi.org/10.1016/S0376-7388(97)00013-6.
84. Skryplonek, K. (2018). The use of acid whey for the production of yogurt-type fermented beverages. *Mljekarstvo*, *68*(2), 139–149. https://doi.org/10.15567/mljekarstvo.2018.0207.

85. Smith, K. (2014). *Current and Future Processing of Whey Ingredients access. http: //oregondairy.org/wp-content/uploads/2014/04/4-2014-ODI.pdf.* (accessed on 12th May 2019).
86. Sodini, I., Morin, P., Olabi, A., & Jiménez-Flores, R. (2006). Compositional and functional properties of buttermilk: A comparison between sweet, sour, and whey buttermilk. *Journal of Dairy Science*, *89*(2), 525–536. https://doi.org/10.3168/jds.S0022-0302(06)72115-4.
87. Statista. (2021). *Cow milk production worldwide from 2015 to 2021. https://www.statista.com/statistics/263952/production-of-milk-worldwide/*. (accessed on 21st September 2022*)*.
88. Steinhauer, T., Leeb, E., Birle, D., & Kulozik, U. (2016). Determination of a molecular fouling model for the micro- and ultrafiltration of whey: A recombination study from single whey proteins to complex mixtures. *International Dairy Journal*, *52*, 50–56. https://doi.org/10.1016/j.idairyj.2015.08.006.
89. Svanborg, S., Johansen, A. G., Abrahamsen, R. K., & Skeie, S. B. (2015). The composition and functional properties of whey protein concentrates produced from buttermilk are comparable with those of whey protein concentrates produced from skimmed milk. *Journal of Dairy Science*, *98*(9), 5829–5840. https://doi.org/10.3168/jds.2014-9039.
90. Szczurek, W. (2008). Produkty przetwarzania serwatki i ich zastosowanie w paszy dla kurcząt brojlerów – aspekt żywieniowy i fizjologiczny. *Wiadomości Zootechniczne*, R.XLVI,4, 41–52.
91. Tan, T. J., Wang, D., & Moraru, C. I. (2014). A physicochemical investigation of membrane fouling in cold microfiltration of skim milk. *Journal of Dairy Science*, *97*(8), 4759–4771. https://doi.org/10.3168/jds.2014-7957.
92. Tarapata, J., Dybowska, B. E., & Zulewska, J. (2022a). Evaluation of fouling during ultrafiltration process of acid and sweet whey. *Journal of Food Engineering*, *328*, 111059. https://doi.org/10.1016/J.JFOODENG.2022.111059.
93. Tarapata, J., Maciejczyk, M., & Zulewska, J. (2022b). Microfiltration of buttermilk: Partitioning of proteins and modelling using a resistance-in-series model. *International Dairy Journal*, *134*, 105445.
94. Tarapata, J., Zieliński, M., & Zulewska, J. (2022c). Valorization of Dairy By-Products: Efficiency of Energy Production from Biogas Obtained in Anaerobic Digestion of Ultrafiltration Permeates. *Energies*, *15*(18), 6829.

https://doi.org/10.3390/en15186829.

95. Tomasula, P. M., & Bonnaillie, L. M. (2015). Crossflow Microfiltration in the Dairy Industry. In: N. Datta & P.M. Tomasula (Eds.), *Emerging Dairy Processing Technologies: Opportunities for the Dairy Industry* (pp. 1–32). Wiley, Chichester, UK. https://doi.org/https://doi.org/10.1002/9781118560471.ch1.
96. United Nations. (2015). *Resolution adopted by the general assembly on 25 September 2015. UN General Assembly Available at: https://www.un.org/en/development/desa/population/migration/generalassembly/docs/globalcompact/A_RES_70_1_E.pdf* (accessed on 21st September 2022).
97. USDA. (2021). *USDA. United States Department of Agriculture. Dairy: World Markets and Trade. 2021. https://downloads.usda.library.cornell.edu/usda-esmis/files/5t34sj56t/sj13b3984/xw42p992f/dairy.pdf* (accessed on 20th September 2022).
98. USDA. (2022). *USDA. United States Department of Agriculture. Dairy: World Markets and Trades. 2022. https://apps.fas.usda.gov/psdonline/circulars/dairy.pdf* (accessed on 20th September 2022).
99. Vanderghem, C., Bodson, P., Danthine, S., Paquot, M., Deroanne, C., & Blecker, C. (2010). Milk fat globule membrane and buttermilks: from composition to valorization. *Biotechnol. Agron. Soc. Environ*, 14(3), 485-500.
100. Villeneuve, W., Bérubé, A., Chamberland, J., Pouliot, Y., Labrie, S., & Doyen, A. (2021). Contribution of biofouling to permeation flux decline and membrane resistance changes during whey ultrafiltration. *International Dairy Journal*, *117*, 105010. https://doi.org/10.1016/J.IDAIRYJ.2021.105010.
101. Wemsy Diagne, N., Rabiller-Baudry, M., & Paugam, L. (2013). On the actual cleanability of polyethersulfone membrane fouled by proteins at critical or limiting flux. *Journal of Membrane Science*, *425–426*, 40–47. https://doi.org/10.1016/J.MEMSCI.2012.09.001.
102. Wen-qiong, W., Yun-chao, W., Xiao-feng, Z., Rui-xia, G., & Mao-lin, L. (2019). Whey protein membrane processing methods and membrane fouling mechanism analysis. *Food Chemistry*, *289*, 468–481. https://doi.org/10.1016/j.foodchem.2019.03.086.
103. Wojciechowski, K. L., & Barbano, D. M. (2015). Modification of the Kjeldahl noncasein nitrogen method to include bovine milk concentrates and milks from other species. *Journal of Dairy Science*, *98*(11), 7510–7526. https://doi.org/10.3168/JDS.2015-9580.

104. Yang, Z., Ma, X. H., & Tang, C. Y. (2018). Recent development of novel membranes for desalination. *Desalination*, *434*, 37–59. https://doi.org/10.1016/j.desal.2017.11.046.
105. Zieliński, M., Dębowski, M., & Krzemieniewski Uniwersytet Warmińsko-Mazurski, M. (2007). The possibility of anaerobic biodegradation of permeate obtained from sour whey nanofiltration. *Rocznik Ochrona Środowiska*, *9*, 199–210.
106. Zotta, T., Solieri, L., Iacumin, L., Picozzi, C., & Gullo, M. (2020). Valorization of cheese whey using microbial fermentations. *Applied Microbiology and Biotechnology*, *104*(7), 2749–2764. https://doi.org/10.1007/s00253-020-10408-2.
107. Zulewska, J., & Barbano, D. M. (2013). Influence of casein on flux and passage of serum proteins during microfiltration using polymeric spiral-wound membranes at 50°C. *Journal of Dairy Science*, *96*(4), 2048–2060. https://doi.org/10.3168/JDS.2012-6032.
108. Zulewska, J., Kowalik, J., & Dec, B. (2018). Flux and transmission of β-casein during cold microfiltration of skim milk subjected to different heat treatments. *Journal of Dairy Science*, *101*(12), 10831–10843. https://doi.org/10.3168/jds.2018-14496.
109. Żegarska, Z. (2000). *Ćwiczenia z Analizy Żywności. Wydawnictwo UWM, Olsztyn, Poland.*

Journal of Food Engineering 328 (2022) 111059

Contents lists available at ScienceDirect

Journal of Food Engineering

journal homepage: www.elsevier.com/locate/jfoodeng

Evaluation of fouling during ultrafiltration process of acid and sweet whey

Justyna Tarapata [a,*], Brygida E. Dybowska [b], Justyna Zulewska [a]

[a] Department of Dairy Science and Quality Management, Faculty of Food Sciences, University of Warmia and Mazury in Olsztyn, Poland
[b] Department of Process Engineering and Equipment, Faculty of Food Sciences, University of Warmia and Mazury in Olsztyn, Poland

ARTICLE INFO

Keywords:
Acid whey
Flux decline
Reversible fouling
Hydraulic resistance
Resistance-in-series model

ABSTRACT

Membrane fouling caused by deposition of whey protein on the membrane surface is still the major factor limiting concentration and fractionation efficiency in dairy industry. This work aims to elucidate the mechanisms of membrane fouling during ultrafiltration (50 °C) of sweet and acid whey obtained after Gouda and Tvarog (acid-coagulated cheese) manufacture using 20 nm ceramic membrane. A resistance-in-series model that accounts for time evolution of hydraulic resistances was considered. The results demonstrated that the higher the protein content the greater the total hydraulic resistance. Moreover, the resistance due to adsorption and concentration polarization dominated from the first minutes of filtration, whereas the growth of cake layer was much slower and gradual for each feed tested. SDS-PAGE electrophoresis showed that α-lactalbumin and β-lactoglobulin were the main contributors to pore blocking.

Credit author statement

Justyna Tarapata: Conceptualization, Methodology, Investigation, Resources, Data curation, Writing – original draft, Visualization. Brygida E. Dybowska: Methodology, Investigation. Justyna Zulewska: Conceptualization, Methodology, Writing – review & editing, Supervision, Project administration, Funding acquisition.

1. Introduction

The production of cheese, caseinates and yogurts generates a green-yellowish by-product known as whey (Wherry et al., 2019). Whey is the liquid remaining after removal of fat and casein, which contains mostly soluble components, including lactose, soluble salts, and globular proteins that comprises ~20% of the total protein content in milk (Chandrapala et al., 2016; Rocha-Mendoza et al., 2021). Whey is classified into sweet whey or acid whey based on its processing conditions. Sweet whey is collected after the coagulation process during ripened cheese production via enzymatic coagulation (González-Siso, 1996). Acid whey is obtained in the manufacture of acid-coagulated cheeses and Greek yogurt (Rocha-Mendoza et al., 2021). The most important differences between acid and sweet whey are protein content (0.5–0.84% vs 0.8–1.0%, respectively), calcium concentration (103–140 mg/100 g vs 45 mg/100 g, respectively) and pH (4.21–4.6 vs 6–7, respectively) (Fox et al., 2000; Smith, 2014; Rocha-Mendoza et al., 2021). Due to its composition, the development of economically and environmentally sustainable application for acid whey is still a hurdle for dairy industry (Zotta et al., 2020). Moreover, the increased demand for acid-coagulated fresh cheese creates a supply of acid whey that must be managed. The European Union has the largest cheese market in the world and, as a result, a large production of acid whey (Rocha-Mendoza et al., 2021). Tvarog (original name Twaróg) is an acidic fresh white cheese very popular in Central and Eastern Europe. The production technology is, to some extent, similar to German Quark. However, the texture of these two products are different, with Quark having a paste like texture and Tvarog is more crumbly and grainy. Poland and Russia are among the biggest producers of Tvarog and Tvarog-type cheeses, which represent up to two-thirds of total cheese consumption in these countries (Treszczynska et al., 2018). It is estimated that the production of 1 kg of Tvarog cheese generates about 6–7 kg of acid whey that must be either disposed or repurposed.

Membrane separation technology became a logical choice for whey recovery, because many whey components can be separated based on their size and whey contains only dilute concentrations of valuable proteins and other biochemical materials (Wen-qiong et al., 2019). In the last decades the ultrafiltration (UF) of whey has grown in importance as a "green" technique (Corbatón-Báguena et al., 2018). However, during filtration of whey, membrane fouling caused by deposition of

* Corresponding author. Department of Dairy Science and Quality Management, Faculty of Food Sciences University of Warmia and Mazury, Oczapowskiego 7, 10-719, Olsztyn, Poland.
E-mail address: justyna.tarapata@uwm.edu.pl (J. Tarapata).

https://doi.org/10.1016/j.jfoodeng.2022.111059
Received 21 October 2021; Received in revised form 12 March 2022; Accepted 14 March 2022
Available online 22 March 2022
0260-8774/© 2022 Elsevier Ltd. All rights reserved.

whey protein on the membrane surface is the major factor limiting concentration and fractionation efficiency (Steinhauer et al., 2015). Main proteins in whey that are associated with fouling tendencies are: α-lactalbumin (α-LA), bovine serum albumin (BSA) and β-lactoglobulin (β-LG) (Barukčić et al., 2015). Additionally, physicochemical properties like increased ionic strength and calcium content enhance the deposit layer formation due to reduction of repulsive forces in protein-protein and protein-membrane interactions (Labbez et al., 2002; Steinahuer et al., 2016; Luján-Facundo et al., 2017). Ultrafiltration of acid whey obtained after lactic acid fermentation is especially difficult to practice because of fouling associated mainly with precipitation of calcium phosphate, the high concentration of minerals, lactic acid content and the resulting insolubility of some individual whey proteins (Konrad et al., 2012).

The main effect of fouling is a decrease in flux. As reported by Konrad et al. (2012) the flux in UF of fermented acid whey with polyethersulfone membranes is directly dependent on pH (2.5–4.5) and the lower the pH (<3.9) the higher the permeation flux. Moreover, the acid whey is non-filterable at pH 4.6 with 10 kDa polymeric membranes at 45 °C and transmembrane pressure of 2 bar. The economic flux for a plant should have acceptable degree of fouling which can be easily removed with a standard cleaning procedure (Damar et al., 2020). High and stable permeate flux can be obtained with shear-enhanced filtration and in order to sustain such flux in long-term operation, critical fouling conditions (the flux at which irreversible fouling appears on a membrane surface) should be studied and an optimum flux needs to be determined (Bacchin, 2004; Luo et al., 2012).

Regarding the mechanisms of flux reduction, these are a result of both concentration polarization (accumulation of solute on the membrane surface) and membrane fouling (Luján-Facundo et al., 2017). As a novelty, a resistance-in series model that accounts for the time evolution of the fouling resistances during UF of whey model solutions was considered recently (Corbatón-Báguena et al., 2018). The results demonstrated that the higher the protein and salt concentrations in the feed solutions the greater the fouling degree. High values of coefficient of determination ($R^2 > 0.96$) indicated that resistance-in-series model can be accurately fitted to the experimental data for either ceramic or polymeric membranes.

The aim of this work was to examine the fouling mechanisms that affect ceramic UF membranes using acid whey obtained after Tvarog manufacture in comparison with sweet whey obtained after rennet cheese (Gouda) production. Based on physicochemical analysis of external and internal foulant streams as well as mathematical modeling of the process a thorough investigation of flux decline was carried out. Unlike other authors (Konrad et al., 2012; Luján-Facundo et al., 2017; Corbatón-Báguena et al., 2018), the whey subjected to UF in this study was obtained from cheesemaking process instead of using model solutions of single or mixed whey proteins or whey derived from reconstitution of milk or whey protein concentrates, thus omitting the potential influence of subsequent processing on protein properties and hence their interactions with other whey components and membrane material.

2. Materials and methods

2.1. Experimental set-up

The experiments were carried out using laboratory scale ultrafiltration unit (Pall Membralox XLAB 5, Pall Corp, Port Washington, NY). This plant was equipped with a temperature control system, a 3.5 L stainless steel feed tank, a progressive cavity pump with frequency converter to select the desired crossflow velocity, a manometer at each side of the membrane module to control the transmembrane pressure and a balance (with an accuracy of ±0.001 g). A complete scheme of the experimental set-up can be found in Zulewska et al. (2018).

2.2. Membrane and feed material

Filtration was performed using monochannel ceramic membrane (ET1-070, zirconia, Pall Corp.). The characteristics of membrane specified by manufacturer were as follows: nominal pore diameter of 20 nm; length of 250 mm; channel diameter of 7 mm; effective area of 0.005 m^2.

The abovementioned system was used to ultrafilter two types of whey: acid whey obtained after Tvarog (acid-coagulated cheese) manufacture (AW-T) and sweet whey (SW) obtained after Gouda cheese production (a reference feed material).

Acid whey AW-T was supplied by Dairy EkoŁukta Ltd. (Łukta, Poland). Tvarog cheese was produced from cheese milk pasteurized at 88.2 ± 2 °C for 21s. Sweet whey was produced during cheesemaking processes in Dairy Research and Educational Center at University of Warmia and Mazury in Olsztyn (Poland). Whey, after separation from curd grains, was subjected to centrifugation at 45 °C using model LWG20 centrifuge (Spomasz, Gniezno, Poland) to remove fat and residual curd, and then pasteurized at 72 °C for 15s. Pasteurization process was carried out with a plate heat exchanger (model P20-HB; Alfa Laval, Lund, Sweden). After that, whey was cooled and stored at 3 °C until processing (at least 24 h).

2.3. Ultrafiltration process

Firstly, the clean membrane was characterized in terms of water permeability (prerun clean water flux, CWF) and clean membrane resistance (R_m) using reverse-osmosis (RO) water. The prerun CWF was determined at ~25 °C based on permeate weight collected in 120 s and the membrane surface area. The following conditions were applied during prerun CWF measurements: the retentate outlet valve was opened to produce transmembrane pressure (TMP) of 1 bar, and the permeate outlet valve was fully opened. The R_m (1/m) was calculated based on prerun CWF according to Corbatón-Báguena et al. (2018), separately for each UF process. The value of R_m was considered as mean (n = 3) for each feed tested.

Whey (~3.5 kg) was ultrafiltered at 50 °C. It was placed in feed tank with all valves closed, except the retentate valve. The pump was turned on, the frequency converter was adjusted to 5 on 0 to 10 scale, resulting in pump motor frequency of 28.3 Hz and crossflow velocity of approximately 4.1 m/s. These parameters created turbulent flow of whey through the filtration unit (Re ~38,000). Whey was recirculated for 5 min and then the permeate valve was slowly opened. Ultrafiltration was conducted under constant TMP of 3 bar recommended by membrane manufacturer. The permeate was collected and the retentate was recirculated in the system. The permeation flux (m^3/m^2h) was determined every 15 min according to eq. (1):

$$J_p = \frac{M}{A_m \times t \times \rho} \quad (1)$$

where M is the permeate weight (kg), A_m is the membrane surface area (m^2), t is time (s), and ρ is the permeate density at the operating temperature (kg/m^3).

At the end of UF run, retentate was drained from the system by opening two valves and all permeate collected during processing run was mixed and each was sampled. The average total time of whey processing was 180 min.

The cleaning step before and after each UF process was done as described by Zulewska et al. (2018).

2.4. Characterization of membrane fouling

To gain an insight into the state of the membrane fouling, RO water rinsing steps were performed immediately after UF run to collect foulants' streams according to modified method described by Tan et al. (2014).

First, the UF unit was flushed with 2 L of RO water at 50 °C for 1 min, to wash out the whey residue from the system. Then, another two rinsing steps were carried out to collect: (i) foulants located on the membrane surface (external foulants, F_e) and (ii) foulants located inside the membrane pores (internal foulants, F_i). First, RO water rinse (2 L) was conducted with the permeate valve fully closed and the retentate valve fully opened. The RO water rinse was performed for 5 min at 50 °C, at pump motor frequency of ~12.9 Hz. The rinse water collected in this manner contained the external foulants (F_e) attached to the membrane surface. The rinsing solution was drained from the UF unit and sampled. Next, RO water rinsing (2 L) was conducted with the permeate valve fully opened and the retentate valve fully closed to collect the internal foulants (F_i) attached to the pore walls. Rinsing and sampling were performed as described for F_e.

When the RO water rinsing was completed, the fouled membrane water flux (FWF) was determined using same settings as for prerun CWF.

Finally, the membrane was cleaned and then rinsed with room-temperature RO water until neutral pH was reached and the postrun CWF was determined under same conditions as for prerun CWF. The postrun CWF was close to the prerun CWF indicating the effectiveness of cleaning procedure which enabled the maintenance of the same conditions before each UF run.

Additionally, the fouling degree (FD) was calculated by comparing the values of permeate flux at the beginning of UF ($J_{p,0}$) and at the end of a run ($J_{p,f}$) (Eq. (2)):

$$FD(\%) = \left[\left(J_{p,0} - J_{p,f}\right) / J_{p,0}\right] \times 100\%. \quad (2)$$

2.5. Chemical and instrumental procedures

The pH of the starting and final UF products was measured using a pH meter (CP-401, Elmetron, Zabrze, Poland) equipped with an electrode IJ-44C IONODE (Elmetron).

The samples of whey before processing, final retentates and permeates were analyzed for total solids (TS), total nitrogen (TN), noncasein nitrogen (NCN), and nonprotein nitrogen (NPN) content using forced-air oven drying (AOAC International, 2007; method 990.20; 33.2.44), Kjeldahl method (AOAC International, 2007; method 991.20; 33.2.11), Kjeldahl method (AOAC International, 2007; method 998.05; 33.2.64) with modifications according to Wojciechowski and Barbano (2015), and Kjeldahl method (AOAC International, 2007; method 991.21; 33.2.12), respectively.

The viscosity of feed materials was determined using rotational rheometer (RheolabQC, Anton Paar, Graz, Austria) at a shear rate of 100 s^{-1} and the temperature of 50 °C.

The density of the permeates was measured with automatic handheld density meter (Densito, Mettler Toledo, Greifensee, Switzerland) with an accuracy of ±0.001 g/cm^3.

The lactic acid content in feed was calculated based on titratable acidity measurements (1°SH = 0.0225 lactic acid %).

The content of mineral components (Ca and P) was evaluated in all processing streams and rinsing solutions. Total calcium content was analyzed using atomic absorption spectrometry according to the method of IDF (2007) at the wavelength of 422.7 nm. Total phosphorus content was evaluated by colorimetric analysis (Żegarska, 2000); the absorbance was measured using spectrophotometer model Carry 60 UV–Vis (Agilent) at the wavelength of 610 nm.

The conductivity of UF streams was measured with conductivity benchtop meter (model InoLab Cond Level 1, WTW, Weilheim, Germany) equipped with conductivity cell TetraCon 325 (WTW).

The feeds and permeates were evaluated for particle-size distribution by dynamic light scattering, using Zetasizer NanoS (model ZEN1600, Malvern Instrument Ltd., UK). Whey samples were diluted with RO water at a ratio of 1:100 before measurement. The parameters necessary for software calculations are provided elsewhere (Dybowska, 2011). The particle size distribution was presented as average of 9 replicates.

2.6. SDS-PAGE electrophoresis

To identify proteins present in UF streams, on the membrane surface and inside the pores contributing to external and internal fouling, respectively, a SDS-PAGE electrophoresis on 12% polyacrylamide gel (Biorad Laboratories, Warsaw, Poland) was used. The fresh samples of whey and permeates were diluted with sample buffer (pH 6.8, 10 mM Tris-HCl, 1.0% SDS, 20% glycerol, 0.02% bromophenol blue tracking dye, and 50 mM dithiothreitol), then immersed in boiling water for 3 min and kept frozen (−26 °C) in plastic vials (Eppendorf microtubes, 3810X; Merc, Darmstadt, Germany) until analysis. Due to small TS content (data not shown), samples of F_e and F_i (20 g each) were first frozen at −26 °C, next lyophilized for 72 h at 0.18 bar (Freeze dryer Alpha 1e2 LD, Christ, Germany), then diluted with 100 μL of sample buffer, immersed in boiling water for 3 min and kept frozen (−26 °C). Before analysis all samples were thawed at room temperature, then wells were loaded with 13.6 μg protein per loading in case of whey and permeates, and with 10 μL of F_e and F_i sample per loading. Running, staining and destaining procedures were performed according to Verdi et al. (1987). The destained gels were scanned using a scanner Lumi Bis Bioimaging Systems DNR (Jerusalem, Israel) and analyzed using TotalLab 1D v 11.3 (New Castle, England).

2.7. Fouling resistance model fitting

Among the different mathematical models available in the literature, the resistance-in-series model is the most often used. It takes into account the contribution of following fouling mechanisms: the adsorption of solute on the membrane surface and also on the pore walls, the concentration polarization and cake formation which are predominant fouling mechanisms that explain the decline of permeate flux during UF of protein based solutions (Katsoufidou et al., 2005). To determine the most predominant fouling mechanism during UF of acid whey, the model parameters of a resistance-in-series model were related to different feed tested. The general equation for the resistance-in-series model is Eq. (3):

$$J_p = \frac{\Delta P}{\mu \times \left(R_m + R_{ads} + R_{cp} + R_{cl}\right)} = \frac{\Delta P}{\mu \times \left(R_m + \left(R_{ads,ss} + R_{cp,ss}\right) \times \left(1 - \exp(-b \times t)\right) + \left(\frac{m_{dep}}{A_m}\right) \times \alpha\right)} \quad (3)$$

where ΔP is the transmembrane pressure; μ is the viscosity of the feed solution, R_m is the resistance of the clean membrane, t is filtration time.

The resistances due to adsorption on membrane surface and on the pore walls and concentration polarization ($R_{ads} + R_{cp}$) are expressed as

Table 1
Prerun clean water flux (CWF), an average permeation flux, fouled water flux (FWF), fouling degree (FD) and concentration factor (CF) obtained during UF of acid whey from tvarog production (AW-T) and sweet whey (SW).

Feed	prerun CWF ($\times 10^{-4}$ m^3/m^2s)	Flux ($\times 10^{-5}$ m^3/m^2s)	FWF ($\times 10^{-5}$ m^3/m^2s)	FD (%)	CF based on retentate and permeate weights
AW-T	1.045[a]	2.51[a]	0.73[b]	37[a]	1.64[a] ± 0.02
SW	1.037[a]	1.60[b]	0.94[a]	26[b]	1.34[b] ± 0.09

[a-c] Means within a column with different superscripts are different ($P < 0.05$).

exponential time dependence that makes these resistances grow at a constant rate b up to a steady-state value expressed as sum of resistance due to solute adsorption at the steady-state ($R_{ads,ss}$) and resistance due to concentration polarization at the steady-state ($R_{cp,ss}$). The resistance due to cake formation (R_{cl}) is expressed as ratio of the protein mass deposited on the membrane surface (m_{dep}) to the membrane area (A_m) multiplied by specific cake resistance (α). Detailed description of the model was done by Corbatón-Báguena et al. (2018). In current experiment the mathematical model was fitted to the experimental data using Microsoft Excel's add-in program Solver. The non-linear least squares minimization was performed to minimize the difference between the experimental and predicted data. The fitting accuracy was evaluated by calculating coefficient of determination (R^2) and standard deviation (SD).

2.8. Statistical analysis

UF runs for two tested whey types were carried out in triplicate. The statistical analysis was performed using the Statistica software (version 13.1, 1984–2016, StatSoft, Inc., Tulsa, OK, USA). Statistical evaluation of data was done using one way ANOVA ($P < 0.05$) followed by Tuckey's post hoc test.

3. Results and discussion

3.1. Ultrafiltration of whey

The average permeate flux observed for two ultrafiltered whey types is presented in Table 1. The flux noted for AW-T was significantly ($P < 0.05$) higher than for SW. Sweet whey contained almost 2.5 times more protein (TP) than AW-T (~0.67% compared to 0.27%, Table 2) which resulted in ~1.5 times lower permeation (1.60×10^{-5} compared to 2.51×10^{-5} m^3/m^2s, Table 1). As confirmed by other researchers (Corbatón-Báguena et al., 2018), the fouling during UF of whey model solutions becomes more severe when whey protein concentration increases.

The evolution of permeate flux and total hydraulic resistance over time for SW and AW-T are shown in Fig. 1 a and b, respectively. It can be observed that the flux rates for each feed material declined sharply after starting the UF process. This phenomenon is related to membrane fouling and suggests that the maximum fouling occurred once the membrane was exposed to whey flow at the very beginning of the filtration process. Similar results during milk filtration have been reported elsewhere (Zulewska and Barbano, 2013; Zulewska et al., 2018).

The flux decline at the start of the UF is connected either with formation of the secondary layer on the membrane surface (Cheryan, 1997) or pore blocking mechanism followed by the formation of a cake layer (Juang et al., 2010). Adsorption of proteins onto membrane surface at the early stages of filtration has also been reported by Tong et al. (1988) who examined the mechanism of membrane fouling by only submersing membranes in milk.

In our study, the course of the curve representing changes of permeate flux in time was different for acid and sweet whey. In case of AW-T, the substantial flux decline was observed during 45 min of UF and after that, much slower, but progressive increase in hydraulic resistance occurred. In case of SW, flux substantially decreased during 30 min after the beginning of UF and after that time, generally the plateau value was reached. It can be concluded that in case of SW, the fouling layer, once built up during 30 min of UF, did not increase substantially during further processing, in contrast to UF of acid whey when the overall fouling evolved with time resulting in subsequent increase in total hydraulic resistance.

Fouling occurring during the production step is still a bottleneck of UF of milk protein suspensions. Therefore, flux optimization in membrane filtration was a subject of many studies (Luo et al., 2012; Diagne et al., 2013). An early concept to avoid excessive pressure causing flux decline was the limiting flux defined as plateau flux which is achieved at

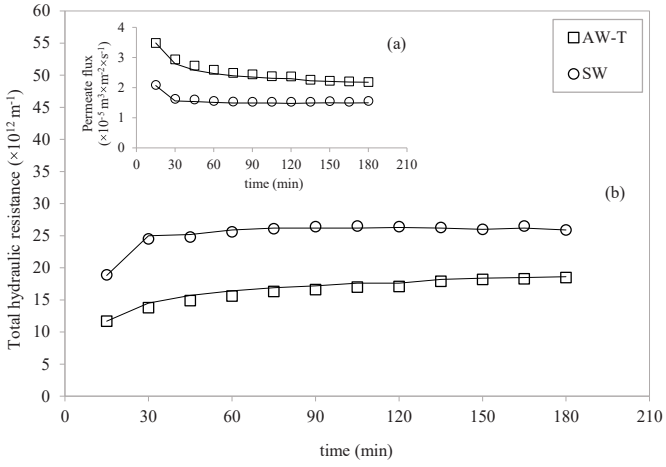


Fig. 1. Changes in permeate flux (a) and total hydraulic resistance (b) during UF of acid whey from tvarog production (AW-T) and sweet whey (SW). Solid lines represent resistance-in-series model predictions and symbols represent experimental data.

Table 2
Means (n = 6) and standard deviations of pH and composition[a] (% by weight) of acid whey from tvarog production (AW-T) and sweet whey (SW) subjected to UF at 50 °C.

Whey	pH	TS	Lactic acid	CP	NCN	NPN	TP	Cn	WP
AW-T	4.66[b] ± 0.08	5.53[a]±0.16	0.58[b] ± 0.02	0.50[c]±0.01	0.48[c]±0.02	0.229[a]±0.004	0.27[c]±0.01	0.02[a]±0.01	0.25[c]±0.01
SW	6.66[a] ± 0.13	5.90[a]±0.51	0.09[c]±0.01	0.86[a]±0.02	0.82[a]±0.03	0.19[b] ± 0.02	0.67[a]±0.01	0.03[a]±0.02	0.64[a]±0.02

[a-c] Means within a column with different superscripts are different ($P < 0.05$).

[a] TS = total solids; CP = crude protein; calculated as total N × 6.38; NCN = noncasein nitrogen × 6.38; NPN = nonprotein nitrogen × 6.38; TP = true protein, calculated as CP–NPN; Cn = casein, calculated as CP–NCN; WP = whey proteins, calculated as TP − Cn.

Table 3
Means (n=9) and standard deviations of viscosity, density at 50°C of acid whey from tvarog production (AW-T) and sweet whey (SW) subjected to UF and calculated limiting and critical flux values.

Feed	Viscosity (mPa × s)	Density (kg/m^3)	Limiting flux	Critical flux (× 10^{-5} m^3/m^{2}s)
			Samuelsson's model[a] (× 10^{-5} m^3/m^{2}s)	
AW-T	0.74[a] ± 0.03	1013[a] ± 7	2.62	1.75
SW	0.77[a] ± 0.70	1018[a] ± 7	2.62	1.75

[a-c] Means within a column with different superscripts are different ($P < 0.05$).
[a] According to the equation: Re × 6.94 × 10^{-10} m/s (Samuelsson et al., 1997).

high TMP; further increases in TMP do not increase the flux (Aimar and Field, 1992). Then, in order to minimize or even eliminate flux decline, a basic method for the fouling control, regarding judicious choice of the permeate flux, has been evolving from critical flux concept proposed back in 1995 (Field et al.) to new threshold flux concept introduced in 2011 (Field and Pearce). The critical flux is the flux below which the fouling is fully reversible whereas above the critical value irreversible fouling starts to occur. Initially two types of critical flux were proposed: strong form, for which the flux is the same as for water, and weak form, when the flux is decreased because of the establishment of a layer resulting from concentration polarization (Diagne et al., 2013). With certain assumptions, critical flux equals two thirds of limiting flux (Bacchin, 2004). According to threshold flux concept, it is the value of flux at or below which a low and nearly constant rate of fouling occurs but above which the rate of fouling increases markedly and the flux decrease is not only caused by concentration polarization but also little irreversible adsorption of fouling species on the membrane (Luo et al., 2012; Diagne et al., 2013).

Limiting and critical flux were calculated based on the data from our study (calculations were performed according to Samuelsson et al., 1997 and Bacchin, 2004, respectively). Determination of the threshold flux would require a different experimental set up, such as finding the break point in flux vs TMP curve. In this experiment, the UF system was not tested in order to find optimal processing parameters because process was carried out under the constant TMP recommended by the membrane manufacturer. Based on the comparison of flux values obtained during whey processing (Table 1) and calculated values of limiting and critical fluxes (Table 3), it can be stated that all UF processes were conducted under limiting flux conditions (2.62 × 10^{-5} m^3/m^{2}s), thus formation of highly irreversible fouling was prevented. The permeation flux during UF of SW was lower than critical flux suggesting that fouling was fully reversible. On the other hand, flux vs time curve for SW (Fig. 1a) indicated that fouling layer did establish once the process was started and flux reached plateau value only after this layer was formed. However, it must be noted that the critical flux was compared with an average value of processing flux. The initial flux for SW was 2.09 × 10^{-5} m^3/m^{2}s, so higher than critical value (1.75 × 10^{-5} m^3/m^{2}s), causing irreversible fouling layer formation. This layer had formed after 30 min of UF resulting in increase in total resistance leading to plateau value of flux of approx. 1.57 × 10^{-5} m^3/m^{2}s (close to average value 1.60 × 10^{-5} m^3/m^{2}s) and was constant till the end of processing, confirming reversible fouling (i.e. concentration polarization with adsorption fouling) occurring after formation of irreversible layer. Whereas flux for AW-T was higher than the critical value indicating continuous build-up of the fouling layer causing subsequent increase in flow resistance which was reflected by the course of total resistance curve as the function of time (Fig. 1b). It proves that during UF of acid whey the irreversible deposition of material occurs and this deposit can be only removed (at best) by cleaning operations. The postrun CWF measured in this experiment after cleaning the fouled membrane (data not shown) was close to prerun CWF, so the fouling layer was chemically removed.

3.2. A physicochemical evaluation of membrane fouling

The data concerning feed and retentate composition is shown in Tables 2 and 4 and Fig. 2. Higher protein content in SW resulted from significantly ($P < 0.05$) higher WP content in comparison with AW-T (0.64% vs 0.25%). Much lower WP content noted for AW-T could result from thermal treatment of milk before Tvarog production (88.2 ± 2 °C for 21s). Thermal processing of milk may cause the denaturation of milk serum proteins and formation of intermolecular disulfide bonds between β-LG and κ-casein (Harland et al., 1952; Zulewska et al., 2018). Thus, some part of serum proteins remain in the cheese matrix. Higher proportion of β-LG:α-LA noted for SW (2.5:1) than for AW-T (2:1) in this study (Fig. 2), suggest that high pasteurization temperature of milk before Tvarog production caused changes in the ratio of β-Lg:α-LA in resulting whey and induced heat denaturation of whey proteins. Moreover, as confirmed by chemical composition analyses (Table 2) and SDS-PAGE electrophoresis (Fig. 2b), trace amounts of casein, mainly β-casein, was also present in both tested feeds and was retained by UF membrane in retentate stream (Table 4). Retention of casein could contribute to fouling, as its presence was also noted in stream containing external foulants (Fig. 3a).

The increase in WP concentration during UF was almost equal to CFs obtained for both whey types tested (Tables 1, 2 and 4), namely ~1.6x for AW-T and ~1.3x for SW.

As revealed by SDS-PAGE electrophoresis, all major whey proteins were present in stream containing surface foulants (Fig. 3a), thus all proteins contributed to external fouling i.e. most likely concentration polarization layer or the protein layer loosely adsorbed to the membrane surface, since foulants extraction was performed at relatively low cross-flow velocity. The analysis of SDS-PAGE gels with samples of permeates and internal foulants streams (Fig. 4 and Fig. 3b, respectively) revealed that some major proteins i.e. α-LA and β-LG were able to cross the

Table 4
Means (n = 6) and standard deviations of pH and composition[a] (% by weight) of retentates obtained after UF of acid whey from tvarog production (AW-T) and sweet whey (SW).

Retentate	pH	TS	CP	NCN	NPN	TP	Cn	WP
AW-T	4.68[b] ± 0.09	5.76[a]±1.28	0.66[c]±0.01	0.63[c]±0.02	0.24a±0.02	0.42[c]±0.02	0.03[b] ± 0.01	0.39[c]±0.02
SW	6.60[a] ± 0.53	6.27[a]±0.53	1.11[a]±0.02	1.07[a]±0.02	0.19 b ± 0.01	0.92[a]±0.02	0.05[a]±0.01	0.87[a]±0.02

[a-c] Means within a column with different superscripts are different ($P < 0.05$).
[a] TS = total solids. CP = crude protein, calculated as total N × 6.38. NCN = noncasein nitrogen × 6.38. NPN = nonprotein nitrogen × 6.38. TP = true protein, calculated as CP–NPN. Cn = casein calculated as CP–NCN. WP = whey proteins calculated as TP − Cn.

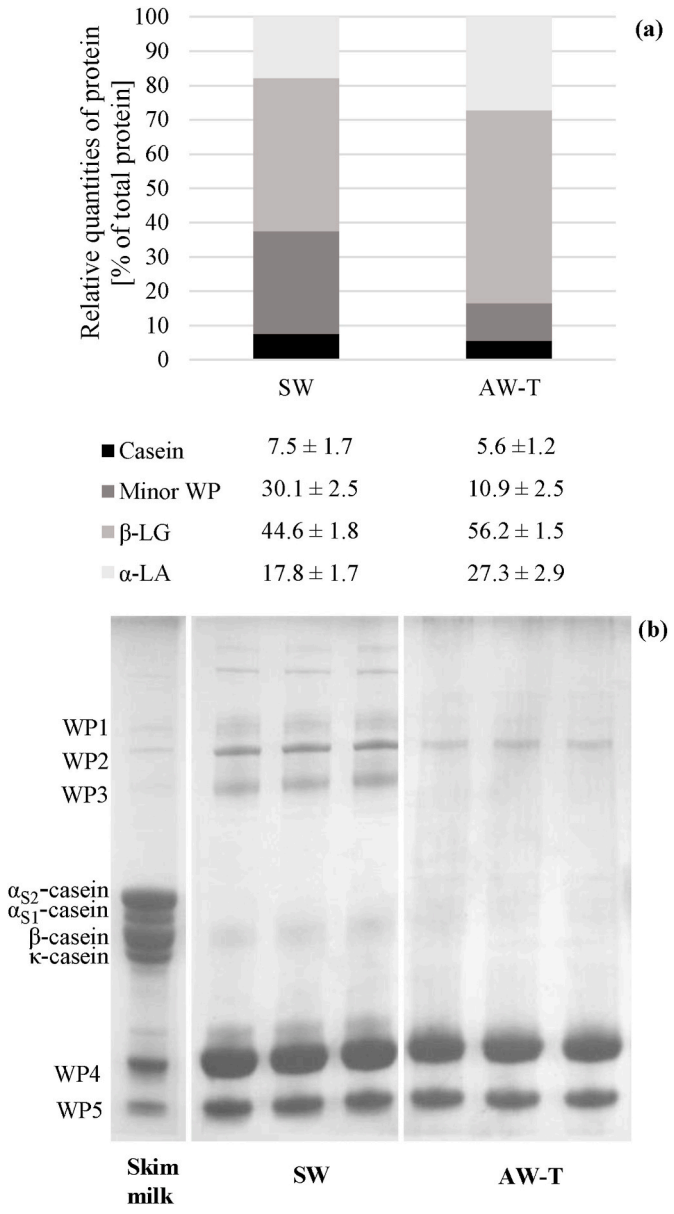


Fig. 2. The relative quantities of proteins (a) and their profile (b) for sweet whey (SW) and acid whey from tvarog production (AW-T) subjected to UF. Bands identified on the gel are: WP1, WP2 and WP3 = minor whey proteins; WP4 = β-LG; WP5 = α-LA. Relative quantities of proteins are expressed as mean ± standard deviation.

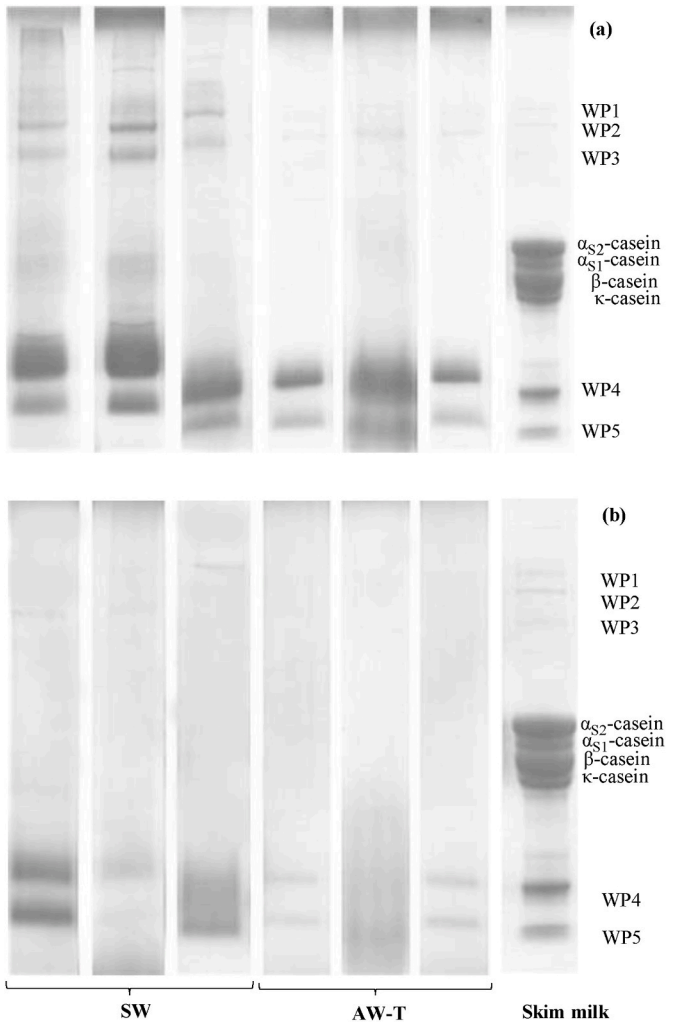


Fig. 3. The protein profile of foulants streams obtained after UF of sweet whey (SW) and acid whey from tvarog production (AW-T): a – external foulants (F_e); b – internal foulants (F_i). Bands identified on the gel are: WP1, WP2 and WP3 = minor whey proteins; WP4 = β-LG; WP5 = α-LA.

membrane toward the permeate side and slightly fouled the membrane pores.

A comparison of the particle size distribution (PSD) between the feed and the UF permeates was conducted. The particle size in tested feeds was between approx. 100 and 1000 nm (Fig. 5a). The same range was previously confirmed for whey pasteurized at 73 °C and related to notable amounts of protein aggregates that were responsible for higher filtration resistance and deposit formation (Barukčić et al., 2015). The intensity-based PSD in UF permeates displayed three distinct peaks (Fig. 5b): one in the 0.5–2 nm range, a second one in the 2–15 nm range and a third one in the 100–1000 nm range indicating the polydisperse nature of UF permeates. According to Heidebrecht and Kulozik (2019) first peak may relate only to α-LA, second one to: α-LA, β-LG, lactoperoxidase or bovine serum albumin, and the last peak covers the range of large particles like caseins or aggregates. In our experiment, some amount of α-LA and β-LG passed through the membrane and its presence may be reflected as a first and a second peak on the intensity-based PSD in UF permeates (Fig. 5b). Whereas peak covering the particle size range between 100 and 1000 nm should rather be related to high instability of proteins and tendency to aggregation, than to casein. The report with results of PSD measurements suggested high polydispersity of permeate samples with the occurrence of large particles, most probably aggregates. Although, the electrophoresis was conducted under reducing conditions and the presence of aggregates cannot be confirmed, this analysis can provide a qualitative data on casein content, excluding this protein from consideration as it was not present in permeate streams (Fig. 4). Additionally, PSD based on volume and number of particles were also measured for UF permeates (Fig. 5c and d). Both of this measurements exhibit single large peak with maximum particle size of 2 nm, corresponding to size of α-LA (Heidebrecht and Kulozik, 2019). In conclusion, the multimodal size distribution in permeate streams shifted towards smaller particle sizes in contrast to unimodal (SW) and bimodal (AW-T) particle size distribution in feeds (Fig. 5a and b) suggests that shear stress during processing caused breakdown of aggregates, enhancing smaller particle (α-LA and β-LG) transmission to permeate stream and thus its adsorption inside the pores. In case of AW-T, the aggregates present in feed, could have been formed at the stage of heat processing (at elevated temperature ~88 °C/21s) of milk before Tvarog production. Whey proteins, including β-LG, α-LA and BSA, are very

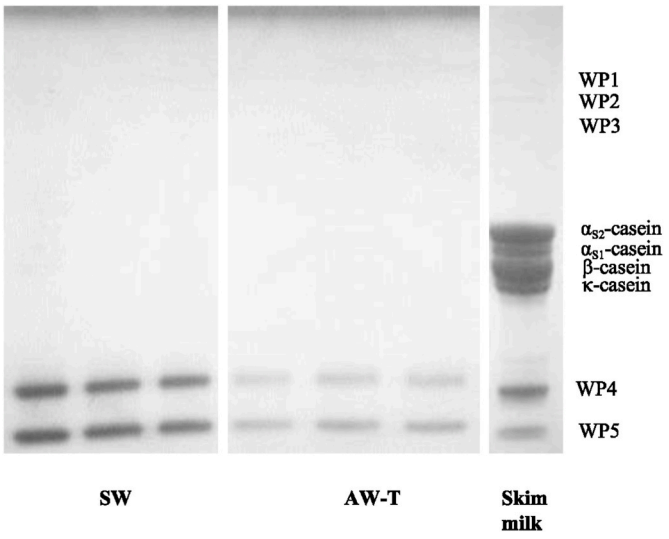


Fig. 4. The protein profile of UF permeates obtained after filtration of sweet whey (SW) and acid whey from tvarog production (AW-T). Bands identified on the gel are: WP1, WP2 and WP3 = minor whey proteins; WP4 = β-LG; WP5 = α-LA.

sensitive to heat treatment. Above 70 °C they form aggregates or gels (Dybowska, 2011). This phenomenon could have enhanced the formation of fouling layer during UF of AW-T. As previously confirmed (Steinhauer et al., 2015), the aggregates of β-Lg were found to accelerate membrane fouling during MF and UF due to covalent thiol/disulfide reactions. Moreover, both of tested feeds contained considerable amount of calcium (>360 mg/L) (Fig. 6a) and as reported by Stuart et al. (1986) and Anderson et al. (1997), α-LA has the ability to strongly bind Ca^{2+} which results in a calcium-mediated salt bridging between α-LA and the membrane. In case of β-LG, it was found that gel network formation is facilitated in the presence of calcium (Steinhauer et al., 2015).

The effect of mineral concentration (Ca and P) on the formation of fouling layer during UF process was also investigated. The concentration of Ca and P in AW-T (1180 mg/L Ca, 612 mg/L P) was significantly higher ($P < 0.05$) than for SW (366 mg/L Ca, 363 mg/L P), and similar relation was observed between resulting UF streams: permeates and retentates obtained from different feed materials (Fig. 6a). The results of mineral content in sweet and acid whey are similar to previously reported data (Wong et al., 1978). The measurements of electrical conductivity remained almost the same for feeds, UF permeates and concentrates (Fig. 7). The membrane was not selective for ashes, which contribute most to the electrical conductivity (Baldasso et al., 2011). The Ca and P concentration in whey either acid or sweet was significantly ($P < 0.05$) correlated with its conductivity, with Person's coefficient at 0.99 and 0.98, respectively. According to Steinhauer et al. (2016) the presence of salt ions has a major impact on protein interaction forces and at higher ion concentrations the deposition probability is higher because of reduced particle repulsions. This may explain why flux decline (FD) (Table 1) noted during UF of SW (26%) was significantly lower ($P < 0.05$) than for AW-T (37%). More severe membrane blockage

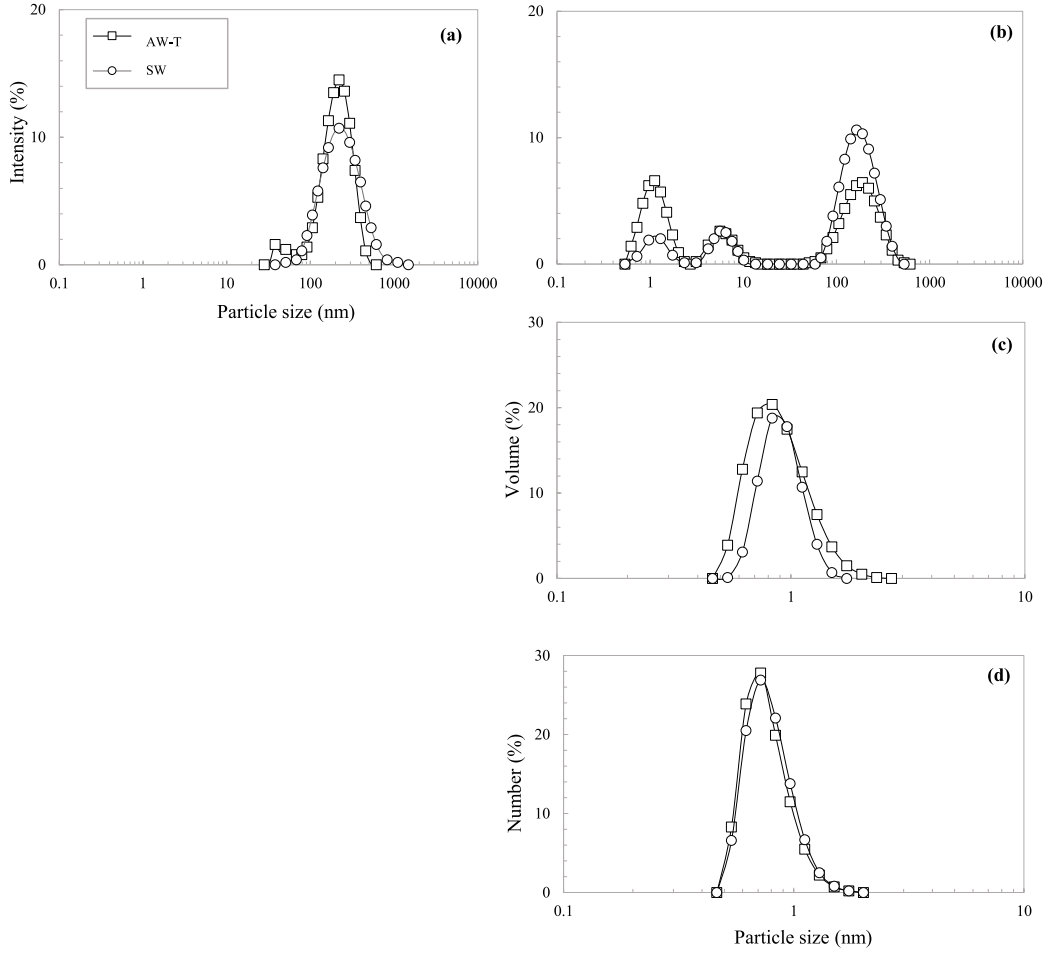


Fig. 5. Particle size distribution (diameter) for: a - whey, b-d - UF permeates measured via dynamic light scattering: SW – sweet whey; AW-T - acid whey from tvarog production.

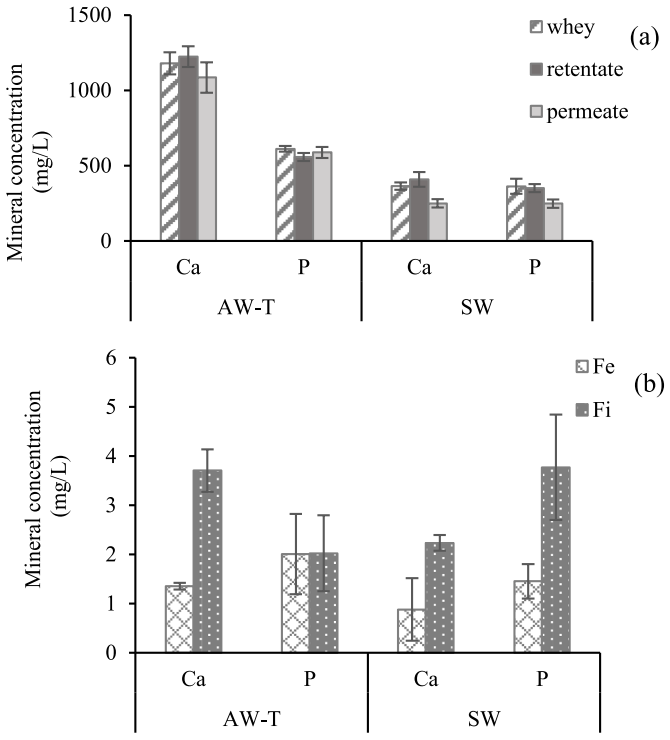


Fig. 6. Mineral concentration in: a - UF streams; b – the foulants streams obtained during filtration of acid whey from tvarog production (AW-T) and sweet whey (SW). Error bars represent one standard deviation (n = 9). F_e = external foulant; F_i – internal foulants.

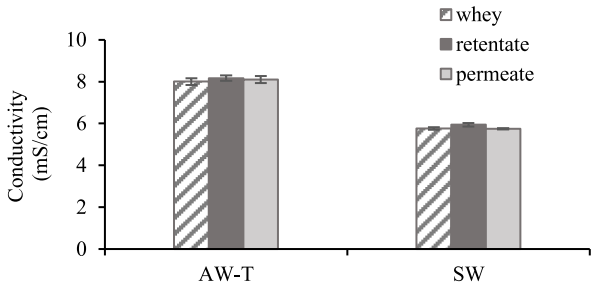


Fig. 7. Electric conductivity of tested whey types and resulting UF permeate and retentate streams. AW-T – acid whey from tvarog production; SW – sweet whey. Error bars represent one standard deviation (n = 9).

Table 5
Values of the fitting parameters for the resistance-in-series model and the goodness of fit (R^2 = coefficient of determination, SD = standard deviation) for two whey types tested: AW-T = acid whey from tvarog production, SW = sweet whey.

Whey	$R_{ads,ss} + R_{cp,ss}$ ($\times 10^{12}$ m^{-1})	b (s^{-1})	$R_{cl,ss}$ ($\times 10^{12}$ m^{-1})	α ($\times 10^{13}$ m/kg)	Goodness of fit	
					R^2	SD
AW-T	10.053	0.016	7.033	8.852	0.979	0.003
SW	17.448	0.283	7.132	12.859	0.994	0.007

$R_{ads} + R_{cp}$ = the resistances caused by adsorption and concentration polarization; b = rate of growth of the resistances due to adsorption and concentration polarization; R_{cl} = resistance caused by the growth of the cake layer; α = specific cake resistance.

after UF of acid whey was also confirmed by FWF, which was significantly lower in case of acidic feed (Table 1) characterized by higher concentration of Ca and P. However, the mineral concentrations measured in all foulants streams were rather low, below 6 mg/L (Fig. 6b), when compared to concentration in feed. Similar findings regarding ceramic membranes were obtained by Tan et al. (2014) during skim milk microfiltration (MF). This may suggest that the minerals might not form a part of the foulant alone, but could catalyze instability of the proteins by helping them cross-link.

Regarding the lower total hydraulic resistance noted for AW-T in comparison with SW (Fig. 1b), the pH of feed should also be considered. In agreement with our results, Steinhauer et al. (2016) reported, that overall fouling resistance for acid whey at pH of 4.6 during cross-flow MF (ceramic system) is considerably lower than the overall fouling resistance occurring in MF of sweet whey at its natural pH (~6.8) when the protein content is comparable for both wheys. The pH influences electrostatic interactions between solutes and membrane material. It was reported (Sats et al., 2014) that the isoelectric points (pI) of whey proteins are as follows: 4.7 for α-LA and BSA, 5.0 for β-LG, 6.5–8.0 for immunoglobulins, 9.0 for lactoferrin and 10.0 for lactoperoxidase. This means that, with no pH adjustment, all molecules in acid whey are positively charged at the pH of 4.6. In addition, other authors reported that pI of the ceramic membranes (made of titania) was about 6.2 (Labbez et al., 2002). Therefore, it could be assumed that the ceramic membrane and the solutes in acid whey are positively charged, thus there can exist electrostatic repulsions between them, preventing from severe fouling. Since the pH of sweet whey is about 6.7, some of its solutes could have opposite charges to each other and to the membrane. Hence, it can be expected that only low electrostatic repulsions or even attraction enhance the deposit layer formation. Regarding our results, the phenomenon described above, could be assigned to the first phase of flux reduction, when sharper increase in resistance at early stage of UF caused by adsorption of solutes was noted for SW than for AW-T. However, in subsequent processing time, fouling during UF of SW was not changed and in case of AW-T gradual increase in flux decline was observed, which means that different mechanism were responsible for resistance growth during the second phase of flux decline.

3.3. Resistance-in-series model

The basis for the modeling of membrane filtration in the presence of fouling is given by Eq. (3). The resistance to permeation might be enhanced by osmotic pressure due to concentration polarization while the hydraulic resistance may be greater than that of membrane material because of material accumulation on the membrane surface or inside the pores (Field and Pearce, 2011).

The prediction of the total hydraulic resistance evolution during UF of whey in time is presented in Fig. 1b. The fitting accuracy of the resistance-in-series model in terms of R^2 and SD is shown in Table 5. Values of R^2 ranged between 0.979 and 0.994 for AW-T and SW, respectively. Standard deviation calculated for three runs was 0.003 and 0.007 for AW-T and SW, respectively. The resistance-in-series model was accurately fitted to the experimental data for each feed tested.

The average (n = 9) clean membrane resistance (R_m) calculated based on water flux was found to be ~1.38×10^{12} m^{-1} which is comparable with the 50 nm (pore size) clean zirconia membrane resistance of 1.20×10^{12} m^{-1} reported by Carić et al. (2000).

The parameters of resistance-in-series model for our experimental conditions are included in Table 5. It was noted that $R_{ads} + R_{cp}$ increased with increasing true protein content in whey (Table 2) and retentate streams (Table 4). The $R_{ads} + R_{cp}$ value noted for AW-T (10.053×10^{12} m^{-1}; 0.27% true protein in feed and 0.42% in retentate) was smaller than for SW (17.445×10^{12} m^{-1}; 0.67% true protein in feed and 0.92% in retentate). These data are in agreement with literature data. Carić et al. (2000) stated that fouling resistance caused by protein adsorption increases as protein concentration increases. According to Cheryan

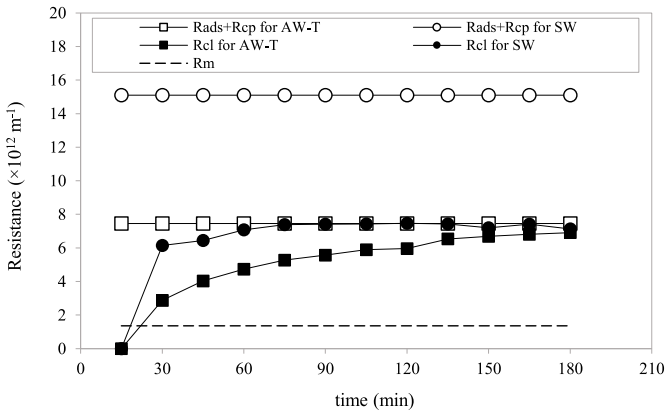


Fig. 8. Time evolution of the fouling resistances during UF of acid whey from tvarog production (AW-T) and sweet whey (SW). Rm = clean membrane resistance, R_{cl} = resistance due to the growth of the cake layer, $R_{ads} + R_{cp}$ = the resistances due to adsorption and concentration polarization.

(1986) and Baldasso et al. (2011) the more concentrated the solution of protein the lower the permeate fluxes. It results from the higher osmotic pressure and the greater accumulation of solute molecules in the polarized layer increasing its thickness and thus its resistance to filtration. In Table 5 it can be observed that the value of parameter b (the rate of growth of the resistances due to adsorption and concentration polarization) for AW-T (~0.016 s^{-1}) is significantly ($P < 0.05$) lower than for SW (0.283 s^{-1}). This result is in contrary to other studies (Carrère et al., 2001; Corbatón-Báguena et al., 2018) with the conclusion that parameter b was independent of the operating conditions. Crobatón-Báguena et al. (2018) considered resistance-in-series model during UF of whey model solutions (pH 7) of different protein concentrations and obtained b value for 15 kDa monotubular ZrO_2–TiO_2 membrane between 0.236 and 0.240 s^{-1}. Whereas Carrère et al. (2001) microfiltered lactic acid fermentation broth (pH 7.5) with a ceramic tubular (Al_2O_3, TiO_2) membrane increasing the TMP and obtained b value between 0.00026 and 0.00037 s^{-1}. The rate of increase in resistance caused by adsorption and concentration polarization for SW in our experiment (pH ~6.7) was close to the one obtained by Corbatón-Báguena et al. (2018), who performed UF using ceramic system, similarly to this research.

Nevertheless, in our study, parameter b was dependent on feed tested and was much lower for acid whey than for sweet whey. This phenomenon is probably related to true protein content as its concentration for SW was significantly higher ($P < 0.05$) than for AW-T. Moreover, the value of parameter b could be also explained by differences in Ca:protein (CP) ratio in feed material. AW-T was characterized by Ca:protein ratio of 1:4, resulting in b value of 0.016. Whereas, this ratio in SW was significantly different and reached the value of 1:22, resulting in significantly higher b value of 0.283. Another factor potentially influencing filtration efficacy might be lactic acid, but in this study both tested feeds were characterized by significantly different ($P < 0.05$) lactic acid content (Table 2), which makes it difficult to compare. To get insight into the effect of different parameters on protein-protein, protein-membrane interactions and thus the value of parameter b in such complex systems, further research should be carried out on model solutions.

The R_{cl} (Table 5) and the determined specific cake resistance coefficient α were higher during SW processing (7.132×10^{12} m^{-1} and 12.859×10^{13} m/kg^{-1}, respectively) than during AW-T processing (7.033×10^{12} m^{-1} and 8.852×10^{13} m/kg^{-1}, respectively). It can be observed that the values of parameter α increased as the size of the molecules in the feed decreased (approx. 245 nm for AW-T and 208 nm for SW). This result is in agreement with previous studies (Salinas-Rodriguez et al., 2015; Corbatón-Báguena et al., 2018).

The time profiles for the predicted resistances are shown in Fig. 8. The fouling related to the adsorption of particles on membrane surface and inside the pores as well as concentration polarization occurred in first minutes of processing and therefore these are the main mechanisms responsible for the sharp decrease in permeate flux at the beginning of UF, which is in agreement with recent reports (Juang et al., 2010; Villeneuve et al., 2021). Additionally, these mechanisms were predominant over the entire processing time regardless the feed tested. However, the total hydraulic resistance during UF of sweet and acid whey increased in time because of gradual growth of cake layer. Regarding the cake layer formation (R_{cl}) during UF of SW, there was an initial period of rapid protein adsorption on the membrane surface followed by a gradual growth of resistance until constant value was reached. The obtained time profile of cake layer formation for AW-T indicated that cake layer was formed slower than in case of SW. At the end of AW-T ultrafiltration, resistance reflecting cake formation (R_{cl}) was almost equal to that caused by adsorption and concentration polarization ($R_{ads} + R_{cp}$). In general, the growth of cake layer was much slower than concentration polarization layer formation regardless the feed composition.

4. Conclusions

The permeation flux for AW-T was considerably higher ($P < 0.05$) than calculated critical value indicating protein deposition on membrane surface. The resistance-in-series model, tested in this work, based on cake formation, concentration polarization and adsorption mechanisms, fitted the experimental data with high accuracy in terms of the regression coefficient and standard deviation. Thus, it can be concluded that this model is appropriate to describe the evolution of permeate flux during UF of acid and sweet whey obtained after cheese manufacture tested at 3 bar and crossflow velocity of 4.1 m s^{-1} with 20 nm ceramic membranes. The higher the protein content in feed the greater the total resistance for both feed tested. In addition, the resistance caused by adsorption and concentration polarization was predominant over the entire ultrafiltration process for both whey types. All major whey proteins were present in stream containing surface foulants, whereas β-lactoglobulin and α-lactalbumin did appear to be the major cause of pore blocking. In UF of acid whey with ceramic membranes, the fouling had both reversible and irreversible components, but it was fully removable by chemical cleaning.

Declaration of competing interest

The authors declare that they have no known competing financial interests or personal relationships that could have appeared to influence the work reported in this paper.

Acknowledgments

Project financially supported by The National Centre for Research and Development, Project No. WPC1/DairyFunInn/2019, amount of funding 1.950.000,00 PLN.

The authors thank to Roman Łaszek, Waldemar Brandt, Anna Lis, Krzysztof Siemianowski and Sławomir Wiśniewski for technical assistance. Justyna Tarapata is a recipient of a scholarship from the Programme Interdisciplinary Doctoral Studies in Bioeconomy (POWR.03.02.00–00-I034/16–00), which is funded by the European Social Fund.

References

Aimar, P., Field, R., 1992. Limiting flux in membrane separations: a model based on the viscosity dependency of the mass-transfer coefficient. Chem. Eng. Sci. 47 (3), 579–586. https://doi.org/10.1016/0009-2509(92)80008-Z.

Anderson, P.J., Brooks, C.L., Berliner, L.J., 1997. Functional identification of calcium binding residues in bovine α-lactalbumin. Biochemistry 36 (39), 11648–11654. https://doi.org/10.1021/bi9709598.

Bacchin, P., 2004. A possible link between critical and limiting flux for colloidal systems: consideration of critical deposit formation along a membrane. J. Membr. Sci. 228 (2), 237–241. https://doi.org/10.1016/j.memsci.2003.10.012.
Baldasso, C., Barros, T.C., Tessaro, I.C., 2011. Concentration and purification of whey proteins by ultrafiltration. Desalination 278 (1–3), 381–386. https://doi.org/10.1016/j.desal.2011.05.055.
Barukčić, I., Božanić, R., Kulozik, U., 2015. Influence of process temperature and microfiltration pre-treatment on flux and fouling intensity during cross-flow ultrafiltration of sweet whey using ceramic membranes. Int. Dairy J. 51, 1–7. https://doi.org/10.1016/j.idairyj.2015.07.002.
Carić, M.D., Milanović, S.D., Krstić, D.M., Tekić, M.N., 2000. Fouling of inorganic membranes by adsorption of whey proteins. J. Membr. Sci. 165 (1), 83–88. https://doi.org/10.1016/S0376-7388(99)00221-5.
Carrère, H., Blaszkow, F., Roux de Balmann, H., 2001. Modelling the clarification of lactic acid fermentation broths by cross-flow microfiltration. J. Membr. Sci. 186 (2), 219–230. https://doi.org/10.1016/S0376-7388(00)00677-3.
Chandrapala, J., Duke, M.C., Gray, S.R., Weeks, M., Palmre, M., Vasiljevic, T., 2016. Nanofiltration and nanodiafiltration of acid whey as a function of pH and temperature. Separ. Purif. Technol. 160, 18–27. https://doi.org/10.1016/j.seppur.2015.12.046.
Cheryan, M., 1986. Ultrafiltration Handbook. Technomic Publishing Company, Inc, Lancaster, pp. 375–380.
Cheryan, M., 1997. Ultrafiltration and microfiltration hand book, 2nd. Technomic Publishing Co, Lancaster, USA.
Corbatón-Báguena, M.J., Álvarez-Blanco, S., Vincent-Vela, M.C., 2018. Evaluation of fouling resistances during the ultrafiltration of whey model solutions. J. Clean. Prod. 172, 358–367. https://doi.org/10.1016/j.jclepro.2017.10.149.
Damar, I., Cinar, K., Gulec, H.A., 2020. Concentration of whey proteins by ultrafiltration: comparative evaluation of process effectiveness based on physicochemical properties of membranes. Int. Dairy J. 111, 104823. https://doi.org/10.1016/j.idairyj.2020.104823.
Diagne, N.W., Rabiller-Baudry, M., Paugam, L., 2013. On the actual cleanability of polyethersulfone membrane fouled by proteins at critical or limiting flux. J. Membr. Sci. 425–426, 40–47. https://doi.org/10.1016/j.memsci.2012.09.001.
Dybowska, B.E., 2011. Whey protein-stabilized emulsion properties in relation to thermal modification of the continuous phase. J. Food Eng. 104 (1), 81–88. https://doi.org/10.1016/j.jfoodeng.2010.11.030.
Field, R.W., Pearce, G.K., 2011. Critical, sustainable and threshold fluxes for membrane filtration with water industry applications. Adv. Colloid Interface Sci. 164 (1–2), 38–44. https://doi.org/10.1016/j.cis.2010.12.008.
Field, R.W., Wu, D.X., Howell, J.A., Gupta, B.B., 1995. Critical flux concept for microfiltration fouling. J. Membr. Sci. 100 (3), 259–272. https://doi.org/10.1016/0376-7388(94)00265-Z.
Fox, P.F., Guinee, T.P., Cogan, T.M., McSweeney, P.L.H., 2000. Fundamentals of Cheese Science. Aspen Publishers Inc., Gaithersburg, USA.
Gonzalez Siso, M.I., 1996. The biotechnological utilization of cheese whey: a review. Bioresour. Technol. 57 (1), 1–11. https://doi.org/10.1016/0960-8524(96)00036-3.
Harland, H.A., Coulter, S.T., Jenness, R., 1952. The effect of the various steps in the manufacture on the extent of serum protein denaturation in nonfat dry milk solids. J. Dairy Sci. 35, 363–368.
Heidebrecht, H.J., Kulozik, U., 2019. Fractionation of casein micelles and minor proteins by microfiltration in diafiltration mode. Study of the transmission and yield of the immunoglobulins IgG, IgA and IgM. Int. Dairy J. 93, 1–10. https://doi.org/10.1016/j.idairyj.2019.01.009.
Juang, R.S., Lin, S.H., Peng, L.C., 2010. Flux decline analysis in micellar-enhanced ultrafiltration of synthetic waste solutions for metal removal. Chem. Eng. J. 161 (1–2), 19–26. https://doi.org/10.1016/j.cej.2010.04.007.
Katsoufidou, K., Yiantsios, S.G., Karabelas, A.J., 2005. A study of ultrafiltration membrane fouling by humic acids and flux recovery by backwashing: experiments and modelling. J. Membr. Sci. 266 (1–2), 40–50. https://doi.org/10.1016/j.memsci.2005.05.009.
Konrad, G., Kleinschmidt, T., Faber, W., 2012. Ultrafiltration flux of acid whey obtained by lactic acid fermentation. Int. Dairy J. 22 (1), 73–77. https://doi.org/10.1016/j.idairyj.2011.08.005.
Labbez, C., Fievet, P., Szymczyk, A., Vidonne, A., Foissy, A., Pagetti, J., 2002. Analysis of the salt retention of a titania membrane using a "DSPM" model: effect of pH, salt concentration and nature. J. Membr. Sci. 208 (1–2), 315–329. https://doi.org/10.1016/S0376-7388(02)00310-1.
Luján-Facundo, M.J., Mendoza-Roca, J.A., Cuartas-Uribe, B., Alvarez-Blanco, S., 2017. Membrane fouling in whey processing and subsequent cleaning with ultrasounds for a more sustainable process. J. Clean. Prod. 143, 804–813. https://doi.org/10.1016/j.jclepro.2016.12.043.
Luo, J., Ding, L., Wan, Y., Jaffrin, M.Y., 2012. Threshold flux for shear-enhanced nanofiltration: experimental observation in dairy wastewater treatment. J. Membr. Sci. 409–410, 276–284. https://doi.org/10.1016/j.memsci.2012.03.065.
Rocha-Mendoza, D., Kosmerl, E., Krents, A., Zhang, L., Badiger, S., Miyagusuku-Cruzado, G., Mayta-Apaza, A., Giusti, M., Jimenez-Florez, R., Garcia-Cano, I., 2021. *Invited review:* acid whey trends and health benefits. J. Dairy Sci. 104 (2), 1262–1275. https://doi.org/10.3168/jds.2020-19038.
Salinas-Rodríguez, S.G., Amy, G.L., Schippers, J.C., Kennedy, M.D., 2015. The Modified Fouling Index Ultrafiltration constant flux for assessing particulate/colloidal fouling of RO systems. Desalination 365, 79–91. https://doi.org/10.1016/j.desal.2015.02.018.
Samuelsson, G., Huisman, I.H., Tragardh, G., Paulsson, M., 1997. Predicting limiting flux of skim milk in crossflow microfiltration. J. Membr. Sci. 129 (2), 277–281. https://doi.org/10.1016/S0376-7388(97)00013-6.
Sats, A., Mootse, H., Pajumagi, S., Pisponen, A., Tatar, V., Poikalainen, V., 2014. Estimation of particle size distribution in bovine colostrum whey by dynamic light scattering (DLS) method. Agron. Res. 12 (3), 801–806.
Smith, K., 2014. Current and Future Processing of Whey Ingredients access. http://oregondairy.org/wp-content/uploads/2014/04/4-2014-ODI.pdf. (Accessed 12 May 2019).
Steinhauer, T., Leeb, E., Birle, D., Kulozik, U., 2016. Determination of a molecular fouling model for the micro- and ultrafiltration of whey: a recombination study from single whey proteins to complex mixtures. Int. Dairy J. 52, 50–56. https://doi.org/10.1016/j.idairyj.2015.08.006.
Steinhauer, T., Marx, M., Bogendorfer, K., Kulozik, U., 2015. Membrane fouling during ultra- and microfiltration of whey and whey proteins at different environmental conditions: the role of aggregated whey proteins as fouling initiators. J. Membr. Sci. 489, 20–27. https://doi.org/10.1016/j.memsci.2015.04.002.
Stuart, D.I., Archaya, K.R., Walker, N.P.C., Smith, S.G., Lewis, M., Phillips, D.C., 1986. α-lactalbumin possesses a novel calcium binding loop. Nature 324, 84–87. https://doi.org/10.1038/324084a0.
Tan, T.J., Wang, D., Moraru, C.I., 2014. A physicochemical investigation of membrane fouling in cold microfiltration of skim milk. J. Dairy Sci. 97 (8), 4759–4771. https://doi.org/10.3168/jds.2014-7957.
Tong, P.S., Barbano, D.M., Rudan, M.A., 1988. Characterization of proteinaceous membrane foulants and flux decline during the early stages of whole milk ultrafiltration. J. Dairy Sci. 71, 604–612. https://doi.org/10.3168/jds.S0022-0302(88)79597-1.
Treszczynska, B., Siwek, A., Kowalik, J., Lobacz, A., Zulewska, J., 2018. Influence of flavors and stabilizers used on the preferences and properties of aerated tvarog curd cheese. Acta Sci. Pol. Technol. Aliment. 17 (4), 335–346. https://doi.org/10.17306/J.AFS.2018.0591.
Verdi, R.J., Barbano, D.M., Dellavalle, M.E., 1987. Variability in true protein, casein, nonprotein nitrogen, and proteolysis in high and low somatic cell count milks. J. Dairy Sci. 70, 230–242. https://doi.org/10.3168/jds.S0022-0302(87)80002-4.
Villeneuve, W., Bérubé, A., Chamberland, J., Pouliot, Y., Labrie, S., Doyen, A., 2021. Contribution of biofouling to permeation flux decline and membrane resistance changes during whey ultrafiltration. Int. Dairy J. 117, 105010. https://doi.org/10.1016/j.idairyj.2021.105010.
Wen-qiong, W., Yun-chao, W., Xiao-feng, Z., Rui-xia, G., Mao-lin, L., 2019. Whey protein membrane processing methods and membrane foulingu mechanism analysis. Food Chem. 289, 468–481. https://doi.org/10.1016/j.foodchem.2019.03.086.
Wherry, B., Barbano, D.M., Drake, M.A., 2019. Use of acid whey protein concentrate as an ingredient in nonfat cup set-style yogurt. J. Dairy Sci. 102 (10), 8768–8784. https://doi.org/10.3168/jds.2019-16247.
Wojciechowski, K.L., Barbano, D.M., 2015. Modification of the Kjeldahl noncasein nitrogen method to include bovine milk concentrates and milks from other species. J. Dairy Sci. 98 (11), 7510–7526. https://doi.org/10.3168/jds.2015-9580.
Wong, N.P., LaCroix, D.E., McDonough, F.E., 1978. Minerals in whey and whey fractions. J. Dairy Sci. 61, 1700–1703. https://doi.org/10.3168/jds.S0022-0302(78)83790-4.
Żegarska, Z. (Ed.), 2000. Ćwiczenia Z Analizy Żywności. Wydawnictwo UWM, Olsztyn, Poland.
Zotta, T., Solieri, L., Iacumin, L., Picozzi, C., Gullo, M., 2020. Valorization of cheese whey using microbial fermentations. J. Appl. Microbiol. Biotechnol. 104, 2749–2764. https://doi.org/10.1007/s00253-020-10408-2.
Zulewska, J., Barbano, D.M., 2013. Influence of casein on flux and passage of serum proteins during microfiltration using polymeric spiral-wound membranes at 50°C. J. Dairy Sci. 96 (4), 2048–2060. https://doi.org/10.3168/jds.2012-6032.
Zulewska, J., Kowalik, J., Dec, B., 2018. Flux and transmission of β-casein during cold microfiltration of skim milk subjected to different heat treatments. J. Dairy Sci. 101 (12), 10831–10843. https://doi.org/10.3168/jds.2018-14496.

International Dairy Journal 134 (2022) 105445



Contents lists available at ScienceDirect

International Dairy Journal

journal homepage: www.elsevier.com/locate/idairyj



Microfiltration of buttermilk: Partitioning of proteins and modelling using a resistance-in-series model



Justyna Tarapata [a, *], Maciej Maciejczyk [b], Justyna Zulewska [a]

[a] Department of Dairy Science and Quality Management, Faculty of Food Science, University of Warmia and Mazury in Olsztyn, Poland
[b] Department of Physics and Biophysics, Faculty of Food Science, University of Warmia and Mazury in Olsztyn, Poland

ARTICLE INFO

Article history:
Received 19 December 2021
Received in revised form
6 June 2022
Accepted 13 June 2022
Available online 24 June 2022

ABSTRACT

The performance of microfiltration ceramic membranes was investigated in terms of protein fractionation efficacy and permeate flux when treating skimmed (0.3% fat) buttermilk. Tests were performed with a 0.1 μm alumina membrane at a transmembrane pressure of 0.2 MPa and a crossflow velocity of 6.3 m s^{-1}. Modelling of the flux was performed using the resistance-in-series model (RIS), combining fouling resistances due to concentration polarisation, adsorption and cake formation. The RIS model was appropriate to describe the main fouling mechanisms with high fitting accuracy ($R^2 > 0.93$). The predominant fouling mechanism was cake layer formation followed by adsorption. The polynomial correction of the exponential growth of mass deposited on the membrane surface was proposed. The function with polynomial correction accurately fit experimental data ($R^2 = 0.99$). Moreover, the thermal processing history of buttermilk resulted in selective transmission of α-LA. However, further studies are required to enhance the efficiency of buttermilk fractionation.

© 2022 Elsevier Ltd. All rights reserved.

1. Introduction

Buttermilk (BM) is a by-product of butter production. It is an aqueous phase of the cream released from the butter mass formed during cream churning. Buttermilk is mainly processed into powder, which has limited functional properties. Although BM powder can be added to baking goods or various dairy products, its added value is still minimal, and its full potential remains to be exploited (Morin, Britten, Jiménez-Flores, & Pouliot, 2007a). Moreover, since the share of BM in the global food market is still negligible (Barukčić, Jakopović, & Božanić, 2019), further studies on processing and potential fields of application for BM should be carried out.

In recent years, the demand for serum proteins (SP) has been increasing in the food sector (Svanborg, Johansen, Abrahamsen, & Skeie, 2015). The major SPs include β-lactoglobulin (β-LG) and α-lactalbumin (α-LA) fractions. β-LG has good emulsifying and foaming properties (Charcosset, 2021). Health benefits have also been reported for bovine α-LA. For example, α-LA contributes to infant and adult nutrition (Rocha-Mendoza et al., 2021). In infant formula, α-LA stimulates the immune system. In adults, α-LA serves as a source of bioactive peptides with antibacterial and prebiotic properties (Layman, Lönnerdal, & Fernstrom, 2018). In addition, α-LA can bind to oleic acid and form complexes that are reported to have anticancer properties (Rammer et al., 2010).

Currently, the main sources of α-LA and β-LG-rich ingredients used in the dairy industry for the production of protein concentrates are cheese whey and skim milk. The SPs derived from skim milk consist of fewer minerals and have no caseinomacropeptide compared with traditional whey proteins from cheese whey (Svanborg et al., 2015). The differences in composition result in different functional properties of both formulations. As revealed by Coppola, Molitor, Rankin, and Lucey (2014), skim milk SPs have superior sensory, foaming and storage properties compared with whey SP. Since BM's chemical composition and casein/SP ratio is similar to that of skim milk (Ali, 2019; Corredig & Dalgleish, 1977), it could serve as a good substrate for SP fractionation, which increases the value of this by-product. Recently, Svanborg et al. (2015) discussed the close similarities in physicochemical properties between SP concentrates produced from BM and skimmed milk. Their study showed that a protein concentrate from BM was equivalent to that from skim milk in its solubility, foaming properties and chemical composition. The protein profiles were comparable, but SP concentrate from skim milk had a higher content of casein (Svanborg et al., 2015). Despite the promising properties, so far, the

* Corresponding author.
E-mail address: justyna.tarapata@uwm.edu.pl (J. Tarapata).

https://doi.org/10.1016/j.idairyj.2022.105445
0958-6946/© 2022 Elsevier Ltd. All rights reserved.

process-oriented isolation of SP from BM has not been thoroughly explored. The majority of studies on BM have been focused on the isolation of MFGM components due to their bioactive properties (Ali, 2019). However, in the future, a technology for the isolation and the use of BM SP for consumption could be developed.

To date, microfiltration (MF) has been considered an efficient technique to fractionate BM into casein and milk fat globule membrane (MFGM)-rich retentate and SP-rich permeate (Morin, Britten, et al., 2007a; Svanborg et al., 2015). However, fouling is one of the major drawbacks in the industrial implementation of membrane processes. It gradually reduces the permeate flux, increases the hydraulic resistance and changes the selectivity of the membrane (Tan, Wang, & Moraru, 2014). To design a cost-effective filtration process, the optimum flux should be selected. The optimum flux means the flux at which an acceptable degree of fouling is created and which can be easily removed with standard cleaning procedure (Damar, Cinar, & Gulec, 2020). The basis for developing solutions to minimise membrane fouling and thus increase product yields during membrane filtration is to understand the fouling mechanisms (Tan et al., 2014). According to Katsoufidou, Yiantsios, and Karabelas (2005) and Luján-Facundo, Mendoza-Roca, Cuartas-Uribe, and Álvarez-Blanco (2017), the mechanisms of flux reduction during filtration of protein-based solutions are a result of both concentration polarisation (accumulation of solute on the membrane surface) and membrane fouling. They can be predicted with mathematical models. Among the different mathematical models available in the literature, the resistance-in-series model (RIS) is the most often used. In recent studies in the field of dairy science, Corbatón-Báguena, Álvarez-Blanco, and Vincent-Vela (2018) fitted a RIS model to the experimental data obtained during the ultrafiltration of whey model solutions with high accuracy (coefficient of determination $R^2 > 0.95$). Those authors included two fouling resistances: the resistance due to adsorption and concentration polarisation and the resistance due to cake layer formation.

As the overall process productivity and chemical composition of the obtained fractions depends on membrane performance, the aim of this work was to examine the MF process of BM (using ceramic graded permeability membranes) in terms of the efficacy of SP fractionation and fouling mechanisms that affect membrane performance. The experimental data were fitted to the RIS model. A time-based evolution of model parameters was determined, and the predominance of each fouling resistance as a function of time was investigated. Moreover, exponential time dependence was proposed to describe changes in protein mass deposited on the membrane surface during MF.

2. Materials and methods

2.1. Modelling using resistance-in-series model

The resistance-in-series model (RIS) is particularly applicable for the analysis of flux decline in MF or UF of protein-based solutions (Corbatón-Báguena et al., 2018). The RIS model applied in this study considers the following fouling mechanisms: adsorption, concentration polarisation and cake formation. In this regard, the permeate flux of the cross-flow MF process (J_p) is described by Eq. (1) (Juang, Chen, & Chen, 2008a):

$$J_p = \frac{TMP}{\mu \times (R_m + R_{ads} + R_{cp} + R_{cl})} \quad (1)$$

where *TMP* is the transmembrane pressure, μ is the viscosity of the feed, R_m is the hydraulic resistance of the membrane itself, R_{ads} is the resistance due to the adsorption of solute on the membrane surface, and also on the pore walls, R_{cp} is the resistance due to concentration polarisation, and R_{cl} is the resistance of the cake layer.

The R_m is determined during the clean water flux (*CWF*) measurements. According to Eq. (1), when the clean water is used as feed, R_{ads}, R_{cp} and R_{cl} are negligible. Eq. (2) shows the calculation of the membrane resistance:

$$R_m = \frac{TMP}{\mu \times CWF} \quad (2)$$

According to previous research conducted by Carrere, Blaszkow, and de Balmann (2001) and Juang, Chen, and Chen (2008b), the experimental variations of R_{ads} and R_{cp} follow an exponential trend that makes these resistances grow at a rate constant b up to a steady-state (ss) values of $R_{ads,ss}$ and $R_{cp,ss}$. Moreover, both mechanisms are simultaneously determined during crossflow filtration experiments and expressed as a one fixed value of $R_{ads,ss} + R_{cp,ss}$ (Eq. (3)):

$$R_{ads} + R_{cp} = (R_{ads,ss} + R_{cp,ss}) \times [1 - \exp(-b \times t)] \quad (3)$$

where $R_{ads,ss}$ is the resistance due to solute adsorption at the steady-state and $R_{cp,ss}$ is the resistance due to concentration polarisation at the steady-state, t is the filtration time. The sum of $R_{ads,ss} + R_{cp,ss}$ and the value of b are determined by fitting experimental data and model equations (Corbatón-Báguena et al., 2018; Juang et al., 2008a).

The resistance caused by the formation of the cake layer (R_{cl}) is defined by Eq. (4):

$$R_{cl} = \left(\frac{m_{dep}}{A_m}\right) \times \alpha \quad (4)$$

where m_{dep} is the protein mass deposited on the membrane surface, A_m is the membrane area and α is the specific cake resistance. The value of α is determined by fitting experimental data and the model equation (Corbatón-Báguena et al., 2018).

Once the permeate flux and protein rejection are known, the changes in protein concentration in the retentate at each time interval can be calculated from Eq. (5) (Juang et al., 2008b):

$$C = \frac{C_0\left[V_0 - (1-\beta)A_m \int_0^t J_p dt\right]}{V_0 - A_m \int_0^t J_p dt} \quad (5)$$

where C is the protein concentration in the retentate stream, V_0 is the initial volume of the feed, and β is the rejection of protein calculated at a steady-state in flux (in this study: the last measured flux value) from Eq. (6):

$$\beta = 1 - \left(\frac{C_p}{C_0}\right) \quad (6)$$

where C_p and C_0 are the concentration of protein in permeate at the steady-state and in the feed, respectively.

Under certain assumptions, the mass deposited on the membrane surface (m_{dep}) can be determined by means of mass equation balance (Eq. (7)) (Juang et al., 2008b):

$$\frac{dm_{dep}}{dt} = A_m \times C \times \left(J_p - J_{p,f}\right) \quad (7)$$

where $J_{p,f}$ is the average permeate flux at the end of the test.

Based on the study of Carbonell-Alcaina et al. (2016), who successfully expressed R_{cl} as an exponential function of time and

considering the fact that R_{cl} depends on protein mass deposited on the membrane surface, in this work, a general equation that accounts for the protein mass deposition on the membrane surface as a function of time was newly proposed and represented in Eq. (8):

$$m_{dep} = m_{dep,ss}[1 - exp(-c \times t)] \quad (8)$$

where $m_{dep,ss}$ is the mass deposited on the membrane surface in the steady-state and c is the rate of protein mass deposit development. The $m_{dep,ss}$ and c can be determined by fitting the m_{dep} values calculated based on Eq. (7) and experimental data to the proposed model.

Substituting Eq. (3), Eq. (4) and Eq. (8) in Eq. (1), the general equation for the RIS model can be obtained (Eq. (9)):

$$J_p = \frac{TMP}{\mu \times \left[R_m + (R_{ads,ss} + R_{cp,ss}) \times [1 - \exp(-b \times t)] + \left(\frac{m_{dep,ss}[1-\exp(-c \times t)]}{A_m}\right) \times \alpha\right]} \quad (9)$$

2.2. Pre-treatment of buttermilk

Three batches of BM (~200 kg each) were supplied by the Dairy Cooperative SM Mlekovita (Poland) and delivered to the Dairy Research and Development Centre (DRDC) located at the University of Warmia and Mazury in Olsztyn. Upon arrival at the DRDC pilot-scale processing plant, the BM was skimmed by a cream separator (model LWG20 centrifuge, Spomasz, Gniezno, Poland) to ~0.3% fat at 45 °C to minimise the differences in the residual fat in the three investigated batches. The average (n = 6) total solid content of the BM after skimming was 8.61 ± 0.22%, and the pH was 6.68 ± 0.10. Next, the BM was subjected to pasteurisation with a heat plate exchanger (model P20-HB; Alfa Laval, Lund, Sweden) at 72 °C for 15 s. After pasteurisation, the MF feed was cooled to 50 °C (processing temperature) and kept at this temperature for a maximum of 30 min before fractionation.

2.3. Microfiltration of buttermilk and membrane cleaning

A pilot-scale graded permeability (GP) MF system (Fig. 1) equipped with Membralox ceramic membranes (model EP1940GL0.1μAGP1020, Alumina, Pall Corp., East Hills, NY, USA) was used to microfilter BM. The membranes (pore diameter of 0.1 μm; total surface area of 0.72 m^2) in a tubular single stainless steel module, consisted of three ceramic tubes (0.24 m^2 each), with 19 channels each with a 4 mm channel diameter. They were 1.02 m long and were mounted vertically in the system. The GP MF unit was equipped with a feed pump (type LKH-10-155-FSS-DIN 3.0 kW) and a retentate recirculation pump (type LKH-10-155-FSS-DIN 4.0 kW), both from Alfa Laval (Kansas City, MO, USA).

Immediately before the processing, a short cleaning procedure of the MF unit was applied. The storage solution was flushed out of the system with 23 °C reverse-osmosis (RO) water until the pH was neutral. The MF system was heated with RO water to 75 °C, and then Divos 120CL VM9 (Diversey, Fort Mill, SC, USA) liquid alkaline membrane cleaner (1.0–1.5%, v/v) was added to the water. The alkaline solution was recirculated for 30 min at a permeate flow of approximately 1000 L h^{-1}, the retentate flow was approximately 5000 L h^{-1}, and all pumps were on. Following the cleaning, the membrane system was slowly cooled (<10 °C per min) to 25 °C with the tubular heat exchanger assembled within the unit. The alkaline cleaning solution was flushed out from the unit with RO water (25 °C) until neutral pH was restored. The prerun clean water flux (CWF) was then determined. The prerun CWF was calculated based on the weight of permeate collected in 90 s and the total membrane surface area. The following conditions were applied during the prerun CWF measurement: temperature of 25 °C, the retentate pressure inlet (R_{pi}) 0.32 MPa, the retentate pressure outlet (R_{po}) 0.20 MPa and the permeate outlet valve fully opened, resulting in a retentate flow of approximately 7000 L h^{-1} and a permeate flow of approximately 750 L h^{-1}. Both pumps were on. According to Zulewska, Kowalik, and Dec (2018), the alkaline cleaning applied prior to the processing is very important to restore the flux. The water flux measured after acidic storage is much lower compared with the values for the measurement done after alkaline cleaning. The measured CWF was used to calculate the R_m value according to Eq. (2) in Section 2.

The pre-treated BM (approximately 160 kg) was microfiltered at 50 °C with a GP MF system described above. The BM was placed in the feed tank with all valves closed except the retentate valve. The BM was recirculated for 5 min, and the permeate valve was then fully opened. Next, the position of the retentate outlet valve was slowly adjusted to balance the flows of retentate and permeate to achieve a 3-fold concentration. At a concentration factor (CF) of 3, the average permeate removal rate was 16.9 L h^{-1}. The constant transmembrane pressure (TMP) was kept at 0.20 ± 0.01 MPa. Typical R_{pi} and P_{po} were 0.25 MPa and 0.15 MPa, respectively, and the permeate valve was fully opened (resulting in P_{po} of 0 MPa). The crossflow velocity was about 6.3 m s^{-1}. The weight of the collected permeate was monitored every 30 min to determine the changes of flux in time. Flux (L m^{-2} h^{-1}) was calculated based on permeate

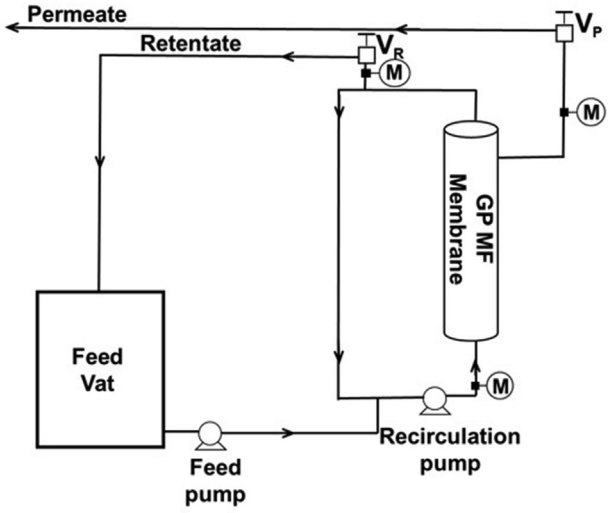


Fig. 1. Simplified scheme of MF system used in the study: M, manometer, V_R, retentate outlet valve, V_P, permeate outlet valve.

weight collected during 30 min and the total filtration area according to Eq. (10):

$$J_p = \frac{M \times 1000}{A_m \times t \times \rho} \quad (10)$$

where M is the permeate weight (kg), A_m is the membrane surface area (m^2), t is time (h), and ρ is the permeate density at the operating temperature (kg m^{-3}).

The retentate and permeate removal flow rates were adjusted every 30 min to keep a CF of 3. Firstly, the retentate and permeate were collected continuously in separate stainless steel tanks (feed and bleed mode) and cooled to 3 °C. After approximately 2.5 h of filtration, the retentate stream was recycled into the feed vat to obtain higher yields of permeate and a final CF of 3. Before the recirculation started, approximately 28 kg of retentate was collected. At the end of the MF run, all retentate and all permeate from the processing run were mixed, and each was sampled. The average total time of BM processing was about 6 h. The MF experiment was replicated three times.

Immediately after processing, 25 °C RO water was flushed through the system with all pumps on. The retentate and permeate removal rates were set at approximately 5000 L and 1000 L, respectively. The MF system was flushed until no BM was visible in the flush water on the retentate side. When the water flush was complete, the fouled membrane water flux (FWF) was determined using the same settings as for prerun CWF. Typically, the fouled membrane flux was about 13 ± 1% of the initial clean membrane water flux (50 ± 4 versus 389 ± 11 L m^{-2} h^{-1}). Next, the MF unit was heated with RO water to 70 °C. The alkaline solution of Divos 120CL VM9 was added to hot RO water in the feed tank (1.0–1.5%, v/v), and the procedure was performed under the same parameters as prior to the MF of BM. After cleaning, the membrane was flushed with 25 °C RO water until neutral pH was reached and the post-run CWF was determined according to the protocol applied in prerun CWF measurement. The post-run CWF was close to the prerun CWF (381 ± 13 L m^{-2} h^{-1}). After determination of the post-run CWF, the MF flow system was heated to 65 °C, and an acidic solution (Pascal VA5, conc. 1.0%, v/v, Diversey, Fort Mill, SC, USA) was recirculated through the membrane at 65 °C for 30 min. After that, the MF system was cooled to 40 °C and then flushed with RO water (25 °C) until neutral pH was reached.

2.4. Collection of foulants

To gain insight into the state of membrane fouling, RO water rinsing steps were performed immediately after the MF run to collect foulant streams according to the modified method described by Tan et al. (2014).

Foulants attached to the membrane surface (external foulants, F_e) and foulants located inside the pores (internal foulants, F_i) were collected during the water flushing stage of the cleaning procedure performed after the MF run. First, the filtration unit was flushed with RO water (four rinsing steps, each of 60 L for 3 min each) at 25 °C to wash out the BM residue from the system. The MF system was flushed until no BM was visible in the flush water on the retentate side. Then, additional two rinsing steps were carried out to collect F_e and F_i, respectively. First, an RO water rinse (approximately 60 L) was conducted with the permeate valve fully closed and the retentate valve fully opened. The RO water rinse was performed for 5 min at 25 °C. The rinse water collected in this manner contained external foulants (F_e) attached to the membrane surface. The samples were collected directly from the retentate outlet after 5 min of circulation. Next, the system was drained to wash out the residual rinsing solution, and another RO water flushing (approximately 60 L, 25 °C) was conducted with the permeate valve fully opened, and the retentate valve fully closed to collect the internal foulants (F_i) attached to the pore walls. The samples were collected directly from the permeate outlet after 5 min of circulation. Both F_e and F_i were collected under the same parameters (temperature of 25 °C, crossflow velocity of 10.3 m s^{-1}) as described in the cleaning procedure in section 2.3. After the foulant collection, the cleaning procedure was continued.

2.5. Fouling coefficient (F_c)

To represent the extent of fouling of the membrane, F_c was calculated according to Rao (2002) with Eq. (11):

$$F_c = 1 - (FWF \,/\, prerun\ CWF) \quad (11)$$

where FWF is fouled water flux, and prerun CWF is the flux of pure water. The F_c varies between 0 (not fouled membrane) and 1 (completely fouled membrane).

2.6. Physicochemical analyses

The BM and final MF products (retentate and permeate) were subjected to physicochemical analysis. The pH was measured using a pH meter (CP-401, Elmetron, Zabrze, Poland) equipped with an electrode IJ-44C IONODE (Elmetron). Total solids (TS) were analysed according to AOAC International method 990.20; 33.2.4 (AOAC, 2007). Total nitrogen (TN), noncasein nitrogen (NCN), and nonprotein nitrogen (NPN) were examined using the Kjeldahl method (AOAC International method 991.20; 33.2.11; AOAC, 2007), the Kjeldahl method (AOAC International method 998.05; 33.2.64; AOAC, 2007) with modifications according to Wojciechowski and Barbano (2015), and the Kjeldahl method (AOAC International method 991.21; 33.2.12; AOAC, 2007), respectively. Determination of fat was performed based on the Rose-Gottlieb method (IDF, 1987a). The amount of lactose was estimated using Milko-Scan™ FT2 (Foss, Hillerød, Denmark). The analysis of ash was performed using the muffle furnace technique at 530 °C (PN-A-86364:1996). Total calcium content was determined using atomic absorption spectrometry (AAS) according to the method of IDF (2007) at the wavelength of 422.7 nm. Total phosphorus content was evaluated by a colorimetric analysis (Żegarska, 2000), and the absorbance was measured using a Carry 60 UV–Vis (Agilent) spectrophotometer at the wavelength of 610 nm. The viscosity was determined using a rotational rheometer (RheolabQC, Anton Paar, Graz, Austria) at a shear rate of 100 s^{-1} and a temperature of 50 °C. The density was measured with an automatic handheld density meter (Densito, Mettler Toledo, Greifensee, Switzerland) with an accuracy of ±0.001 g cm^{-3}.

2.7. SDS-PAGE electrophoresis

To identify the proteins present in MF streams and proteins attached to the membrane surface and pore walls contributing to external and internal fouling, respectively, an SDS-PAGE electrophoresis on 12% polyacrylamide gel (Biorad Laboratories, Warsaw, Poland) was used. The fresh samples of BM, MF retentate and MF permeate were diluted with a sample buffer (pH 6.8, 10 mM Tris–HCl, 1.0% SDS, 20% glycerol, 0.02% bromophenol blue tracking dye, and 50 mM dithiothreitol), then immersed in boiling water for 3 min and kept frozen (−26 °C) in plastic vials (Eppendorf microtubes, 3810X; Merc, Darmstadt, Germany) until analysis. Due to the small TS content (data not shown), samples of F_e and F_i (20 g each) were first frozen at −26 °C, lyophilised for 72 h at 0.18 bar (Freeze dryer Alpha 1e2 LD, Christ, Germany), then diluted with 100 μL of

sample buffer, immersed in boiling water for 3 min and kept frozen (−26 °C). Before the analysis, all samples were thawed at room temperature, and the wells were then loaded with 22.4 μg protein per loading for BM, retentate and permeate, and with 10 μL of F_e and F_i sample per loading. In addition, 4 μL of an SDS-PAGE molecular mass standard (Dual Xtra Standard, Bio-Rad) was applied to one well. Running, staining and destaining procedures were performed according to Verdi, Barbano, Dellavalle, and Senyk (1987). The destained gels were scanned using a Lumi Bis Bioimaging Systems DNR scanner (Jerusalem, Israel) and analysed using TotalLab 1D v 11.3 (Newcastle, UK).

2.8. Statistical analysis and model fitting procedure

All physicochemical analyses were carried out in triplicate. The statistical analysis was performed using the Statistica software (version 13.1, 1984–2016, StatSoft, Inc., Tulsa, OK, USA). The statistical evaluation of the data was conducted using a one way ANOVA ($P < 0.05$) followed by Tukey's post hoc test. The mathematical model explained in Section 2 was fitted to the experimental data using Microsoft Excel's add-in Solver and LabPlot software (LabPlot Team, 2022). The non-linear least-squares minimisation was performed to minimise the difference between the experimental and predicted data. The fitting accuracy was evaluated using the regression coefficient (R^2) and the standard deviation (SD).

3. Results and discussion

3.1. Microfiltration flux – experimental and model

The MF process of BM was conducted until reaching CF of 3.21 ± 0.05. The average permeation flux noted was 23.4 L m^{-2} h^{-1}. The evolution of permeate flux with time obtained during the MF experiments is shown in Fig. 2. The flux decline during the first minutes of operation was more rapid than in later stages of the process, as was expected and reported previously (Hansen et al., 2018; Zulewska et al., 2018). According to Juang, Lin, and Peng (2010) and Carbonell-Alcaina et al. (2016), the initial permeate flux decline with time is due to the pore-blocking phenomena, which is usually followed by the formation of a cake layer.

The recirculation of retentate, which started after 2.5 h of processing, caused no sudden or substantial changes in the rate of flux decline with time. There was no significant difference ($P > 0.05$) in the rate of flux decline noted between two subsequent measurements (the last measurement before recirculation was started and the first measurement after recirculation was started, data not shown). Following recirculation, the permeation flux decreased gradually under the constant rate from the third hour of MF until the end of processing. This was reflected in nonsignificant ($P > 0.05$) changes between the rate of flux decline noted from the third hour until the end of the MF process.

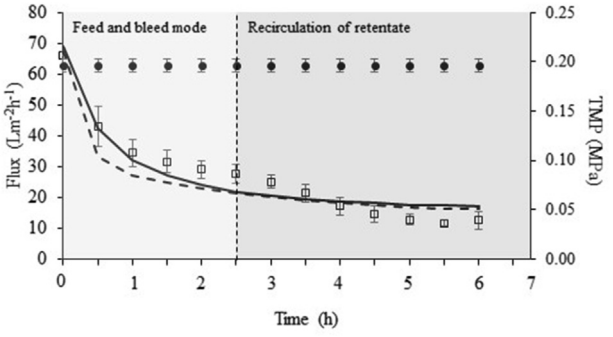


Fig. 2. Time evolution of the permeate flux and transmembrane pressure (TMP) noted during MF of buttermilk. Solid line represents standard resistance-in-series model predictions, dotted line represents corrected model predictions and symbols represent experimental data: □ flux; ● TMP. Error bars represent one standard deviation. Some error bars are too small to be visible in the figure.

The percentage of flux decline obtained at the end of the MF process was 71 ± 5%, and the calculated F_c was 0.88 ± 0.01, indicating severe fouling of the ceramic membrane used. Comparison with other flux decline or F_c values reported in the literature is difficult due to different processing conditions. Nevertheless, similar to the current study, Rombaut, Dejonckheere, and Dewettinck (2006) observed F_c values of 0.98 during the MF (50 °C, TMP = 0.1 MPa) of butter serum (9.78% of TS) on cellulose acetate membranes with a pore diameter of 0.15 μm. The authors suggested that the higher the dry matter content, the more pronounced the fouling was. In the current experiment, the TS of BM (8.61%, Table 1) was slightly lower than that reported by Rombaut et al. (2006), and it resulted in a slightly lower F_c. Additionally, the authors reported that more intense pore blocking by casein micelles is most likely the cause of the high fouling rate. Moreover, according to Rao (2002), a higher F_c may indicate the presence of a deposit layer strongly adhering to the membrane surface, which could not be easily removed by rinsing. As revealed by SDS-PAGE electrophoresis of the foulants (Fig. 3) conducted in the current study, casein was the major protein responsible for both pore blocking and cake layer formation. However, apart from casein, the cake layer was also composed of high molecular mass SP (i.e., lactoferrin). According to Morin et al. (2007a), casein accumulates at the surface of the membrane, creating a porous layer that limits permeation. Therefore, it appears that during the MF process of BM, the flux is mainly controlled by the adsorption of casein to the pore walls and the formation of a cake layer composed of casein and high molecular mass SP. Additionally, based on similar prerun and postrun CWF values, it can be stated that water flux was restored after the cleaning procedure, indicating a reversible form of fouling existing in the study.

To gain some insight into the fouling mechanism controlling the flux over the MF process of BM, the RIS model (which accounts for the time evolution of the fouling resistances) was fitted to experimental data obtained in the current study. As described in Section 2 (Eq. (1)), the total hydraulic resistance is the sum of the original

Table 1
Chemical composition and pH of buttermilk and products of microfiltration (MF) process: MF retentate and MF permeate.[a]

Milk component	Buttermilk		MF retentate		MF permeate	
	Mean	SD	Mean	SD	Mean	SD
TS (%)	8.61	0.22	14.47	0.90	5.25	0.07
TN (%)	2.80	0.10	7.43	0.70	0.25	0.03
NCN (%)	0.31	0.01	0.40	0.07	0.22	0.01
NPN (%)	0.16	0.02	0.17	0.02	0.16	0.01
TP (%)	2.64	0.11	7.26	0.69	0.09	0.02
Casein (%)	2.49	0.11	7.03	0.73	0.03*	0.03
SP (%)	0.15	0.02	0.23	0.08	0.06	0.02
Lactose (%)	4.74	0.05	4.35	0.02	4.77	0.12
Fat (%)	0.27	0.02	1.29	0.41	0.04	0.01
Ash (%)	0.66	0.01	1.00	0.05	0.46	0.01
Ca (mg L^{-1})	843	379	2442	669	323	81
P (mg 1000 g^{-1})	666	47	1013	318	450	230
pH	6.68	0.10	6.51	0.18	6.46	0.03

[a] Abbreviations are: NCN, noncasein nitrogen; NPN, nonprotein nitrogen; TN, total nitrogen; TP, total protein [(TN −NPN) × 6.38]; casein, (TN − NCN) × 6.38; SP, TP − casein. Values are expressed as means (n = 6) and their standard deviation (SD); an asterisk indicates that the result obtained should not be taken under consideration due to the large standard deviation. Additionally the results of SDS-PAGE electrophoresis confirmed that casein was not present in MF permeate.

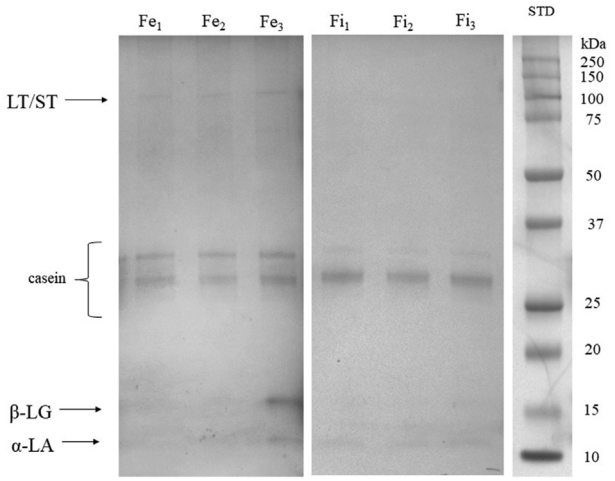


Fig. 3. Sodium dodecyl sulphate-PAGE patterns of external (F_e) and internal (F_i) foulants located on the membrane surface and inside the pores, respectively, collected after microfiltration of buttermilk. Subscripts indicate replicates. Lane STD was loaded with 4 μL of molecular mass standard. Numbers to the right of lane STD indicate molecular masses (kDa). Identification of proteins is provided on the left side of the figure: LT, lactotransferrin; ST, serotransferrin; β-LG, β-lactoglobulin; α-LA, α-lactalbumin.

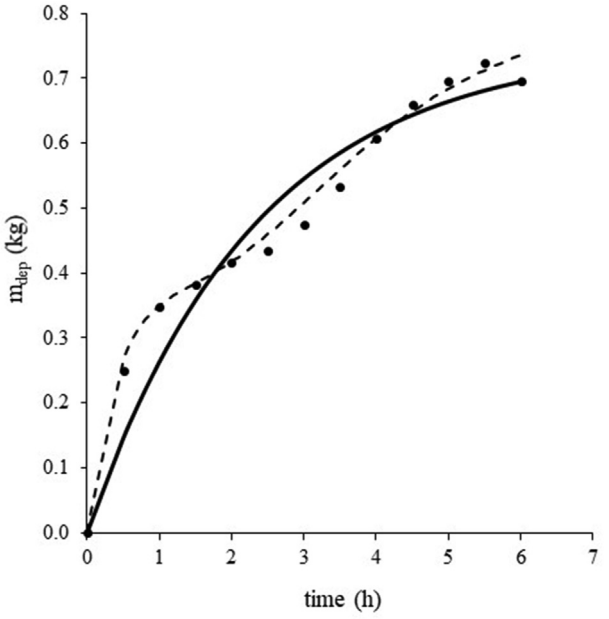


Fig. 4. Fitted analytical curves of standard (solid line) and corrected (dotted line) models of mass deposited on the membrane surface.

membrane resistance (R_m), the adsorption and concentration polarisation resistance ($R_{ads} + R_{cp}$), and the cake layer resistance (R_{cl}). While R_m is characteristic of the membrane and remains constant during the experiment, $R_{ads} + R_{cp}$ and R_{cl} may vary with time (Carbonell-Alcaina et al., 2016; Corbatón-Báguena et al., 2018). As the R_{cl} is the function of protein mass deposited on the membrane surface (m_{dep}), a general equation that accounts for the changes in deposit mass as a function of time was newly proposed based on the results obtained in this work (Eq. (12)):

$$m_{dep}(t) = m_{dep,ss}\,[1 - exp(-c \times t)] \tag{12}$$

where $m_{dep,ss}$ is a steady-state deposited mass, and c is a time constant which describes the speed of the cake formation. Eq. (12) is the functional form of the solid line presented in Fig. 4 and refers to a standard model. The solid line was fitted to the average values of experimental data using LabPlot software. The fitted parameters for the standard model with their uncertainties are collected in Table 2. According to Eq. (12), the predicted $m_{dep,ss}$ for the steady-state, corresponding to the last flux measurement performed during BM processing, equals 0.750 kg. This value is very close to the protein mass loss calculated based on the mass balance after MF of BM (Table 3). However, the mass loss refers to the proteins that were 'trapped' within the whole system, not only the membrane. Whereas m_{dep} is the mass of proteins deposited on/in the membrane. The average density of proteins is approximated to 1.47 ± 0.05 kg dm^{-3} (Quillin & Matthews, 2000). Therefore, if all channels of the membrane are filled with pure proteins theoretical maximum of protein mass deposition is 1.07 ± 0.04 kg, significantly more than m_{dep} estimated in our experiment. Of course one should not expect that the membrane is filled only with proteins, as significant amount of water molecules should still be present. We can estimate the volume of water which should be present in the membrane. Simple physical considerations lead to $V_{w,s} = 0.22 \pm 0.04$ dm^3 and $V_{w,c} = 0.19 \pm 0.03$ dm^3 for $m_{dep,s} = 0.75 \pm 0.06$ kg (standard model) and $m_{dep,c} = 0.80 \pm 0.04$ kg (corrected model), respectively. Based on this result we can postulate that roughly 2/3 of the total volume of membrane is filled with proteins and 1/3 with water. These results show that mass of deposited protein obtained from the proposed model is perfectly possible, although proteins in the membrane must be very densely packed and most of bulk water must be removed.

It should be noted that the investigated process is affected by the change of processing conditions from feed and bleed process to recirculation mode, which generates a visible disturbance of exponential growth of the deposited mass in the approximate time interval 1–4 h. Therefore, the authors propose an analytical polynomial correction of the fitted function which models this effect. Thus, another function of the following form was fitted to the experimental data:

$$m_{dep}(t) = m_{dep,ss}[1 - g(t) \times exp(-c \times t)] \tag{13}$$

where $g(t) = d \times t^2 + e \times t + f$ is the polynomial correction of the exponential growth. The results of fitting are collected in the last column of Table 2. The quality of the fit of the corrected function (dotted line) is significantly better than that of the standard one (see solid line in Fig. 4). The deposited mass only slightly increased (within the estimated error) compared with that obtained from the standard model. The time constant c increased more than twice, although it should be noted that the time-dependence of this process does not depend only on this parameter in the corrected model but also on d, e and f parameters. Further research is needed to gain insight into the definition and interpretation of additional parameters.

The modelled (standard and corrected) permeation fluxes are plotted in Fig. 2. The values of model parameters and fitting accuracy are shown in Table 4. The RIS model accurately fit the experimental data with $R^2 > 0.93$ and SD < 0.04. The values of

Table 2
The parameters fitted to experimental data within standard and corrected model.

Parameter	Standard model	Corrected model
$m_{dep,ss}$ (kg)	0.75 ± 0.06	0.80 ± 0.04
c (s^{-1})	1.2 ± 0.2 × 10^{-4}	2.6 ± 0.3 × 10^{-4}
d (s^{-2})	–	4.8 ± 1.4 × 10^{-8}
e (s^{-1})	–	−5.3 ± 3.0 × 10^{-5}
f	–	1.00 ± 0.03
R^2	0.93	0.99

Table 3
The protein mass (kg) balance after microfiltration (MF) of 159 kg of buttermilk (BM).[a]

Buttermilk (159 kg)		MF retentate (46 kg)		MF permeate (109 kg)		Loss of protein mass (kg)	
Mean	SD	Mean	SD	Mean	SD	Mean	SD
4.19	0.18	3.36	0.32	0.12	0.03	0.71	0.24

[a] Values are expressed as means and their SD (n = 3).

Table 4
Values of the fitting parameters for the resistance-in-series model and the goodness of fit.[a]

Model	$R_{ads,ss} + R_{cp,ss}$ ($\times 10^{12}$ m^{-1})	b (s^{-1})	$R_{cl,ss}$ ($\times 10^{13}$ m^{-1})	α ($\times 10^{13}$ mkg^{-1})	$m_{dep,ss}$ (kg)	c ($\times 10^{-4}$ s^{-1})	Goodness of fit	
							R^2	SD
Standard	8.029	0.238	3.005	3.118	0.75	1.2	0.951[a]	0.015
Corrected	8.029	0.238	3.184	3.118	0.80	2.6	0.934[a]	0.037

[a] Abbreviations are: $R_{ads,ss} + R_{cp,ss}$, the resistances caused by adsorption and concentration polarisation at the steady state; b, rate of growth of the resistances due to adsorption and concentration polarization; $R_{cl,ss}$, resistance caused by the growth of the cake layer at the steady state; α, specific cake resistance; $m_{dep,ss}$, mass deposited on the membrane surface at the steady state; c, the rate of protein mass deposit growth; R^2, coefficient of determination, SD, standard deviation. Means within a column with different superscripts are significantly different ($P < 0.05$).

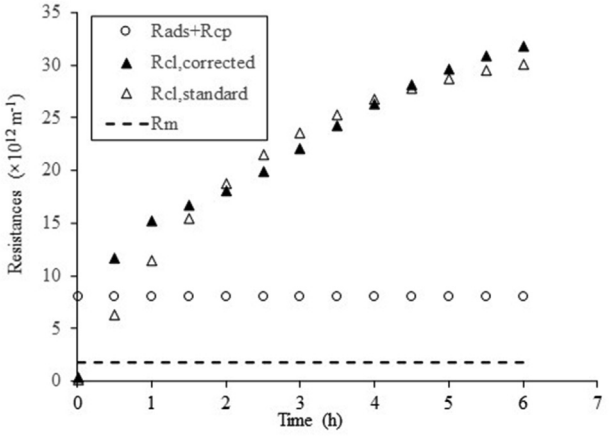


Fig. 5. Time evolution of the fouling resistances during MF of buttermilk calculated with RIS model. $R_{ads} + R_{cp}$ = the resistances due to adsorption and concentration polarisation, $R_{cl,standard}$ = resistance due to the growth of the cake layer calculated according to standard model, $R_{cl,corrected}$ = resistance due to the growth of the cake layer calculated according to corrected model R_m = clean membrane resistance.

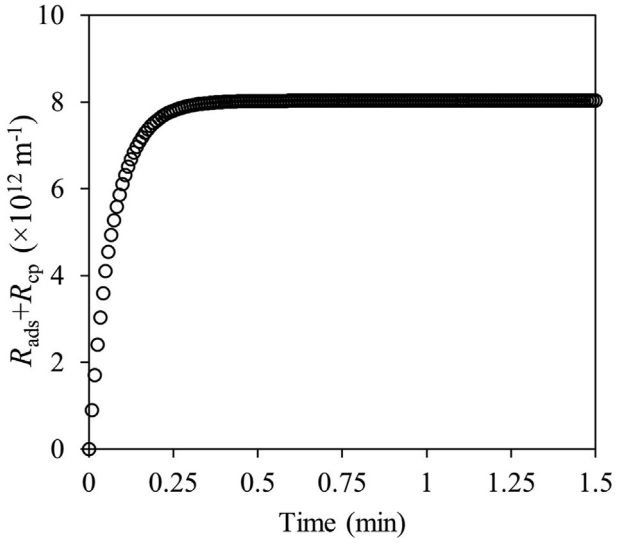


Fig. 6. Initial predicted evolution of the resistance due to adsorption and concentration polarisation ($R_{ads} + R_{cp}$) during MF of buttermilk. The $R_{ads} + R_{cp}$ increased during first seconds of MF process and then reached constant value unchanged until the end of processing.

$R_{ads,ss} + R_{cp,ss}$ and $R_{cl,ss}$ shown in Table 4 correspond to the steady-state filtration. Since the $R_{cl,ss}$ obtained in this test was greater than $R_{ads,ss} + R_{cp,ss}$ (3×10^{13} versus 8×10^{12} m^{-1}), the cake formation mechanism dominated at the steady-state for the operating parameters applied. In Fig. 5, the evolution of different resistances with time is shown. It can be observed that at the beginning of the MF process, the dominant resistance is due to adsorption (either on the surface or on the pore walls of the membrane) and concentration polarisation. At the start of the test, a rapid increase in adsorption and concentration polarisation resistance ($R_{ads} + R_{cp}$) takes place. In Figs. 5 and 6, it can be observed that the maximum value of the resistance due to adsorption and concentration polarisation was achieved at very low time scales, while the growth of the cake resistance was slower. Adsorption of proteins onto the membrane surface at the early stages of filtration has also been reported by Tong, Barbano, and Rudan (1988), who examined the mechanism of membrane fouling by only submersing membranes in milk. However, as the MF time advances, the initial pattern for both permeate flux and hydraulic resistance slows down due to the gradual growth of the cake layer (Fig. 5). The change in the dominant fouling mechanism from adsorption and concentration polarisation to the cake layer formation was noted in this experiment after less than 1 h of the MF process.

To the best of the authors' knowledge, there are a limited number of studies that consider the RIS model and account for the time evolution of the fouling resistances during membrane filtration of liquid dairy products. Recently, Corbatón-Báguena et al. (2018) reported on the fitting accuracy of the RIS model to the permeation resistance noted during UF of whey model solutions. Based on that research, some similarities between the UF of whey model solutions performed with 15 kDa ceramic membrane and the MF process performed in the current study can be identified. During the UF of WPC solution (44.4 g L^{-1}), the resistance due to cake formation increased over the entire ultrafiltration time, being predominant at the end of the filtration process. Moreover, the parameter $R_{cl,ss}$ (characterising the resistance due to the cake layer at the steady-state in the UF process of WPC solutions) was similar to that obtained during the filtration of BM in the current study (~3×10^{13} m^{-1}). However, the structure of this layer would differ significantly due to the different protein compositions of tested feeds. This was reflected in different α values calculated in both studies. It was previously observed that this parameter increases as

the size of the molecules in the feed solution decreases (Salinas-Rodriguez, Amy, Schippers, & Kennedy, 2015). This pattern can be clearly distinguished when comparing the values of α obtained by Corbatón-Báguena et al. (2018) (28.39×10^{13} m kg^{-1}) and α from this study (3.118×10^{13} m kg^{-1}, Table 4). Filtration of the feed containing whey proteins characterised by a particle size of 1–40 nm resulted in higher specific cake resistance than that calculated after MF of BM containing casein micelles with a particle size of 70–1000 nm.

3.2. Composition of MF fractions

The average composition of MF fractions from BM is shown in Table 1. More than a 3-fold concentration of BM resulted in an almost 1.7-fold concentration of TS and an almost 3-fold increase in casein content. Rejection rates (R) were also calculated and are shown in Table 5. The 0.1 μm ceramic membrane rejected nearly 100% of casein present in the feed. Fat was also well retained by the membrane, as the rejection coefficient was about 91.9% (Table 5). Quite high R values were observed for ash (~55.6%), which is also reflected in retention calculated for Ca (87.7%). A comparable rejection of lipids and ash (89% and 59%, respectively) was reported by Morin et al. (2007a), who microfiltered BM on a 0.5 μm ceramic membrane. However, in the abovementioned research, the high R factors were obtained after a 4-fold concentration of BM followed by diafiltration. Additionally, a 0.5 μm membrane enabled (to some extent) the separation of MFGM proteins (retained in retentate) from SP and casein, which were transmitted through the membrane to the permeate stream. In conclusion, the establishment of the concentration polarisation layer at the very beginning of the MF process and subsequent formation of a cake layer composed of casein micelles could have influenced the selectivity of the 0.1 μm membrane used in the current study, resulting in improved rejection of other milk components. Such a change in membrane selectivity resulted in the different and still potentially beneficial composition of obtained MF streams.

The protein profile was evaluated by SDS-PAGE electrophoresis, and the results are shown in Fig. 7. Caseins and MFGM proteins were mostly retained by the membrane. However, the ratio of β-LG to α-LA in feed (71:29), retentate (81:19) and permeate (40:60), indicates evidence of the selective transmission of α-LA to permeate stream. This could result from a high pasteurisation temperature in the butter production process. Thermal processing of milk proteins may cause the denaturation of serum proteins and the formation of intermolecular disulfide bonds between β-LG and κ-casein (Harland, Coulter, & Jenness, 1952; Zulewska et al., 2018). Thus, some part of β-LG remained in the retentate stream.

Densitometry analysis of the gel revealed the almost unchanged ratio of MFGM proteins to caseins when comparing BM with obtained retentate (13:87 versus 15:85). The relative protein content in permeate was as follows: 17% of MFGM proteins, 33% of β-LG and 50% of α-LA. Since observation of MFGM particles by electronic microscopy in previous studies (Morin et al., 2007b) demonstrated high variability in particle size, ranging from 0.1 to 3–4 μm, it can be expected that smaller MFGM particles will pass through the membrane (Morin, Jiménez-Flores, & Pouliot, 2007b). Although some MFGM proteins were observed in the permeate samples, it has to be considered that SDS-PAGE wells were loaded with an equal amount of protein, so even if small amounts of MFGM proteins are found in the permeate, they would represent a relatively small percentage due to the low total protein content in permeate.

Table 5
Rejection percentage after microfiltration of buttermilk.[a]

TS	Fat	Casein	SP	Ash	Ca
63.5 ± 2.3	91.9 ± 2.5	99.6 ± 0.4	68.2 18.3	55.6 ± 0.4	87.7 ± 0.6

[a] Rejection percentage = $[1 - (C_P/C_R)] \times 100$ where C_P and C_R are concentration of the component in the permeate and retentate, respectively; casein = (TN − NCN) × 6.38; SP, serum proteins (total protein − casein). Values are expressed as means and their SD (n = 3).

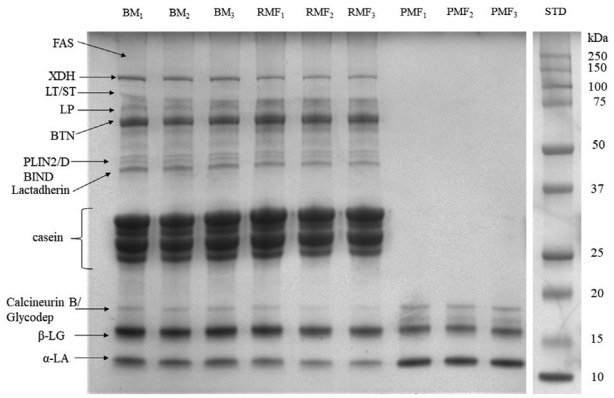


Fig. 7. Sodium dodecyl sulphate-PAGE patterns of buttermilk (BM), MF retentate (RMF) and MF permeate (PMF). Subscripts indicate replicates. Lane STD was loaded with 4 μL of molecular mass standard. Numbers to the right of lane STD indicate molecular masses (kDa). Identification of proteins is provided on the left side of the figure: FAS, fatty acid synthase; XDH, xanthine dehydrogenase; LT, lactotransferrin; ST, serotransferrin; LP, lactoperoxidase; BTN, butyrophilin; PLIN2, perilipin 2; DBIND, vitamin D-binding protein; Glycodep, glycosylation-dependent protein 1; β-LG, β-lactoglobulin; α-LA, α-lactalbumin.

Overall, the parameters applied during the MF process of BM examined in this research resulted in the production of two fractions with different compositions, thus probably different properties and distinct potential applications. As mentioned in Section 1, the separation of BM into MFGM and casein-rich retentate and SP-rich permeate may increase the value of BM. Moreover, the permeate containing α-LA could be especially interesting due to the contribution of this protein to infant and adult nutrition (Rocha-Mendoza et al., 2021). However, the low yield of serum proteins in the permeate stream (only 27% of the SP in the feed actually partitioned to the permeate; Table 1) challenges the feasibility of the process, which results from the composition and thermal processing history of BM. Nevertheless, further studies are underway to investigate the possibilities of process modifications and the application of permeate from buttermilk MF.

4. Conclusions

In summary, this study demonstrates that the resistance-in-series model accounting for the time evolution of the fouling resistances during microfiltration of buttermilk accurately fit the experimental data in terms of high R^2 and low SD. The resistance due to adsorption and concentration polarisation was predominant during the first minutes of operation as it sharply increased with time. However, the resistance due to the cake formation increased over the entire microfiltration time, being predominant at the latter stages of the filtration process. It was observed that the cake layer was mainly composed of casein and high molecular weight serum proteins. Apart from cake layer formation, casein was also involved in the pore-blocking mechanism. The results showed that applied processing parameters enabled selective partitioning of α-lactalbumin, resulting in transmission of this protein to the permeate stream. Nevertheless, further studies on optimised fractionation conditions enhancing the efficiency of the MF process should be performed.

CRediT authorship contribution statement

Justyna Tarapata: Conceptualization, Methodology, Investigation, Resources, Data curation, Writing – original draft, Visualization, Modeling of fouling. Maciej Maciejczyk: Modeling of cake layer formation. Justyna Zulewska: Conceptualization, Methodology, Writing – review & editing, Supervision, Project administration, Funding acquisition.

Declaration of competing interest

None.

Acknowledgments

The authors thank to Waldemar Brandt, Anna Lis, Roman Łaszek, Hanna Nowak, Krzysztof Siemianowski, Sławomir Wiśniewski and Justyna Ziajka for technical assistance. Justyna Tarapata is a recipient of a scholarship from the Programme Interdisciplinary Doctoral Studies in Bioeconomy (POWR.03.02.00–00-I034/16–00), which is funded by the European Social Funds. The research was financially supported by The National Centre for Research and Development, Project No. WPC1/DairyFunInn/2019, amount of funding 1,950,000.00 PLN.

References

Ali, A. H. (2019). Current knowledge of buttermilk: Composition, applications in the food industry, nutritional and beneficial health characteristics. *International Journal of Dairy Technology, 72*, 169–182.

Aoac. (2007). *Official methods of analysis* (18th edn.). Gaithersburg, MD, USA: AOAC International.

Barukčić, I., Jakopović, K. L., & Božanić, R. (2019). Whey and buttermilk – neglected sources of valuable beverages. *Natural Beverages, 13*, 209–242.

Carbonell-Alcaina, C., Corbatón-Báguena, M. J., Álvarez-Blanco, S., Bes-Piá, M. A., Mendoza-Roca, J. A., & Pastor-Alcañiz, L. (2016). Determination of fouling mechanisms in polymeric ultrafiltration membranes using residual brines from table olive storage wastewaters as feed. *Journal of Food Engineering, 187*, 14–23.

Carrere, H., Blaszkow, F., & de Balmann, H. R. (2001). Modelling the clarification of lactic acid fermentation broths by cross-flow microfiltration. *Journal of Membrane Science, 186*, 219–230.

Charcosset, C. (2021). Classical and recent applications of membrane processes in the food industry. *Food Engineering Reviews, 13*, 322–343.

Coppola, L. E., Molitor, M. S., Rankin, S. A., & Lucey, J. A. (2014). Comparison of milk-derived whey protein concentrates containing various levels of casein. *International Journal of Dairy Technology, 67*, 467–473.

Corbatón-Báguena, M. J., Álvarez-Blanco, S., & Vincent-Vela, M. C. (2018). Evaluation of fouling resistances during the ultrafiltration of whey model solutions. *Journal of Cleaner Production, 172*, 358–367.

Corredig, M., & Dalgleish, D. G. (1977). Isolates from industrial buttermilk: Emulsifying properties of materials derived from the milk fat globule membrane. *Journal of Agricultural and Food Chemistry, 45*, 4595–4600.

Damar, I., Cinar, K., & Gulec, H. A. (2020). Concentration of whey proteins by ultrafiltration: Comparative evaluation of process effectiveness based on physicochemical properties of membranes. *International Dairy Journal, 111*, Article 104823.

Hansen, S. F., Petrat-Melin, B., Rasmussen, J. T., Larsen, L. B., Ostenfeld, M. S., & Wiking, L. (2018). Placing pasteurisation before or after microfiltration impacts the protein composition of milk fat globule membrane material. *International Dairy Journal, 81*, 35–41.

Harland, H. A., Coulter, S. T., & Jenness, R. (1952). The effect of the various steps in the manufacture on the extent of serum protein denaturation in nonfat dry milk solids. *Journal of Dairy Science, 35*, 363–368.

Juang, R. S., Chen, H. L., & Chen, Y. S. (2008a). Resistance-in-series analysis in cross-flow ultrafiltration of fermentation broths of *Bacillus subtilis* culture. *Journal of Membrane Science, 323*, 193–200.

Juang, R. S., Chen, H. L., & Chen, Y. S. (2008b). Membrane fouling and resistance analysis in dead-end ultrafiltration of *Bacillus subtilis* fermentation broths. *Separation and Purification Technology, 63*, 531–538.

Juang, R. S., Lin, S. H., & Peng, L. C. (2010). Flux decline analysis in micellar-enhanced ultrafiltration of synthetic waste solutions for metal removal. *Chemical Engineering Journal, 161*, 19–26.

Katsoufidou, K., Yiantsios, S. G., & Karabelas, A. J. (2005). A study of ultrafiltration membrane fouling by humic acids and flux recovery by backwashing: Experiments and modeling. *Journal of Membrane Science, 266*, 40–50. https://doi.org/10.1016/j.memsci.2005.05.009

LabPlot Team. (2022). *LabPlot: A free, open source, cross-platform data visualization and analysis software accessible to everyone* (Version 2.9) [Computer software] https://labplot.kde.org.

Layman, D. K., Lönnerdal, B., & Fernstrom, J. D. (2018). Applications for α-lactalbumin in human nutrition. *Nutrition Reviews, 76*, 444–460.

Luján-Facundo, M. J., Mendoza-Roca, J. A., Cuartas-Uribe, B., & Álvarez-Blanco, S. (2017). Membrane fouling in whey processing and subsequent cleaning with ultrasounds for a more sustainable process. *Journal of Cleaner Production, 143*, 804–813.

Morin, P., Britten, M., Jiménez-Flores, R., & Pouliot, Y. (2007a). Microfiltration of buttermilk and washed cream buttermilk for concentration of milk fat globule membrane components. *Journal of Dairy Science, 90*, 2132–2140.

Morin, P., Jiménez-Flores, R., & Pouliot, Y. (2007b). Effect of processing on the composition and microstructure of buttermilk and its milk fat globule membranes. *International Dairy Journal, 17*, 1179–1187.

Quillin, M. L., & Matthews, B. W. (2000). Accurate calculation of the density of proteins. *Acta Crystallographica Section D, 56*, 791–794.

Rammer, P., Groth-Pedersen, L., Kirkegaard, T., Daugaard, M., Rytter, A., Szyniarowski, P., et al. (2010). BAMLET activates a lysosomal cell death program in cancer cells. *Molecular Cancer Therapeutics, 9*, 24–32.

Rao, H. G. R. (2002). Mechanisms of flux decline during ultrafiltration of dairy products and influence of pH on flux rates of whey and buttermilk. *Desalination, 144*, 319–324.

Rocha-Mendoza, D., Kosmerl, E., Krentz, A., Zhang, L., Badiger, S., Miyagusuku-Cruzado, G., et al. (2021). Acid whey trends and health benefits. *Journal of Dairy Science, 104*, 1262–1275.

Rombaut, R., Dejonckheere, V., & Dewettinck, K. (2006). Microfiltration of butter serum upon casein micelle destabilization. *Journal of Dairy Science, 89*, 1915–1925.

Salinas-Rodriguez, S. G., Amy, G. L., Schippers, J. C., & Kennedy, M. D. (2015). The modified fouling index ultrafiltration constant flux for assessing particulate/colloidal fouling of RO systems. *Desalination, 365*, 79–91.

Svanborg, S., Johansen, A. G., Abrahamsen, R. K., & Skeie, S. B. (2015). The composition and functional properties of whey protein concentrates produced from buttermilk are comparable with those of whey protein concentrates produced from skimmed milk. *Journal of Dairy Science, 98*, 5829–5840.

Tan, T. J., Wang, D., & Moraru, C. I. (2014). A physicochemical investigation of membrane fouling in cold microfiltration of skim milk. *Journal of Dairy Science, 97*, 4759–4771.

Tong, P. S., Barbano, D. M., & Rudan, M. A. (1988). Characterization of proteinaceous membrane foulants and flux decline during the early stages of whole milk ultrafiltration. *Journal of Dairy Science, 71*, 604–612.

Verdi, R. J., Barbano, D. M., Dellavalle, M. E., & Senyk, G. F. (1987). Variability in true protein, casein, nonprotein nitrogen, and proteolysis in high and low somatic cell milks. *Journal of Dairy Science, 70*, 230–242.

Wojciechowski, K. L., & Barbano, D. M. (2015). Modification of the Kjeldahl non-casein nitrogen method to include bovine milk concentrates and milks from other species. *Journal of Dairy Science, 98*, 7510–7526.

Żegarska, Z. (2000). Ćwiczenia z analizy żywności. *Olsztyn, Poland*. Wydawnictwo UWM.

Zulewska, J., Kowalik, J., & Dec, B. (2018). Flux and transmission of β-casein during cold microfiltration of skim milk subjected to different heat treatments. *Journal of Dairy Science, 101*, 10831–10843.

energies

MDPI

Article

Valorization of Dairy By-Products: Efficiency of Energy Production from Biogas Obtained in Anaerobic Digestion of Ultrafiltration Permeates

Justyna Tarapata [1], Marcin Zieliński [2,*] and Justyna Zulewska [1]

[1] Department of Dairy Science and Quality Management, Faculty of Food Science, University of Warmia and Mazury in Olsztyn, Oczapowskiego 7, 10-719 Olsztyn, Poland
[2] Department of Environmental Engineering, Faculty of Geoengineering, University of Warmia and Mazury in Olsztyn, Warszawska 117, 10-719 Olsztyn, Poland
* Correspondence: marcin.zielinski@uwm.edu.pl

Abstract: This study aimed at evaluating the methane potential of two ultrafiltration (UFP) and two diafiltration (DFP) permeates generated during milk protein concentration. The permeates were characterized by a different chemical oxygen demand (COD) ranging from 7610 mg O_2/L to 57,020 mg O_2/L. The CH_4 production efficiency was recorded for 20 days and ranged from 149 to 181 NL/kg COD_{added}. Moreover, the possibilities of the use of UFP/DFP to produce electricity and heat with a combined heat and power (CHP) unit was analyzed to underline the impact of the implementation of anaerobic digestion on the electric and thermal energy requirements of a dairy plant. It was concluded that the application of anaerobic digestion to UFP and DFP treatments generates the energy required to cover all the large-scale dairy plant energy demands and produce extra income. The amount of permeates generated annually in the analyzed dairy plant will enable the production of approx. 22,699 MWh of electricity and 85,516 GJ of heat. This would require a biogas plant with a 3 MW yield. Additionally, the lactose production from UFP/DFP was considered as an alternative or parallel solution for its management. The study confirmed that the biogas and lactose production from UFP/DFP enables plant owners to adjust a plant's management towards one of these two solutions.

Keywords: UF permeate; lactose; dairy wastes; anaerobic digestion; biogas

check for updates

Citation: Tarapata, J.; Zieliński, M.; Zulewska, J. Valorization of Dairy By-Products: Efficiency of Energy Production from Biogas Obtained in Anaerobic Digestion of Ultrafiltration Permeates. *Energies* **2022**, *15*, 6829. https://doi.org/10.3390/en15186829

Academic Editor: Byong-Hun Jeon

Received: 11 August 2022
Accepted: 15 September 2022
Published: 18 September 2022

Publisher's Note: MDPI stays neutral with regard to jurisdictional claims in published maps and institutional affiliations.

Copyright: © 2022 by the authors. Licensee MDPI, Basel, Switzerland. This article is an open access article distributed under the terms and conditions of the Creative Commons Attribution (CC BY) license (https://creativecommons.org/licenses/by/4.0/).

1. Introduction

The significant growth of the global population in the last decades has resulted in the development of the industrialization of the food production and processing sectors. The dairy industry is a part of the food sector that fulfills the demand for products such as milk, cheese, milk powder, etc. [1]. The consumption of dairy products has experienced a significant rise in many countries, resulting in the establishment of large-scale production factories [2].

While serving the global demand for milk-based products, the dairy industry generates a significant amount of pollution due to its use of water and its emission of effluents into the environment. In Europe, nearly 29 million tons of dairy products end up as waste each year. Within this waste, there are processing effluents as well as spoiled and mishandled products [1,3].

The cheese sector produces high quantities of whey and milk permeate that represent a major disposal problem [4]. Ultrafiltration (UF) and diafiltration (DF) permeates are the effluents generated during the concentration of milk or whey proteins (Figure 1). The diafiltration process is a variation of a membrane process, in which fresh solvent is added to the retentate produced during the first stage of the filtration process to replenish the filtered volume; consequently, the small molecules such as salts are washed away from the retained

macromolecules. The purpose of applying a DF stage is to obtain a retentate of a higher purity [5–9]. The effluents generated during milk and whey processing are characterized by an extreme chemical oxygen demand (COD) up to approximately 70,000 mg O_2/L [10]. Based on a simple mass balance, it is estimated that for 100 kg of raw milk between 80 to 87.5 kg of UF permeate is produced, while only 12.5–20 kg is transformed into the final product—milk protein concentrate (MPC) in liquid form [11]. The concentration of whey or milk serum (the permeate obtained after the microfiltration of skim milk, with a chemical composition similar to whey) generates even higher amounts of UF/DF permeate due to the higher volume reduction factor achieved during protein concentration. The UF/DF permeate contains primarily water, lactose, minerals, and a small number of nitrogen-containing compounds. Most of the nitrogen content of the UF/DF permeate from milk consists of nonprotein nitrogen compounds normally found in milk [12]. Generally, the UF permeates generated in the dairy industry are considered a potential source of lactose production in large-scale dairy plants (Figure 1). The primary feed material for lactose production is the UF permeate of sweet/cheese whey generated during the production of whey protein concentrates (WPC) and whey protein isolates (WPI). About 4.2 million tons of whey protein powders were produced worldwide in 2018 [13]. A less valuable source of feed for lactose isolation is the production of MPC and milk protein isolates (MPI). Their annual production reached approximately 190 thousand tons globally in 2017 [14]. The industrial-scale producers prefer lactose sources that demand the least amount of processing and create minimal waste [15]. Thus, the management of UF permeates from MPC and MPI production is still a challenge for the dairy industry.

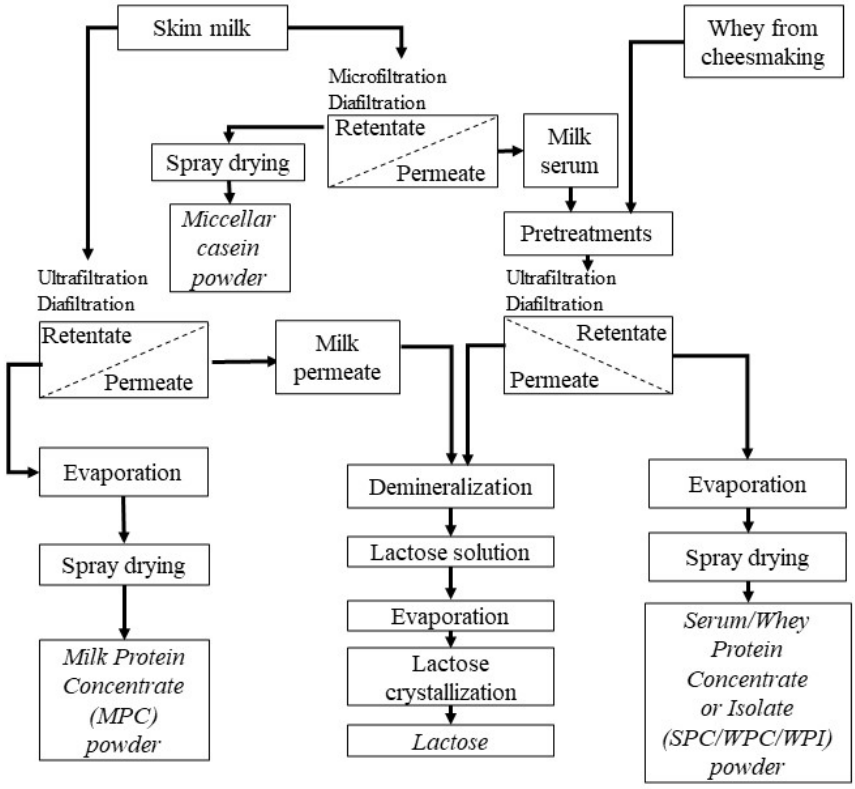


Figure 1. Flow diagram for concentration of proteins and lactose production in dairy industry. The final products are marked in italics.

Anaerobic digestion (AD) can be employed as the first biological treatment process necessary for the partial stabilization of food-processing wastes (such as dairy wastewater) prior to their utilization or disposal, as well as for the production of biogas [16–18]. In addition to reducing the pollutive potential of these wastes, the biogas produced from AD could be used for space and water heating in food-processing plants. AD has been used as

a means for dairy waste neutralization [19,20]. The AD of dairy wastewater (mainly cheese whey) has been widely studied using single- and two-stage systems [21–23]. However, several authors [24–29] reported a low biogas productivity and methane yield associated with the low pH of the fermented whey or its high COD. Differently constructed reactors have been used to enhance the treatment of dairy wastewater [4]. Nevertheless, the vast majority of published research is focused on the management of whey, whose components can be successfully recovered in a dairy factory, whereas little is known about exploiting the potential of UF permeates containing a relatively high concentration of lactose.

The biochemical methane potential (BMP) test is often applied to assess the anaerobic biodegradability of a tested substrate, whereby its specific methane yield may be evaluated [30]. BMP tests can indicate the potential for biogas production from various substrates [31].

Due to the microbial role in the AD process, kinetic methods are commonly used to simulate anaerobic biodegradation. Hydrolysis is often assumed to be the rate-limiting step in AD, and the researchers often model batch BMP data using a first-order kinetic model. A first order kinetic model has been successfully applied to AD using different kinds of reactors [32,33].

Moreover, AD was recently recognized as an environmentally friendly technology for producing renewable energy as biogas [34,35]. Therefore, biogas production allows for the increase in the share of renewable sources in the national energy scheme, which is the EU's goal as set out in the renewable energy directive (RED II) [36]. Due to the still-growing energy demand in European countries, it is predicted that there will be a rapid development of biogas plants [37]. These installations enable the production of biogas (under controlled conditions), which is a mixture of methane (45–74%), carbon dioxide (25–54%), and trace amounts of other components, i.e., hydrogen sulfide, ammonia, hydrogen, nitrogen, and oxygen, in a concentration up to 1–2% of the total biogas volume. The methane content in the produced gas is mainly affected by the components found in the fermentation substrate [37].

Additionally, the production of biogas in agricultural areas may provide extra income from agricultural activities, which creates an opportunity to develop the local economy in rural areas and promote circular economic principles in local communities [35,38–40]. An on-site biogas plant can be a significant source of additional income for a plant specialized in dairy production [20]. Moreover, local farmers may benefit from either selling the wastes generated from agricultural production as a co-substrate used in a biogas plant or from receiving high-quality organic fertilizer left over from biogas production [41]. New biogas plants will also offer job opportunities.

The aim of this study is to analyze the possibilities of using the waste from dairy processing to produce electricity and heat from the biomethane generated in the process of anaerobic digestion. The analysis is based on the effluents produced by a large-scale dairy factory. BMP tests were performed using four different substrates, namely, UF and DF permeates obtained after the filtration of milk and milk serum. Their energy potentials were calculated and a simplified financial analysis concerning the profits generated via energy vs. lactose sale was conducted.

The key novelty of this study is the assessment of the possibility of valorizing the permeates generated during DF by using them in biogas production and comparing their effects with typical UF. Attempts were made to estimate the relationship between the degree of lactose recovery and the amount of biogas obtained. A case study was proposed for a dairy plant using membrane techniques.

2. Materials and Methods

2.1. Materials

The ultrafiltration permeates (UFP—wastes from dairy processing) used in research experiments were obtained from Dairy Research and Development Center located at University of Warmia and Mazury in Olsztyn. These permeates were produced from

ultrafiltration (UF) and diafiltration (DF) processes of two different dairy products (100 L of milk and 170 L of milk serum, Figure 2). The UF and DF processes were carried out using UF module (Koch Membrane Systems, Wilmington, MA, USA) fitted with 3838-HFK-131 membrane (spiral wound element; semipermeable polyethersulfone layer on a polyester backing material) with a membrane area of 6.7 m^2, molecular weight cut-off value of 10,000 Da, and a feed spacer model N 31 mil (used in accordance with manufacturer's specifications). The unit was operated under a constant transmembrane pressure of 4 bar at 50 °C for either UF or DF processes. Milk was ultra-filtrated to achieve a concentration factor of approximately 4.6×. The UF retentate was diluted with reverse osmosis water at 50 °C to bring the weight back to the original total weight of the starting feed for DF. Then, the diluted UF retentate was diafiltrated to achieve a concentration factor of 6.6×. Diafiltration was continued until the protein content of the retentate, measured by MilkoScan™ FT2 (Foss, Hillerød, Denmark), was 13.5%. Milk serum was UF to achieve a concentration factor of approximately 5.5×. The UF retentate was diluted with reverse osmosis water at 50 °C to bring the weight back to the original total weight of the starting feed for DF. Then, the diluted UF retentate was diafiltrated to achieve a concentration factor of 8.5×. Diafiltration was continued until the protein content of the retentate, measured by MilkoScan™ FT2 (Foss, Hillerød, Denmark), was 2.2% of protein in the retentate. The permeates were sampled in a representative manner, and then stored at 4 °C.

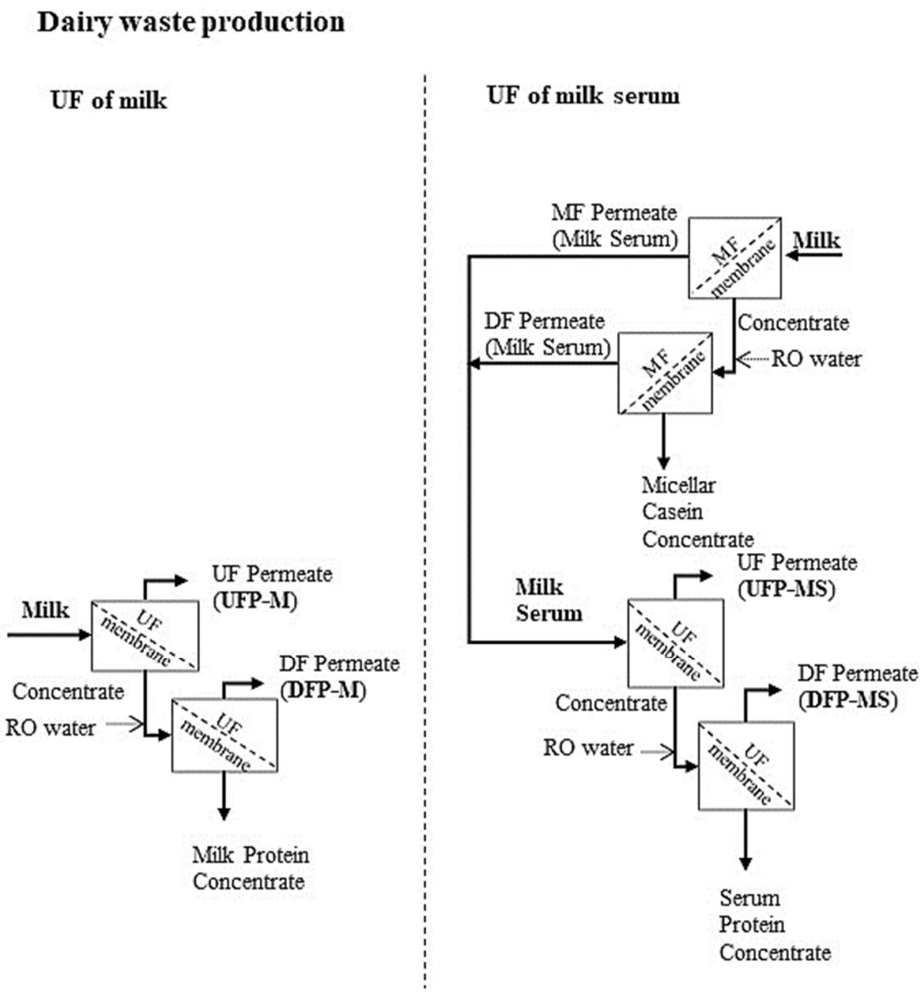


Figure 2. Production of dairy wastes (ultrafiltration permeates = fermentation substrates): UFP-M = milk ultrafiltration permeate; DFP-M = milk diafiltration permeate; UFP-MS = milk serum ultrafiltration permeate; DFP-MS = milk serum diafiltration permeate; UF = ultrafiltration; DF = diafiltration; MF = microfiltration; RO = reverse osmosis.

The fermentative inoculum (anaerobic sludge—the source of methanogenic bacteria) came from a bioreactor operating under mesophilic conditions at 36 ± 1 °C. The parameters of the sludge are reported in Table 1.

Table 1. The parameters of anaerobic sludge used as inoculum.

Trait	Anaerobic Sludge
TS [%]	6.8 ± 0.2
VS [% TS]	73.5 ± 0.9
Ash [% TS]	26.5 ± 0.9
C [% TS]	41.1 ± 0.8
N [% TS]	3.7 ± 0.0
C/N ratio	11.2 ± 0.2

TS—total solids; VS—volatile solids; C—carbon; N—nitrogen; C/N—carbon to nitrogen; ±standard deviation.

2.2. Analysis of Physicochemical Parameters

The pH of the substrates was measured using a pH meter (CP-401, Elmetron, Zabrze, Poland) equipped with an electrode IJ-44C IONODE (Elmetron). The permeate samples were analyzed to obtain content of total solids (TS) and volatile solids (VS) using a gravimetric method. The samples were dried at 105 °C [42]. The total nitrogen (TN) content was determined using Kjeldahl method (AOAC International, Gaithersburg, MD, USA, 2007; method 991.20; 33.2.11). The total calcium content was analyzed using atomic absorption spectrometry. The measurements were carried out in accordance with ISO 8070-2007 IDF 119:2007(E) (ISO/IDF, 2007) using Thermo Scientific iCE 3000 Series AA Spectrometer (Thermo Fisher Scientific, Franklin, MA, USA) and at the wavelength of 422.7 nm. The amount of lactose was estimated using Milko-Scan™ FT2 (Foss, Hillerød, Denmark). The analysis of ash was performed using the muffle furnace technique at 530 °C (PN-A-86364:1996). The chemical oxygen demand (COD) of the samples was determined with the aid of cuvette test LCK 914 (HACH LANGE GmbH, Berlin, Germany). The composition and percentage of individual components of the biogas outflow (CH_4, CO_2) were analyzed using a gas chromatograph (GC, 7890A Agilent, Santa Clara, CA, USA) equipped with a thermoconductometric detector (TCD). Biogas was collected from the bioreactors with a 10 mL gas-tight syringe. The carrier gases used were argon (Ar) and helium (He) at a volume flow of 0.9 NL/h. The injection and detector port temperatures were 150 and 250 °C, respectively.

2.3. Biogas Efficiency Research

The methane yield of tested substrates was determined using a volumetric gas production method, namely, the Automated Methane Potential Test System II (AMPTS II, BPC Instruments AB, Lund, Sweden). The fermentation measurements were performed at 37 ± 1 °C. The measurement system recorded changes in partial pressure coupled with reactors. Each AMPTS reactor (glass vessel of 500 mL total volume) was equipped with an individual automated stirrer (100 rpm for 30 s every 10 min). There were 15 AMPTS bottles: [four substrates and one control] × triplicate replication, where the substrates were UFP-M, DFP-M, UFP-MS, and DFP-MS, and control was inoculum only. Tests were performed by filling the reactors with approximately 200 g of the anaerobic sludge and then the fermentation substrates were added. The initial organic load rate (OLR) was approximately 5 g COD/L. Anaerobic conditions in the reactors were achieved by flushing pure nitrogen through the mixture of sludge and substrate. Using the bioprocess control software, a gas production report was recorded every day. This program generates results of the volume of gas already normalized (standard atmospheric pressure 101.3 kPa, at 0 °C, and with zero moisture content). The measurement was carried out until the available organic compounds were fully decomposed. Subsequent measurements of the amount of biogas were automatically compared with each other, and when ten consecutive gas volume measurements did not differ by more than 1%, the measurement was completed. The endogenous biogas generated by anaerobic sludge was excluded from the calculations

of biomethane production in the tests. Biomethane yields were calculated as a biomethane volume produced over a period of 20 days and expressed as NL per kilogram of added COD (COD_{added}).

2.4. Kinetic Analysis

Nonlinear regression was used to obtain the rate constants of methane production from plots of volume of methane per mass of COD_{added} versus time. According to the approach reported by Llabres-Luengo and Mata-Alvarez [43], the first order linear regression is defined as:

$$Y(t) = -Y_{max}(e^{-kt} - 1) \quad (1)$$

where Y—methane yield (NL CH_4/kg COD_{added}), Y_{max}—maximal methane yield (NL CH_4/kg COD_{added}), k—kinetic constant (1/day), and t—time (day). The methane production rate was calculated as the product of the k and the maximal volume of methane per mass of COD_{added} obtained from the first order kinetics.

To evaluate the model results, Statistica software (version 13.1, 1984–2016, StatSoft, Inc., Tulsa, OK, USA) was used for calculations of the determination coefficient R^2.

2.5. Energetic Calculations

The calculations of the energy potential of substrates (UFP-M, DFP-M, UFP-MS, and DFP-MS) were based on the conducted fermentation tests and methodology described by Cieślik et al. [44] and Kozłowski et al. [20]. The amount of electricity and heat produced from combined heat and power (CHP) unit were determined using Equations (2) and (3):

$$E_E = V_{CH_4} \times Re_{CH_4} \times \eta_e \quad (2)$$

where E_E—amount of produced energy [MWh/kg COD_{added}], V_{CH4}—volume of produced methane [m^3/kg COD_{added}], Re_{CH4}—energy efficiency ratio of methane [0.00917 MWh/m^3], and η_e—electrical efficiency of CHP. For the purpose of these calculations, the efficiency of 43% was assumed for the unit offered by PAKTOMA (Łódź, Poland), a Polish manufacturer of modern co-generation units for biogas plants).

Heat produced in CHP unit was determined from Equation (3):

$$E_H = V_{CH_4} \times Re_{CH_4} \times \eta_t \quad (3)$$

where E_H—amount of produced heat [MWh/kg COD_{added}], V_{CH4}—volume of produced methane [m^3/kg COD_{added}], Re_{CH4}—energy efficiency ratio of methane [0.00917 MWh/m^3], and η_t—heat efficiency of CHP. For the purpose of these calculations, the efficiency of 45% was assumed for the unit offered by PAKTOMA, a Polish manufacturer of modern co-generation units for biogas plants).

2.6. Case Study

This paper describes potential heat and electric power produced from biogas generated by anaerobic digestion of liquid by-products obtained from protein concentration in a large-scale dairy plant. The data regarding daily milk and whey throughput along with the usage of electric energy come from the reports published by the company and the community council. Waste yield was calculated from raw milk and whey throughput and processing using membrane technology.

The assumption is that the dairy plant process daily about 1200 t of raw milk, which is solely dedicated for the production of milk concentrates. The whole milk is first supplied to the separator and consequently discharged as two flows, skim milk and cream, of which the cream normally represents about 10% of the total throughput [45]. The total amount of liquid discharged as skim milk will then be 1080 t. In a typical UF process, pasteurized skim milk is concentrated to a final volume of one-fifth to one-eighth of the volume of the original skim milk to produce milk protein concentrate (MPC) that has 65 to 75% content

of protein relative to total solids. For the production of MPC with higher protein content, ultrafiltration is used in conjunction with the DF process [46]. Considering the amount of skim milk processed in the analyzed dairy plant, the filtration process characterized by volume concentration factor of 5 will generate about 864 t of permeate at each stage of filtration.

Another side stream processed by the factory is whey (800 t/day). Composition of whey is similar to that of milk serum, which is why its processing is easily comparable with processing of milk serum. In a typical UF process, pasteurized whey is concentrated to a final volume of between one-sixth to one-ninth of the volume of the original whey (based on the research performed previously) to produce serum protein concentrate (SPC60 or WPC60) that contains 60% content of protein. For the production of SPC with higher protein content, UF is used in conjunction with the DF process. Considering the amount of whey processed in analyzed dairy plant, the filtration process characterized by volume concentration factor of 8.5 will generate about 706 t of permeate at each stage of filtration.

The daily demand for electric power in this particular dairy plant equals 11 MWh. This covers the demand of all processing departments. Apart from manufacturing milk and whey concentrates, the factory also produces cheese, yogurts, and buttermilk.

2.7. Statistical Analysis

The statistical analysis was performed using the Statistica software (version 13.1, 1984–2016, StatSoft, Inc., Tulsa, OK, USA). Statistical evaluation of data was conducted using one-way ANOVA ($p < 0.05$) followed by Tukey's post hoc test.

3. Results and Discussion

3.1. Analysis of Methane Production

To calculate the energetic potential of the substrates, it is essential to assess their physical and chemical properties. The basic parameters—such as the TS content, VS content, COD, and pH—characterizing the substrates used for the fermentation process performed in this study are presented in Table 2.

Table 2. The physicochemical parameters of the fermentation substrates.

Parameter	Substrate			
	UFP-M	**DFP-M**	**UFP-MS**	**DFP-MS**
TS [%]	5.60 ^{a} ± 0.06	1.81 ^{c} ± 0.05	3.8 ^{b} ± 0.02	0.86 ^{d} ± 0.09
VS [%]	5.13 ^{a} ± 0.06	1.65 ^{a,b} ± 0.08	3.46 ^{b} ± 0.07	0.79 ^{a,b} ± 0.03
Ash [%]	0.45 ^{a} ± 0.01	0.15 ^{c} ± 0.01	0.332 ^{b} ± 0.004	0.07 ^{d} ± 0.01
Ca [mg/L]	185.5 ^{a} ± 9.6	34.8 ^{c} ± 2.0	54.4 ^{b} ± 2.1	3.6 ^{d} ± 0.1
TN [%]	0.18 ^{a} ± 0.03	0.06 ^{c} ± 0.01	0.097 ^{b} ± 0.003	0.021 ^{d} ± 0.002
Lactose [%]	4.97 ^{a} ± 0.02	1.59 ^{c} ± 0.18	3.37 ^{b} ± 0.02	0.76 ^{d} ± 0.01
pH	6.55 ^{b} ± 0.18	6.84 ^{c} ± 0.10	6.84 ^{c} ± 0.04	7.03 ^{a} ± 0.06
COD [mg O_2/L]	57,020 ^{a} ± 510	19,150 ^{c} ± 1500	38,600 ^{b} ± 780	7610 ^{d} ± 430

TS—total solids; Ca—calcium; TN—total nitrogen calculated as total N × 6.38; COD—chemical oxygen demand; UFP-M = milk ultrafiltration permeate; DFP-M = milk diafiltration permeate; UFP-MS = milk serum ultrafiltration permeate; DFP-MS = milk serum diafiltration permeate; Data are expressed as mean (n = 6) ± standard deviation; $^{a–d}$ Means within a row with different superscripts are different ($p < 0.05$).

The results concerning the TS content indicated the significant ($p < 0.05$) difference between the four tested materials. The permeates obtained in the DF stage, during either the milk or milk serum UF process, contained mostly water (over 98%) and a very low number of solids (Table 2). An about three to four times greater volume of DF permeate— for DFP-M and DFP-MS, respectively—is required to obtain the same organic load as in the permeates obtained after first stage of processing for the UF/concentration (UFP-M and UFP-MS, respectively).

The respective streams obtained either during UF (UFP-M vs. UFP-MS) or DF (DFP-M vs. DFP-MS) were characterized by a higher TS content when milk was subjected to

filtration in comparison with milk serum. That is why, from a biogas plant exploitation point of view, the effluents generated during the filtration of the milk (UFP-M and DFP-M) used as substrates may result in a much higher profitability when compared to the streams obtained after milk serum processing (UFP-MS and DFP-MS, respectively).

The concentrations of organic matter expressed as the COD in the permeates after the UF process were 38,600 and 57,020 mg O_2/L for UFP-MS and UFP-M, respectively. Whereas the COD values of the permeates obtained in the DF process were equal to 7610 and 19,150 mg O_2/L for DFP-MS and DFP-M, respectively (Table 2). The permeates generated after the UF process in the dairy industry contribute a high COD as they are rich in lactose [12]. Lactose contributes around 90% of the COD. High COD values indicate that the dairy wastes produced are strong and fluctuating types [10]. In general, the COD value of the dairy effluents depends on the protein, fat, and carbohydrate content, which was confirmed by the Person's correlation coefficient ($r > 0.97$, $p < 0.05$) obtained in the current study (Table 3). The waste load equivalents of these constituents are 1 kg of fat, which contributes 3 kg of COD; 1 kg of protein, which contributes 1.36 kg of COD; and 1 kg of lactose, which contributes 1.13 kg of COD [10,47].

Table 3. The Pearson's correlation coefficients for the analyzed traits.

Trait	COD	VS	Ash	Ca	TN	Lactose	pH	TS	CH_4 Production
COD	1.00								
VS	0.11	1.00							
Ash	1.00 *	0.05	1.00						
Ca	0.93 *	0.30	0.90 *	1.00					
TN	0.97 *	0.23	0.95 *	0.98 *	1.00				
Lactose	1.00 *	0.10	1.00 *	0.93 *	0.97 *	1.00			
pH	−0.87 *	−0.34	−0.84 *	−0.94 *	−0.94 *	−0.87 *	1.00		
TS	1.00 *	0.11	1.00 *	0.93 *	0.97 *	1.00 *	−0.87 *	1.00	
CH_4 production	−0.08	0.06	−0.06	−0.17	−0.15	−0.07	0.32	−0.07	1.00

* significant values ($p < 0.05$).

The biochemical methane potential value obtained in the current experiment is expressed by the volume of methane produced per kilogram of added organic matter, which is expressed in COD, as the permeate is a liquid. The methane potential of the UF/DF permeates, noted at the end of the experiments, ranged from 149 to 181 NL CH_4 per kg of added COD (Table 4). There were no significant ($p > 0.05$) differences detected between the methane yields generated from the four tested dairy waste samples at the end of the experiment (20 days). Moreover, the methane content in the biogas did not differ significantly between the four tested samples and reached about 69% (Table 5).

Table 4. Methane yield, methane production rate, and reaction rate constant (k) obtained in conducted experiments.

Variant	Methane Yield [NL/kg COD_{added}]	Methane Production Rate [NL/kg COD/d]	k [1/d]	R^2
UFP-M	150 ^{a} ± 32	52	0.37 ^{a}	0.91
DFP-M	149 ^{a} ± 13	51	0.37 ^{a}	0.87
UFP-MS	181 ^{a} ± 3	46	0.28 ^{a}	0.91
DFP-MS	169 ^{a} ± 28	48	0.29 ^{a}	0.99

K—the rate constant of methane production; UFP-M = milk ultrafiltration permeate; DFP-M = milk diafiltration permeate; UFP-MS = milk serum ultrafiltration permeate; DFP-MS = milk serum diafiltration permeate; Data are expressed as mean (n = 3) ± standard deviation; ^{a}—Means within a column sharing the same superscript are not significantly different from each other ($p > 0.05$).

Table 5. Methane (CH_4) and carbon dioxide (CO_2) content in produced biogas.

Variant	CH_4 [%]	CO_2 [%]
UFP-M	69.39 [a]	30.61 [a]
DFP-M	69.23 [a]	30.77 [a]
UFP-MS	68.82 [a]	31.18 [a]
DFP-MS	69.29 [a]	30.71 [a]

[a]—Means within a column sharing the same superscript are not significantly different from each other ($p > 0.05$).

The efficiency of biomethane production from dairy waste varies across publications and depends on the applied parameters. For instance, in the research performed by Fernández et al. [48], a yield of 314 L CH_4/kg COD_{added} was demonstrated during single-stage anaerobic digestion of whey under thermophilic conditions, with an OLR up to 1.5 kg O_2/m^3day. In another study, described by Kisielewska et al. [49], who evaluated the digestion of a solution of dried ultra-filtrated whey permeate in a mesophilic system (UASB methanogenic reactor; 35 °C) at OLR rates from 4.6 to 6.9 kg COD/m^3, the obtained methane yield reached about 120 L CH_4/kg COD_{added}.

The fermentation charts for all the tested substrates are presented in Figure 3. The amount of generated methane increased during the first 10 days of measurements in all the cases of the tested substrates. After this time, the methane yield remained at a constant level. This indicated a fast hydrolysis process and a good adaptation of the anaerobic sludge to the substrate.

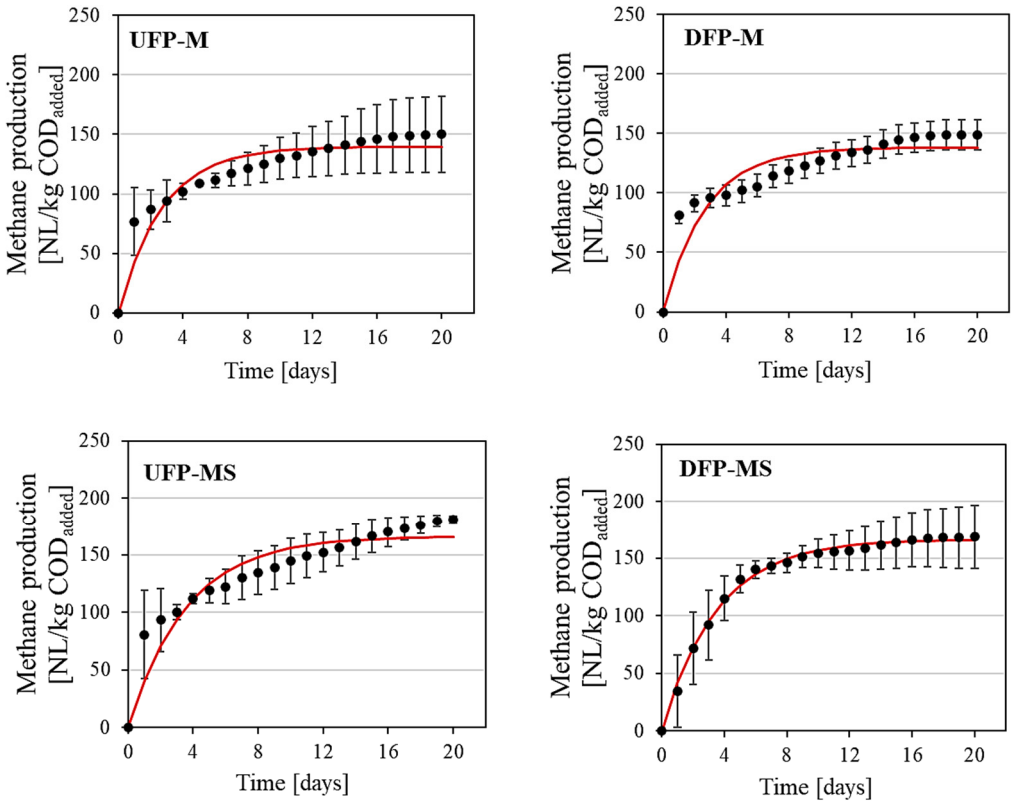


Figure 3. Comparison between measured data (points) and data calculated with the first order regression (red line) for specific methane production from ultrafiltration permeates in the 20-day test: UFP-M = milk ultrafiltration permeate; DFP-M = milk diafiltration permeate; UFP-MS = milk serum ultrafiltration permeate; DFP-MS = milk serum diafiltration permeate. The gas from the inoculum has been subtracted and the data have been expressed as volume of CH_4 per kg of COD_{added}.

In the current experiment, the registration of the volume of produced CH_4 was carried out until the available organic compounds were fully decomposed. The methane potential

test was terminated when the difference between the subsequent ten reads was equal to or less than 1%. In all cases of the tested permeates, the measurement did not last less than 20 days. For comparison, the time of decomposition obtained in the study performed by Kozłowski et al. [20] (with batch culture technology, and mesophilic conditions of 39 °C ± 1 °C), who used whey as a fermentation substrate, was seven days shorter than that noted in the current experiment (13 days vs. 20 days). The decomposition time is a crucial parameter to consider at the planning stage for future biogas plants. It enables the estimation of the size of the reactor.

3.2. Kinetic Analysis

The comparison between the measured data and the data calculated with the first order regression is presented in Figure 3. The coefficients for the tested model are presented in Table 4. The results from the first order regression accurately fitted the measured data. The determination coefficient for the four tested waste types is between 0.87 and 0.99. Regarding the kinetic constant, the first order regression yielded values ranging from 0.29 to 0.37/day. However, the difference between the mean values for the four tested permeates was nonsignificant ($p > 0.05$). The kinetic constant obtained in this experiment is comparable with the kinetic constants reported in the literature for dairy liquid wastes such as cheese whey [33] (with a hydrolysis constant k between 0.36–0.55/day; a COD of substrates between 50,000–78,000 mg/L; an inoculum/substrate ratio of 6; and a temp. of 35 °C). Mainardis et al. [33] obtained a good correlation ($R^2 > 0.97$) between the predicted and measured methane potential values using a first-order kinetic model.

Moreover, the CH_4 flux analysis conducted in the current study revealed one peak on the first day of digestion (35–81 NL CH_4/kg COD_{added}/day), followed by a less intense successive peak (<6 NL CH_4/kg COD_{added}/day) on the fourth day. According to Mainardis et al. [33], this outcome can be ascribed to the different molecules present in the substrate, which are consecutively degraded. A significant fraction of the permeates was easily biodegradable by the used biomass.

3.3. Energy Analysis

The results of the simplified economic and energy calculations are presented in Table 6. The maximum generated electric power was estimated at 10,632 MWh/a for UFP-M and a minimum of 1374 MWh/a for DFP-MS. In general, the higher the COD of the substrates, the higher the electric power produced and thus the higher profitability of the biogas plant. In the work by Kozłowski et al. [20], energy data from a dairy factory, producing 400 t of whey per day (two times lower than in the case of the dairy plant analyzed in this study), were reported: they claimed a biomethane yield of 3,508,487 m^3 per annum, which is a significantly greater amount than the summarized methane yield noted for UFP-MS and DFP-MS in this study (2,167,430 m^3/a). It is also important to highlight that in the research conducted by Kozłowski et al. [20], whey was used as a fermentation substrate, and its amount was almost half of that of UFP-MS. Whey contains more TS than UF/DF permeate, which is why the amount of biogas generated is expected to be higher than that from milk serum permeates. Therefore, in the future research, the co-digestion of UF/DF permeates in combination with other wastes should also be considered. The results presented by Comino et al. [50] indicate that the co-digestion of a high volume of whey (up to 65% in volume) and cattle slurry is possible without the use of chemicals for pH correction, but also that this kind of mix has a similar energetic potential for anaerobic digestion as energy crops such as maize. Anaerobic co-digestion can overcome most of the limitations of anaerobic mono-digestion by producing more CH_4 due to the synergy of the substrates and the supplementation of the missing nutrients by the co-substrates [51,52].

As calculated, the dairy plant can generate approximately 23,000 MWh of electricity and about 85,500 GJ of heat on an annual basis while using all the generated permeates considered in this study. The total electric energy output value corresponds to approximately 2.8 MW of the gross nominal capacity, which not only covers the annual demand of

the whole factory (0.5 MW, calculated based on the daily demand of 11 MWh/d) but also enables the sale of remaining energy. In the case of an electric power calculation expressed in MW, the working time of the CHP during the whole year of exploitation was assumed to be equal to 8100 h/a. It should be mentioned that the feasible working time in a typical biogas plant is between 7200 and 8100 h/a [35]. This is much lower than the 8760 h/a value corresponding to the entire year's 24/7 operating time. This is related to many exploitation issues and breaks in biogas generation due to, i.e., mixing system failures and other mechanical damages.

Based on the data reported by Kozłowski et al. [20], it is assumed that a 3 MW biogas plant is capable of generating 24,000 MWh of electric power, which means that in the analyzed case there is still an approx. 4% power reserve for a potential increase in waste processing. The reserve may be used for an anaerobic digestion of wastes obtained by other dairy plants of the same owner, which are much smaller and do not have appropriate equipment for the further utilization of the obtained permeate. However, the transportation cost should then be considered. In the analyzed case, the manufacturer has an advantage in that they do not have to acquire a substrate for biogas production, because they can use their own effluents.

Apart from serving as potential substrates for anaerobic digestion, the UF permeates may also be considered a profitable source material for lactose production. This is especially relevant in the case of large-scale dairy factories possessing appropriate equipment since the manufacture of lactose powder requires additional investment and operation costs for equipment dedicated to the further processing of the permeate [53]. A large amount of crystalline lactose is produced globally. The major source for lactose production is the UF permeate of sweet whey. However, any other sources rich in lactose such as the UF permeates of milk may be used [15]. Therefore, the potential income of the dairy factory from the sale of lactose powder is also presented in Table 6. The degree of lactose production was estimated based on an annual generation of UF/DF permeates calculated in the case study analyzed in the current research. It should be noted that the operating costs were not included in Table 6. According to the analysis conducted by Silva et al. [54], for the manufacture of 1 kg of lactose, an approximately EUR 0.20 expenditure is required.

Table 6. Simplified possible electricity and heat production from dairy waste in comparison to lactose production.

Parameter	Unit	UFP-M	DFP-M	UFP-MS	DFP-MS
Daily consumption of raw milk	t/d	1200	-	-	-
Daily consumption of milk serum/whey	t/d	-	-	800	-
			Biomethane production		
Daily generated permeate	t/d	864	864	706	706
Annually generated permeate	t/a	315,360	315,360	257,690	257,690
Dairy OLR (COD)	kg O_2/L	0.057	0.019	0.039	0.008
Total yearly OLR (COD)	kg O_2/a	17,975,520	5,991,840	10,049,910	2,061,520
Methane efficiency	Nm^3/kg COD	0.150	0.149	0.181	0.169
Methane production	m^3/a	2,696,328	892,784	1,819,033	348,397
Annual electric energy	MWh/a	10,632	3520	7173	1374
Daily electric energy	MWh/d	29.1	9.6	19.7	3.8
Heat	GJ/a	40,055	13,263	27,022	5176
Electric power	MW	1.3	0.4	0.9	0.2
Electric power price [1]	EUR/MWh	96.50			
Heat price [2]	EUR/GJ	8.77			
Electric power value	EUR/a	1,025,988	339,680	692,195	132,591
Heat value	EUR/a	351,282	116,317	236,983	45,390
Total electric power value	EUR/a	2,190,454			
Total heat value	EUR/a	749,972			

Table 6. *Cont.*

Parameter	Unit	UFP-M	DFP-M	UFP-MS	DFP-MS
		Lactose powder production (edible; non-pharmaceutical range)			
Yearly production [3]	t/a	10,971	3532	6083	1387
Lactose powder price [4]	EUR/t		899		
Lactose powder value	EUR/a	9,862,929	3,175,268	5,468,617	1,246,913
Total lactose value	EUR/a	19,753,727			

UFP-M = milk ultrafiltration permeate; DFP-M = milk diafiltration permeate; UFP-MS = milk serum ultrafiltration permeate; DFP-MS = milk serum diafiltration permeate; UF = ultrafiltration; OLR—organic load rate; COD—chemical oxygen demand; [1]—price estimated according to Energy Regulatory Office [55]; [2]—the price of heat produced from Poland's most popular energy carrier, i.e., hard coal, was used; [3]—amount of powder estimated based on production yield of 70% [53]; [4]—price estimated based on the report published by CLAL.it [56].

Thus, the total lactose value from Table 6 should be reduced by the cost of production, resulting in an approximately EUR 15.4 MM profit generated from lactose sale. In purely financial terms, food-grade lactose production exceeds the profitability of biogas production in the on-site biogas plant. However, other aspects such as the renewable energy demand and the geopolitical situation should also be considered by the plant owners. It is worth noting that one of the current objectives of the Bioeconomy Strategy for the EU is a reduction in energy dependence on non-renewable and unsustainable sources [57].

In summary, considering that the UF/DF permeates obtained during milk serum production are not primary sources of lactose [15] and considering the promising results of biomethane potential analysis conducted in this study, as well as the global growing demand for renewable energy, these effluents should be used as substrates in anaerobic digestion rather than lactose production. Additionally, the biomethane generated solely from UF/DF permeates of milk serum in a biogas plant can still provide an energy supply in an amount exceeding the needs of a large-scale dairy factory (1.1 MW vs. 0.5 MW) and simultaneously enabling the generation of additional profits from the sale of energy excess. Such a situation (the surplus of UF/DF permeates) enables plant owners to adjust UF/DF permeate management towards one of two analyzed solutions: lactose versus biogas production. Additionally, the rationale for the plant owner to opt for a less profitable form of gas production may stem from the fact that the development of a biogas plant requires fewer investment costs than a technological line dedicated to lactose production [20,54]. It is estimated that the return on investment in the construction of a 1 MW biogas plant is 3 years [58].

4. Conclusions

The methane generation potential of four UF/DF permeates with different lactose concentrations (0.76–4.97%) was tested. A higher lactose content contributed to a higher COD of the tested effluents. The methane yield obtained in this study (~0.16 $Nm^3/kg\ COD_{added}$) was comparable with that of the previously reported data on anaerobic digestion of UF whey permeates. This indicated the potential of using UF/DF permeates as substrates for anaerobic digestion, which may be another efficient means for its utilization. The economic analysis of the simulated electric and heat energy production with the CHP unit showed that the implementation of anaerobic digestion at the dairy plant level could provide a level of electricity and heat exceeding the amount necessary for the functioning of a large-scale factory. This could contribute to the improvement of a plant's energy balance and to a reduction in transport and management costs. When selling the energy, the profits should also be considered. Moreover, the estimated profit from lactose production, considered as alternative permeate-processing method, showed that it is an even more profitable approach. However, different aspects such as the geopolitical situation and energy market prices should also be considered while making decisions regarding the management of UF/DF permeates. It is very likely that the energy prices will rise in the near future due to the limited availability of fossil fuels. The proven efficiency of biogas

and lactose production through ultrafiltration permeates enables plant owners to adjust their management towards one of these two solutions.

Author Contributions: Conceptualization, J.T., J.Z. and M.Z.; methodology, J.T., J.Z. and M.Z.; formal analysis, J.T.; investigation, J.T.; writing—review and editing, J.T., J.Z. and M.Z.; validation, J.Z. and M.Z.; data curation, J.T., J.Z. and M.Z.; writing—original draft preparation, J.T.; visualization, J.T.; supervision J.Z. and M.Z.; resources, J.Z. and M.Z.; funding acquisition, J.Z. and M.Z. All authors have read and agreed to the published version of the manuscript.

Funding: This research was funded by The National Centre for Research and Development, Project No. WPC1/DairyFunInn/2019, amount of funding 1.950.000.00 PLN.

Data Availability Statement: Not applicable.

Acknowledgments: Justyna Tarapata is a recipient of a scholarship from the Program Interdisciplinary Doctoral Studies in Bioeconomy (POWR.03.02.00-00-I034/16-00), which is funded by the European Social Funds.

Conflicts of Interest: The authors declare no conflict of interest.

References

1. Usmani, Z.; Sharma, M.; Gaffey, J.; Sharma, M.; Dewhurst, R.J.; Moreau, B.; Newbold, J.; Clark, W.; Thakur, V.K.; Gupta, V.K. Valorization of Dairy Waste and By-Products through Microbial Bioprocesses. *Bioresour. Technol.* **2022**, *346*, 126444. [CrossRef] [PubMed]
2. Chokshi, K.; Pancha, I.; Ghosh, A.; Mishra, S. Microalgal Biomass Generation by Phycoremediation of Dairy Industry Wastewater: An Integrated Approach towards Sustainable Biofuel Production. *Bioresour. Technol.* **2016**, *221*, 455–460. [CrossRef] [PubMed]
3. Mahboubi, A.; Ferreira, J.A.; Taherzadeh, M.J.; Lennartsson, P.R. Value-Added Products from Dairy Waste Using Edible Fungi. *Waste Manag.* **2017**, *59*, 518–525. [CrossRef]
4. Wang, S.; Rao, N.C.; Qiu, R.; Moletta, R. Performance and Kinetic Evaluation of Anaerobic Moving Bed Biofilm Reactor for Treating Milk Permeate from Dairy Industry. *Bioresour. Technol.* **2009**, *100*, 5641–5647. [CrossRef] [PubMed]
5. Lee, E.K.; Koros, W.J. Membranes, Synthetic, Applications. In *Encyclopedia of Physical Science and Technology*; Academic Press: Cambridge, MA, USA, 2003; pp. 279–344. [CrossRef]
6. Lipnizki, F. Membrane Processes for the Production of Bulk Fermentation Products. *Membr. Technol.* **2010**, 121–153. [CrossRef]
7. Chamberland, J.; Bouyer, A.; Benoit, S.; Provault, C.; Bérubé, A.; Doyen, A.; Pouliot, Y. Efficiency Assessment of Water Reclamation Processes in Milk Protein Concentrate Manufacturing Plants: A Predictive Analysis. *J. Food Eng.* **2020**, *272*, 109811. [CrossRef]
8. Tomasula, P.M.; Bonnaillie, L.M. Crossflow Microfiltration in the Dairy Industry. In *Emerging Dairy Processing Technologies*; Wiley: Hoboken, NJ, USA, 2015; pp. 1–32. ISBN 9781118560471.
9. Çınar, K. Membrane Filtration of Milk: Separation and Fractionation of Milk Proteins. *J. Innov. Sci. Eng.* **2022**, *6*, 61–75. [CrossRef]
10. Bella, K.; Rao, P.V. Anaerobic Digestion of Dairy Wastewater: Effect of Different Parameters and Co-Digestion Options—A Review. *Biomass Convers. Biorefin.* **2021**. [CrossRef]
11. Marella, C.; Salunke, P.; Biswas, A.C.; Kommineni, A.; Metzger, L.E. Manufacture of Modified Milk Protein Concentrate Utilizing Injection of Carbon Dioxide. *J. Dairy Sci.* **2015**, *98*, 3577–3589. [CrossRef]
12. Barbano, D.M.; Sciancalepore, V.; Rudan, M.A. Characterization of Milk Proteins in Ultrafiltration Permeate. *J. Dairy Sci.* **1988**, *71*, 2655–2657. [CrossRef]
13. Global Whey Protein (Powder & Concentrate) Market Study 2019–2024-ResearchAndMarkets.Com. available online: https://www.Businesswire.Com/News/Home/20190417005321/En/Global-Whey-Protein-Powder-Concentrate-Market-Study-2019-2024---ResearchAndMarkets.Com (accessed on 16 September 2020).
14. Milk Protein Concentrate (MPC) Market 2020: Global Industry Analysis by Top Countries Data with Size, Share, Segments, Drivers and Growth Insights to 2026. available online: https://www.Marketwatch.Com/Press-Release/Milk-Protein-Concentrate-Mpc-Market-2020-Global-Industry-Analysis-by-Top-Countries-Data-with-Size-Share-Segments-Drivers-Andgrowth-Insights-to-2026-2020-09-01 (accessed on 4 September 2020).
15. Kravtsov, V.A.; Kulikova, I.K.; Anisimov, G.S.; Evdokimov, I.A.; Khramtsov, A.G. Variety of Dairy Ultrafiltration Permeates and Their Purification in Lactose Production Variety of Dairy Ultrafiltration Permeates and Their Purification in Lactose Production. *IOP Conf. Ser. Earth Environ. Sci.* **2021**, *677*, 32001. [CrossRef]
16. Ghaly, A.E.; Ben-Hassan, R.M. Continuous Production of Biogas from Dairy Manure Using an Innovative No-Mix Reactor. *Appl. Biochem. Biotechnol.* **1989**, *20–21*, 541–559. [CrossRef]
17. Parsons, R.A. On-Farm Biogas Production. In *North-East Agricultural Engineering Service*; Cornell University: Ithaca, NY, USA, 1984.
18. Kugleman, I.J.; Jerri, J.S. Anaerobic Digestion. In *Sludge Treatment*; Eckenfelder, W.W., Jr., Santhanan, C.J., Eds.; Mercel Dekker: New York, NY, USA, 1981.

19. Dębowski, M.; Korzeniewska, E.; Kazimierowicz, J.; Zieliński, M. Efficiency of Sweet Whey Fermentation with Psychrophilic Methanogens. *Environ. Sci. Pollut. Res.* **2021**, *28*, 49314–49323. [CrossRef] [PubMed]
20. Kozłowski, K.; Pietrzykowski, M.; Czekała, W.; Dach, J.; Kowalczyk-Juśko, A.; Jóźwiakowski, K.; Brzoski, M. Energetic and Economic Analysis of Biogas Plant with Using the Dairy Industry Waste. *Energy* **2019**, *183*, 1023–1031. [CrossRef]
21. Rugele, K.; Mezule, L.; Dalecka, B.; Larsson, S.; Vanags, J.; Rubulis, J. Application of Fluorescent in Situ Hybridisation for Monitoring Methanogenic Archaea in Acid Whey Anaerobic Digestion. *Agron. Res.* **2013**, *11*, 373–380.
22. Saddoud, A.; Hassaïri, I.; Sayadi, S. Anaerobic Membrane Reactor with Phase Separation for the Treatment of Cheese Whey. *Bioresour. Technol.* **2007**, *98*, 2102–2108. [CrossRef]
23. Ghaly, A.E. A Comparative Study of Anaerobic Digestion of Acid Cheese Whey and Dairy Manure in a Two-Stage Reactor. *Bioresour. Technol.* **1996**, *58*, 61–72. [CrossRef]
24. Mah, R.A. Interaction of Methanogens and Non-Methanogens in Microbial Ecology. In Proceedings of the Third International Symposium on Anaerobic Digestion, Boston, MA, USA, 14–19 August 1983; pp. 11–22.
25. Ghaly, A.E.; Pyke, J.B. Amelioration of Meth- Ane Yield in Cheese Whey by Controlling the PH of the Methanogenic Stage. *Appl. Biochem. Biotechnol. J.* **1991**, *27*, 217–237. [CrossRef]
26. Yan, J.Q.; Lo, K.V.; Liao, P.H. Anaerobic Digestion of Cheese Whey Using Upflow Anaerobic Sludge-Blanket Reactor. *Biol. Wastes* **1989**, *27*, 289–305. [CrossRef]
27. Clanton, C.J.; Backus, B.D.; Goodrich, P.R.; Fox, E.J.; Morris, H.A. Anaerobic Digestion of Cheese Whey. In Proceedings of the 1987 Food Processing Waste Conference, Atlanta, Georgia, 1–2 September 1987.
28. Lo, K.V.; Liao, P.H. Digestion of Cheese Whey with Anaerobic Rotating Biological Contact Reactor. *Biomass* **1986**, *10*, 243–252. [CrossRef]
29. Wolfe, R.S. Fermentation and Anaerobic Respira-Tion in Anaerobic Digestion. In Proceedings of the Third International Symposium on Anaerobic Digestion, Boston, MA, USA, 14–19 August 1983; pp. 3–10.
30. Pugliese, A.; Bidini, G.; Fantozzi, F. Anaerobic Digestion of Macrophytes Algae for Eutrophication Mitigation and Biogas Production. *Energy Procedia* **2015**, *82*, 366–373. [CrossRef]
31. Barua, V.B.; Kalamdhad, A.S. Biochemical Methane Potential Test of Untreated and Hot Air Oven Pretreated Water Hyacinth: A Comparative Study. *J. Clean. Prod.* **2017**, *166*, 273–284. [CrossRef]
32. Kafle, G.K.; Kim, S.H. Anaerobic Treatment of Apple Waste with Swine Manure for Biogas Production: Batch and Continuous Operation. *Appl. Energy* **2013**, *103*, 61–72. [CrossRef]
33. Mainardis, M.; Flaibani, S.; Trigatti, M.; Goi, D. Techno-Economic Feasibility of Anaerobic Digestion of Cheese Whey in Small Italian Dairies and Effect of Ultrasound Pre-Treatment on Methane Yield. *J. Environ. Manag.* **2019**, *246*, 557–563. [CrossRef]
34. Ratanatamskul, C.; Onnum, G.; Yamamoto, K. A Prototype Single-Stage Anaerobic Digester for Co-Digestion of Food Waste and Sewage Sludge from High-Rise Building for on-Site Biogas Production. *Int. Biodeterior. Biodegrad.* **2014**, *95*, 176–180. [CrossRef]
35. Pochwatka, P.; Kowalczyk-Juśko, A.; Sołowiej, P.; Wawrzyniak, A.; Dach, J. Biogas Plant Exploitation in a Middle-Sized Dairy Farm in Poland: Energetic and Economic Aspects. *Energies* **2020**, *13*, 6058. [CrossRef]
36. RED, I. Renewable Energy—Recast to 2030 (RED II) EU Science Hub. 2013. Available online: https://Ec.Europa.Eu/Jrc/En/Jec/Renewable-Energy-Recast-2030-Red-Ii (accessed on 10 October 2020).
37. Kozłowski, K.; Dach, J.; Lewicki, A.; Cieślik, M.; Czekała, W.; Janczak, D. ENVIRONMENTAL AND PROCESS PARAMETERS OF METHANE FERMENTATION IN CONTINUOSLY STIRRED TANK REACTOR (CSTR). *Inżynieria Ekol.* **2016**, *50*, 153–160. [CrossRef]
38. Luo, T.; Khoshnevisan, B.; Huang, R.; Chen, Q.; Mei, Z.; Pan, J.; Liu, H. Analysis of Revolution in Decentralized Biogas Facilities Caused by Transition in Chinese Rural Areas. *Renew. Sustain. Energy Rev.* **2020**, *133*, 110133. [CrossRef]
39. Garcia, N.H.; Mattioli, A.; Gil, A.; Frison, N.; Battista, F.; Bolzonella, D. Evaluation of the Methane Potential of Different Agricultural and Food Processing Substrates for Improved Biogas Production in Rural Areas. *Renew. Sustain. Energy Rev.* **2019**, *112*, 1–10. [CrossRef]
40. Zemo, K.H.; Panduro, T.E.; Termansen, M. Impact of Biogas Plants on Rural Residential Property Values and Implications for Local Acceptance. *Energy Policy* **2019**, *129*, 1121–1131. [CrossRef]
41. Michalska, K.; Pazera, A.; Bizukojć, M. Innowacje dla branży mleczarskiej—Biogazownie przyzakładowe (Innovations for the dairy industry—Biogas compounds). *Acta Innov.* **2013**, *9*.
42. Dębowski, M.; Kisielewska, M.; Kazimierowicz, J.; Rudnicka, A.; Dudek, M.; Romanowska-Duda, Z.; Zielínski, M. The Effects of Microalgae Biomass Co-Substrate on Biogas Production from the Common Agricultural Biogas Plants Feedstock. *Energies* **2020**, *13*, 2186. [CrossRef]
43. Llabrés-Luengo, P.; Mata-Alvarez, J. Kinetic Study of the Anaerobic Digestion of Straw-Pig Manure Mixtures. *Biomass* **1987**, *14*, 129–142. [CrossRef]
44. Cieślik, M.; Dach, J.; Lewicki, A.; Smurzyńska, A.; Janczak, D.; Pawlicka-Kaczorowska, J.; Boniecki, P.; Cyplik, P.; Czekała, I.; Jóźwiakowski, K. Methane Fermentation of the Maize Straw Silage under Meso- and Thermophilic Conditions. *Energy* **2016**, *115*, 1495–1502. [CrossRef]
45. Bylund, G. *Mleczarstwo Technika i Technologia*; Tetra Pak: Warszawa, Poland, 2013.
46. Gavazzi-April, C.; Benoit, S.; Doyen, A.; Britten, M.; Pouliot, Y. Preparation of milk protein concentrates by ultrafiltration and continuous diafiltration: Effect of process design on overall efficiency. *J. Dairy Sci.* **2018**, *101*, 9670–9679. [CrossRef] [PubMed]

47. Ahmad, T.; Aadil, R.M.; Ahmed, H.; Rahman, U.U.; Soares, B.C.V.; Souza, S.L.Q.; Pimentel, T.C.; Scudino, H.; Guimarães, J.T.; Esmerino, E.A.; et al. Treatment and Utilization of Dairy Industrial Waste: A Review. *Trends Food Sci. Technol.* **2019**, *88*, 361–372. [CrossRef]
48. Fernández, C.; Cuetos, M.J.; Martínez, E.J.; Gómez, X. Thermophilic Anaerobic Digestion of Cheese Whey: Coupling H_2 and CH_4 Production. *Biomass Bioenergy* **2015**, *81*, 55–62. [CrossRef]
49. Kisielewska, M.; Wysocka, I.; Rynkiewicz, M.R. Continuous Biohydrogen and Biomethane Production from Whey Permeate in a Two-Stage Fermentation Process. *Environ. Prog. Sustain. Energy* **2014**, *33*, 1411–1418. [CrossRef]
50. Comino, E.; Riggio, V.A.; Rosso, M. Biogas Production by Anaerobic Co-Digestion of Cattle Slurry and Cheese Whey. *Bioresour. Technol.* **2012**, *114*, 46–53. [CrossRef]
51. Bolen, T.J.; Hasan, M.; Conway, T.; Yaméogo, D.D.S.; Sanchez, P.; Rahman, A.; Azam, H. Feasibility Assessment of Biogas Production from the Anaerobic Co-Digestion of Cheese Whey, Grease Interceptor Waste and Pulped Food Waste for WRRF. *Energy* **2022**, *254*, 124144. [CrossRef]
52. Mata-Alvarez, J.; Dosta, J.; Romero-Güiza, M.S.; Fonoll, X.; Peces, M.; Astals, S. A Critical Review on Anaerobic Co-Digestion Achievements between 2010 and 2013. *Renew. Sustain. Energy Rev.* **2014**, *36*, 412–427. [CrossRef]
53. Durham, R.J. Modern Approaches to Lactose Production. In *Dairy-Derived Ingredients Food Nutraceutical Uses*; Woodhead Publishing Limited: Cambridge, UK, 2009; pp. 103–144. [CrossRef]
54. da Silva, A.N.; Perez, R.; Minim, V.P.R.; Martins, D.D.S.A.; Minim, L.A. Integrated Production of Whey Protein Concentrate and Lactose Derivatives: What Is the Best Combination? *Food Res. Int.* **2015**, *73*, 62–74. [CrossRef]
55. Energy Regulatory Office. Reference Prices in 2021. Available online: https://Www.Ure.Gov.Pl/Pl/Oze/Aukcje-Oze/Ceny-Referencyjne/6539,Ceny-Referencyjne.Html (accessed on 17 July 2022).
56. Weekly Prices of Lactose. Available online: https://Www.Clal.It/En/Index.Php?Section=lattosio (accessed on 17 July 2022).
57. European Commission Bioeconomy Strategy. *A Sustainable Bioeconomy for Europe: Strengthening the Connection between Economy, Society and the Environment*; European Commission: Brussels, Belgium, 2018. Available online: https://Ec.Europa.Eu/Research/Bioeconomy/Pdf/Ec_bioeconomy_strategy_2018.Pdf (accessed on 25 February 2020).
58. Available online: https://Www.Gramwzielone.Pl/Bioenergia/2795/Ile-Kosztuje-Budowa-Biogazowni-i-Kiedy-Sie-Zwroci (accessed on 6 September 2022).

Olsztyn, 22.09.2022 r.

M. Sc. eng. Justyna Tarapata
Department of Dairy Science and Quality Management
Faculty of Food Science
University of Warmia and Mazury in Olsztyn

STATEMENT

I declare that in the publications:

1. Tarapata, J., Dybowska, B. E., & Zulewska, J. (2022). Evaluation of fouling during ultrafiltration process of acid and sweet whey. *Journal of Food Engineering*, *328*, 111059. https://doi.org/10.1016/J.JFOODENG.2022.111059.
   My contribution was 70% and consisted of conceptualization, design of methodology, investigation, resources, data curation, writing – original draft, visualization.

2. Tarapata, J., Maciejczyk, M., & Zulewska, J. (2022). Microfiltration of buttermilk: Partitioning of proteins and modelling using a resistance-in-series model. *International Dairy Journal*, *134*, 105445.
   https://doi.org/10.1016/J.IDAIRYJ.2022.105445.
   My contribution was 75% and consisted of conceptualization, design of methodology, investigation, resources, data curation, writing – original draft, visualization, modeling of fouling.

3. Tarapata, J., Zieliński, M., & Zulewska, J. (2022). Valorization of Dairy By-Products: Efficiency of Energy Production from Biogas Obtained in Anaerobic Digestion of Ultrafiltration Permeates. *Energies*, *15*(18), 6829.
   https://doi.org/10.3390/en15186829.
   My contribution was 70% and consisted of conceptualization, design of methodology, formal analysis, investigation, writing - review & editing, data curation, writing – original draft presentation, visualization.

Justyna Tarapata

UNIVERSITY
OF WARMIA AND MAZURY
IN OLSZTYN

Justyna Żulewska Ph.D.
DEPARTMENT OF DAIRY SCIENCE AND QUALITY MANAGEMENT
Head of the Department

Olsztyn, 03.10.2022 r.

STATEMENT

I declare that in the publications:

1. Tarapata, J., Dybowska, B. E., & Zulewska, J. (2022). Evaluation of fouling during ultrafiltration process of acid and sweet whey. *Journal of Food Engineering*, *328*, 111059. https://doi.org/10.1016/J.JFOODENG.2022.111059.
   My contribution was 20% and consisted of conceptualization, design of methodology, writing – review & editing, supervision, project administration and funding acquisition.

2. Tarapata, J., Maciejczyk, M., & Zulewska, J. (2022). Microfiltration of buttermilk: Partitioning of proteins and modelling using a resistance-in-series model. *International Dairy Journal*, *134*, 105445.
   https://doi.org/10.1016/J.IDAIRYJ.2022.105445.
   My contribution was 20% and consisted of conceptualization, design of methodology, writing - review & editing, supervision, project administration, funding acquisition.

3. Tarapata, J., Zieliński, M., & Zulewska, J. (2022). Valorization of Dairy By-Products: Efficiency of Energy Production from Biogas Obtained in Anaerobic Digestion of Ultrafiltration Permeates. *Energies*, *15*(18), 6829.
   https://doi.org/10.3390/en15186829.
   My contribution was 10% and consisted of conceptualization, design of methodology, writing - review & editing, validation, data curation, supervision, resources, funding acquisition.

Justyna Żulewska

DEPARTMENT OF DAIRY SCIENCE AND QUALITY MANAGEMENT
FACULTY OF FOOD SCIENCE
UNIVERSITY OF WARMIA AND MAZURY IN OLSZTYN
ul. Oczapowskiego 7, 10-719 Olsztyn

P. +48 89 523 34 02 e-mail: kmizj@uwm.edu.pl
F. +48 89 523 34 02 http://www.uwm.edu.pl/wnz/kmizj/

Olsztyn, 29.09.2022 r.

prof. dr hab. eng. Marcin Zieliński

Department of Environmental Engineering

Faculty of Geoengineering

University of Warmia and Mazury in Olsztyn

STATEMENT

I declare that in the publication:

Tarapata, J., Zieliński, M., & Zulewska, J. (2022). Valorization of Dairy By-Products: Efficiency of Energy Production from Biogas Obtained in Anaerobic Digestion of Ultrafiltration Permeates. *Energies*, *15*(18), 6829. https://doi.org/10.3390/en15186829.

My contribution was 20% and consisted of conceptualization, design of methodology, writing - review & editing, validation, data curation, supervision, resources, funding acquisition.



Olsztyn, 29.09.2022 r.

dr hab. Maciej Maciejczyk, prof. UWM

Department of Physics and Biophysics

Faculty of Food Science

University of Warmia and Mazury in Olsztyn

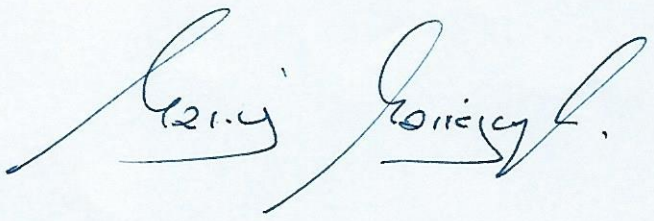
maciej.maciejczyk@uwm.edu.pl

STATEMENT

I declare that in the publication:

Tarapata, J., Maciejczyk, M., & Zulewska, J. (2022). Microfiltration of buttermilk: Partitioning of proteins and modelling using a resistance-in-series model. *International Dairy Journal*, *134*, 105445. https://doi.org/10.1016/J.IDAIRYJ.2022.105445.

My contribution was to model the cake layer formation and I estimate it as 5%.



Olsztyn, 28.09.2022 r.

dr hab. eng. Brygida Ewa Dybowska

brygida.dybowska@uwm.edu.pl

STATEMENT

I declare that in the publication:

Tarapata, J., Dybowska, B. E., & Zulewska, J. (2022). Evaluation of fouling during ultrafiltration process of acid and sweet whey. *Journal of Food Engineering*, *328*, 111059. https://doi.org/10.1016/J.JFOODENG.2022.111059.

My contribution was to develop a measurement methodology and investigation of particle size distribution in tested samples and I estimate it as 10%.

Brygida Dybowska